The role of small heat shock proteins in mutant superoxide dismutase-linked familial amyotrophic lateral sclerosis

Victoria Ellen Licence

The role of small heat shock proteins in mutant superoxide dismutase-linked familial amyotrophic lateral sclerosis

Victoria Ellen Licence

PhD thesis

University of Durham
Department of Biological and Biomedical Sciences

2005

ABSTRACT

The mechanisms by which mutations in the gene encoding superoxide dismutase 1 (SOD1) lead to amyotrophic lateral sclerosis (ALS) remain incompletely understood. Mutant SOD1 inclusions are observed in both ALS patients and animal models of the disease. Chaperone proteins have been shown to reduce mutant SOD1 inclusion formation in both cell and animal systems and, up-regulation of heat shock proteins (HSPs) in a mouse model of ALS increases their life expectancy. The results presented in this thesis are based on an investigation into the role of small heat shock proteins (sHSPs) in mutant SOD1 inclusion formation, using a model HEK293 cell system.

Over-expression of yellow fluorescent protein (YFP)-tagged G85R mutant SOD1 in HEK293 cells and subsequent treatment with proteasome inhibitor leads to mutant SOD1-inclusion formation, as shown by immunofluorescence (IMF) microscopy. Using this model of mutant SOD1-inclusion formation, we demonstrate that over-expression of sHSPs decreases the proportion of insoluble mutant SOD1 present within these cells. Mutations in these sHSPs prevent this function, and further increase the proportion of insoluble mutant SOD1. These mutant sHSPs also cause an increase in the insolubility of normally soluble proteins, such as wild-type SOD1. Similar results were observed in Neuro 2a cells, where over-expression of sHSPs caused the phenotype of the mutant SOD1 inclusions to change, from dense, tight structures to more diffuse ones.

We have shown that sHSPs decrease the amount of insoluble mutant SOD1 in HEK293 cells, supporting reports that chaperone proteins prevent mutant SOD1-inclusion formation and are beneficial in a mouse model of ALS.

Whether the clinical use of these proteins will be of therapeutic benefit in the treatment of ALS patients remains to be determined.

TABLE OF CONTENTS

LIST OF FIGURES AND TABLES

DECLARTION

I hereby declare that no part of my thesis entitled 'The role of sHSPs in mutant SOD1 linked-FALS' has been or is being submitted for any other degree or diploma, at this or any other University.

The experimental work described here was carried out at the University of Durham, Department of Biological and Biomedical Sciences, under the supervision of Professor R A Quinlan. These results represent my own work and includes nothing which is the outcome of work done in collaboration.

Victoria Licence, May 2005

STATEMENT OF COPYRIGHT

ACKNOWLEDGEMENTS

I would like to thank my supervisor, Roy Quinlan, for providing me with the opportunity to undertake this project and all the members of the RAQ group – Heather, Vilius, Fred, Ming, Fang and Yuki - for their generous help and advice. Thanks to everyone from RAQ, AM and CJH labs for their help, advice, ideas and, more importantly for all the coffee and cakes! Durham has been a great experience and I will miss you all when I'm gone.

Thanks to my family for support, with extra special thanks to Stephen for encouragement, proof-reading and all those references Durham University could not provide!

And lastly, thanks to Motor Neurone Disease Association UK, who funded this studentship, and especially Belinda (Cupid), for introducing me to people and being a good friend in Milan.

ABBREVIATIONS

ALLN - N-Acetyl-Leu-Leu-Nle-CHO

ALS – amyotrophic lateral sclerosis

APP – β-amyloid precursor protein

ATP – adenosine triphosphate

BSA – bovine serum albumin

CCS – copper chaperone for SOD1

CDK5 – cyclin dependent kinase 5

CMT – Charcot-Marie-Tooth

CNS – central nervous system

CNTF – ciliary neurotrophic factor

COX-2 – cyclo-oxygenase-2

DAPI - 4',6-diamidino-2-phenylindole, dihydrochloride

DMEM - Dulbecco's Modified Eagle Medium

DTT – dithiothreitol

EAAT2 – excitatory amino acid transporter 2

ECL – enhanced chemiluminescence

EC SOD – extracellular superoxide dismutase

EDTA – ethylene diamine tetra-acetic acid

FALS – familial amyotrophic lateral sclerosis

FCS – foetal calf serum

GEF – guanine nucleotide exchange factor

HSE – heat shock element

HSF – heat shock factor

HSP – heat shock protein

ICE - interleukin-β-converting enzyme

IF – intermediate filament

IGF-1 – insulin growth factor-1

IgG – immunoglobulin G

IP - immunoprecipitation

IPTG – isopropylthio-β-D-galactosidase

kDa – kilo Dalton

LSB - Laemmli's sample buffer

MCSs – multiple cloning sites

MEM - Modified Eagle Medium

MN – motor neurone

Mn SOD – mitochondrial manganese superoxide dismutase

MT – microtubule

MTOC – microtubule organising centre

NF - neurofilamnet

NO – nitric oxide

P - pellet

PAGE – polyacrylamide gel electrophoresis

PBS – phosphate buffered saline

PCR – polymerase chain reaction

PMSF – phenlmethylsulphonyl fluoride

SALS – sporadic amyotrophic lateral sclerosis

SBMA – spinobulbar muscular atrophy (or Kennedy's disease)

SCA-1 – spinocerebellar ataxia type-1

SDS – sodium dodecyl sulphate

SEC – size exclusion chromatography

sHSP – small heat shock protein

SMA – spinal muscular atrophy

SN – supernatant

snRNP - small nuclear ribonucleoprotein

SOD1 – Cu/Zn superoxide dismutase

TBS – tris buffered saline

TNF-α - tumour necrosis factor-α

TRITC – tetramethylrhodamine isothiocyanateTTBS

TTBS - TBS containing 0.2% (v/v) Tween

Ub – ubiquitin

UPS – ubiquitin proteasome system

wt – wild type

YFP – yellow fluorescent protein

CHAPTER 1
INTRODUCTION

Amyotrophic Lateral Sclerosis: background and clinical aspects

The motor neurone diseases are a group of heterogeneous disorders, which affect motor neurones (MNs). MNs are large nerve cells which are the effectors of the nervous system. They relay processed information from the brain to the muscle, thereby controlling muscle movement. Upper MNs originate in the brain and pass down the spinal cord towards the body. Lower MNs leave the spinal cord in ventral roots and innervate their specific effector muscles. Motor neurone diseases are characterised by muscle weakness and/or spastic paralysis, which results from damage to MNs. The most common adult onset motor neurone disease is amyotrophic lateral sclerosis (ALS). Other motor neurone diseases include spinobulbar muscular atrophy (SBMA or Kennedy's disease), spinal muscular atrophy (SMA) and hereditary spastic paraplegia. SBMA and SMA affect lower MNs and hereditary spastic paraplegia affects upper MNs.

ALS was first described by Charcot in 1869. The disease has an incidence of 2 in 100,000 and an approximate worldwide prevalence of 7 in 100,000 individuals. It is estimated that up to 5000 people in the UK have ALS. Although ALS can affect any adult individual, the highest occurrence is in the 50-70 year age range, with men being slightly more affected than women. Loss of both upper and lower MNs occurs in ALS, giving rise to muscle atrophy, stiffness and fasciculation (muscle twitching). It is less well recognised that approximately 30% of small interneurons in the motor cortex and spinal cord also degenerate. The progressive decline in muscle function seen in ALS results in paralysis, speech defects and eventually death, due to respiratory

failure (from denervation of respiratory muscles and the diaphragm). This usually occurs within one to five years of clinical onset. In ALS patients, as well as MN loss, various abnormalities have been observed in the remaining MNs. Proximal axonal swellings, termed spheroids, occur and these have been shown to contain neurofilaments (NFs) (Carpenter, 1968). Other protein accumulations are also observed, and these have been shown to contain ubiquitin (Ub) (Leigh et al., 1991). Furthermore, fragmentation of the Golgi apparatus is also a prominent feature (Gonatas et al., 1992). The primary pathogenic processes underlying ALS are presently unknown, but it is probably the case that multiple factors contribute to the disease mechanism. Major hypotheses have been put forward to explain disease progression, and these include cytoskeletal abnormalities (Xu et al., 1993, Cote et al., 1993), excitotoxicity (Rothstein et al., 1992, Shaw et al., 1994) and protein aggregation (Deng et al., 1993, Shibata et al., 1996, Durham et al., 1997). These and some other contributing factors are discussed in detail in later sections.

Mutant genes in ALS

Approximately 10% of all ALS cases are inherited; familial amyotrophic lateral sclerosis (FALS). Of these, 20% are caused by mutations in the superoxide dismutase 1 (SOD1) gene (Rosen, 1993), and most of these follow an autosomal dominant pattern of inheritance. Despite this fact, the disease pathogenesis in FALS and sporadic amyotrophic lateral sclerosis (SALS) cases is remarkably similar. SOD1, located on chromosome 21q22.1, encodes Cu/Zn superoxide dismutase (SOD1), a ubiquitously expressed cytosolic metallo-enzyme which catalyses the conversion of superoxide radicals (a by-product of oxidative phosphorylation in the mitochondria) to hydrogen peroxide (H_2O_2) and

water (H_2O) (Fridovich, 1986). The SOD1 protein is a homodimer consisting of 153 amino acids with copper and zinc binding sites. There are two other forms of SOD: extracellular SOD (EC SOD) and manganese SOD (Mn SOD), which is located in mitochondria. Presently, eighty-nine mutations in SOD1 have been linked to ALS. These are widely, albeit unevenly distributed throughout the gene, and in most cases are mis-sense mutations occurring in exons 4 and 5 (Gaudette et al., 2000, Andersen, 2001, Andersen et al., 2003). An updated list of these mutations can be found at http://www.alsod.org; the online database for ALS genetics.

Other mutations have also been linked to ALS. Mutations in glutamate transporters have been reported in SALS cases (Aoki et al., 1998), and a mutation in dynactin, a protein involved in axonal transport, leads to lower motor neurone disease (Puls et al., 2003). Mutations in NFs are also involved. Some SALS patients show mutations in NF subunits (Al-Chalabi et al., 1999), and similarly, a mutation in the light NF subunit is the primary cause of Charcot-Marie-Tooth (CMT) disease type II.

ALS2 is a recessive form of juvenile ALS, which is a rare, slowly progressing disease which has been mapped to chromosome 2q33 (Hentati et al., 1994). Hadano et al., (2001), reported two independent mutations in the same gene, ALS2, in two unrelated families with the disease. Other related MN disorders have also been identified as being linked to mutations in this gene (Yang et al., 2001). ALS2 is expressed in various tissues and cell types, including neurons in the brain and spinal cord, and encodes a 184kDa protein; alsin, which contains 3 guanine nucleotide exchange factor (GEF) domains. One mutation (in Tunisian ALS2) results in the generation of a truncated protein, and the other, (Kuwaiti ALS2), is a frameshift mutation which results in

the generation of seventy new amino acids before a premature stop codon. Otomo et al., (2003), employed biochemical and cell biological analyses to determine the functions of alsin and demonstrated that it binds specifically to a small GTPase, Rab5, involved in endosomal trafficking. Alsin localises with Rab5 and early endosomal antigen-1 (EEA-1) onto early endosomal compartments and stimulates endosomal enlargement *in vitro*. These data suggest a role for alsin as a Rab5 GEF and implicate the disruption of endosomal dynamics in ALS2. A subsequent report, (Yamanaka et al., 2003), demonstrated that ALS2 mutants are highly unstable, as these proteins could not be detected in lymphoblasts from patients suffering from this form of the disease. As a result they proposed that the loss of function of alsin results in MN degeneration in these MN disorders.

Two recent reports have implicated mutant small heat shock proteins (sHSPs) in neurodegenerative diseases. Mutations in HSP 27 have been linked to CMT disease and distal hereditary motor neuropathy (Evgrafov et al., 2004), and the viability of neuronal cells transfected with mutated HSP 27 was reduced when compared to cells expressing wt protein. Similarly, mutations in HSP 22 have been identified in families with distal hereditary motor neuropathies (Irobi et al., 2004) and cultured cells transfected with mutated HSP 22 formed intracellular inclusions.

Continuing research is being carried out to try and identify other candidate genes that might be involved in ALS; indeed in 2003, three independent reports were published which, in three separate families, linked FALS to a locus on chromosome 16q12.1-16q12.2. Also of interest is the report that a mouse modifier gene has been identified that can suppress ALS onset (Kunst et al., 2000). The region of chromosome 13 linked to the delayed onset

of the disease in these mice contains candidate genes such as SMN (survival motor neuron) and NAIP (neuronal apoptosis inhibitor protein) (Kunst et al., 2000). Both genes have been linked to SMA. The identification of the gene(s) that are able to suppress ALS in this mouse model may help to elucidate the disease mechanisms in ALS.

Mutant SOD1-linked FALS

The mechanism whereby mutant SOD1 gives rise to ALS remains unclear. What is well established, however, is that it is not loss of function of SOD1, but rather one or more toxic gain of functions that gives rise to the disease. Evidence for this toxic gain of function includes: (a) SOD1 null mice do not develop motor neuron disease (Reaume et al., 1996). In this study, a mouse line was produced with targeted inactivation of the SOD1 gene. These mice, shown to be deficient in cytosolic SOD1, develop normally with no evidence of motor neuron disease. Whereas mutant SOD1 transgenic mice (Gurney et al., 1994, Wong et al., 1995) demonstrate limb tremors and neuronal pathology as early as 3 months of age, SOD1 null mice show no detectable morphological changes in the spinal cord by 4 months of age and no motor deficits by 6 months of age. (b) SOD1 activity in a mutant SOD1 transgenic mouse model remains unchanged (Ripps et al., 1995) and mice expressing G37R mutant SOD1 in the presence of elevated levels of wild-type (wt) SOD1 develop ALS (Wong et al., 1995). (c) changes in wt SOD1 levels in transgenic mutant SOD1 mice do not affect disease (Bruijn et al., 1998). Here, the effect of wt SOD1 on the onset and progression of ALS was determined by either increasing or eliminating wt SOD1 in mutant SOD1 transgenic mice. Increasing wt SOD1 levels in G85R mutant SOD1 transgenic mice had no affect on either the time of

onset or disease progression and did not affect disease pathology; both MN degeneration and death remained the same, independent of SOD1 level. Similarly, either decreasing or eliminating wt SOD1 had no effect in G85R mutant SOD1 transgenic mice: disease onset and progression remained unchanged, as did MN degeneration and death. (d) some mutant forms of SOD1 retain full activity. A study looking at the specific activities of 6 different mutant SOD1s (Borchelt et al., 1994), showed that although the G85R mutant lacked activity, the G37R mutant demonstrated specific activity which was greater than or equal to that of wt SOD1. Four other mutants, namely A4V, G41D, G93C and I113T, retained 30-65% of wt specific activity. (e) disease onset and progression do not appear to correlate to SOD1 activity levels (Bowling et al., 1995).

Mutant SOD1 mediated toxicity is non-cell autonomous

Expression of SOD1 is ubiquitous, so why is it that MNs alone are affected in mutant SOD1 linked FALS? When mutant SOD1 is selectively expressed in astrocytes (Gong et al., 2000), or MNs (Lino et al., 2002), mice do not develop any kind of motor neurone disease. Using chimeric mice, (Clement et al., 2003), demonstrated that mutant SOD1 toxicity to MNs is non-cell autonomous, i.e. damage to both neuronal and non-neuronal cells is required for mutant SOD1-mediated toxicity. In these experiments, MNs which expressed either G37R or G93A mutant SOD1 at levels which usually cause disease, could escape degeneration and death if surrounded by normal non-neuronal cells. Another interesting finding was that normal MNs, surrounded by mutant SOD1 expressing non-neuronal cells, acquired Ub containing deposits. This suggests that the presence of mutant SOD1 in these non-neuronal cells may somehow

induce protein aggregation in MNs. These data show that the cellular environment is important in ALS pathogenesis and that dysfunction and death of MNs is partially dependent on support from surrounding non-neuronal cells.

Mutant SOD1 transgenic mice

Three of the FALS-linked SOD1 mutations have been characterised in mouse models of ALS, namely G37R, G85R and G93A (Gurney et al., 1994, Wong et al., 1995, Ripps et al., 1995). Mice expressing these mutant SOD1 transgenes develop an age-dependent ALS-like disorder, exhibiting hind limb weakness, degeneration of spinal cord MNs, increased astrogliosis, activation of microglia and presence of NF- and Ub-containing cytoplasmic inclusions in surviving MNs and astrocytes. Such mice have provided a useful tool in the study of mutant SOD1-linked ALS pathogenesis.

Is aberrant catalytic activity the cause of mutant SOD1 toxicity?

It is possible that mutant SOD1 toxicity may be caused by aberrant enzymatic activity. It has been suggested that disruption of amino acids in and around the active site may cause conformational changes in mutant SOD1 thus resulting in greater access to abnormal substrates. One of these is peroxynitrite (ONO_2^-) which is produced by the reaction between SOD1 and nitric oxide (NO) and is a powerful oxidant. It reacts with SOD1 to produce a nitronium-like intermediate, which nitrates tyrosine residues (Beckman, 1993). Thus mutant SOD1 toxicity may be mediated by increased nitration of proteins, which is damaging to the cell. Increased levels of free nitrotyrosine have been reported in ALS (Beal et al., 1997, Bruijn et al., 1997a). Direct biochemical measurement and immunohistochemical studies demonstrated increased concentrations of free 3-

nitrotyrosine and its major metabolite, 3-nitro-4-hydroxyphenylacetic acid, in the spinal cord of ALS patients. Elevated 3-nitrotyrosine was also detected in the MNs of ALS patients (Beal et al., 1997). Another report demonstrated that, although increased levels of 3-nitrotyrosine in G37R mutant SOD1 transgenic mice are detectable, no such increase in protein bound nitrotyrosine in either the spinal cord or MNs of these mice, or in spinal cord extracts from ALS patients was observed (Bruijn et al., 1997a). Also, levels of nitrated NF are the same in both control and ALS cases (Strong et al 1998). These latter reports argue against the peroxynitrite/nitration theory and therefore it is unlikely that it is a contributing factor in SOD1-mediated toxicity. Other evidence opposing this theory is that as NO is critical in the formation of peroxynitrite, it would be expected that altering NO synthesis would affect disease progression. However, a report by Facchinetti et al., (1999) concluded that NO was unlikely to have a role in pathogenesis of G93A mutant SOD1 transgenic mice, as the expression of G93A mutant SOD1 in a NO null background had no beneficial effect on survival, as compared to the expression of G93A alone.

Another cause of mutant SOD1-mediated toxicity may be linked to hydroxyl radicals. Wiedau-Pazos et al. (1996) have shown that mutant SOD1 is able to utilise H_2O_2 as a substrate more efficiently than wt SOD1. This reaction produces a highly reactive hydroxyl radical. Toxic hydroxyl radials and the resultant oxidative damage have been shown to be increased in the spinal cord of mutant SOD1 transgenic mice, coincident with features of motor neuron disease (Ferrante et al., 1997, Bogdanov et al., 1998). However, another report, (Bruijn et al., 1997a), showed that levels of hydroxyl radicals and lipid peroxidation (arising from free radical-mediated damage) remain unchanged in G37R mutant SOD1 transgenic mice, compared with non-transgenic control

littermates. These conflicting data would suggest that hydroxyl radicals are unlikely to be a contributing factor in SOD1-mediated toxicity.

The report by Bruijn et al., (1998), also disagrees with the aberrant catalysis hypothesis. If more efficient use of peroxynitrite by mutant SOD1 has a role in disease pathogenesis, then altering the levels of wt SOD1 in G85R mutant SOD1 transgenic mice would be expected to alter disease progression. However, this report demonstrates that this is not the case. In the case of H_2O_2 the same reasoning applies: if mutant SOD1 utilises H_2O_2 more efficiently than wt SOD1, then altering the levels of wt SOD1 in the G85R mutant SOD1 transgenic mice should alter disease progression. However, this is not the case. That wt SOD1 does not influence disease in mutant SOD1 transgenic mice challenges the idea that toxicity arises from increased oxidative stress.

Both hypotheses of aberrant catalytic activity as a possible cause of toxicity ultimately involve copper, as this element acts as a co-factor for SOD1, interacting with substrates in the active site. In 1997, Culotta et al. showed that in yeast, copper loading onto SOD1 is dependent on a specific copper chaperone – CCS: copper chaperone for SOD1. Subsequent studies have shown that wt and various SOD1 mutant proteins bind copper via the action of CCS. This supports a hypothesis that aberrant copper mediated chemistry, catalysed by less tightly folded mutant SOD1 enzymes, may be responsible for MN degeneration (Corson et al., 1998). Elimination of CCS in mutant SOD1 transgenic mice had no effect on either disease onset or progression, showing that CCS-dependent copper loading of mutant SOD1 plays no role in disease pathogenesis in these mice (Subramaniam et al., 2002). However, CCS is not the only means by which SOD1 can acquire copper. It has recently been shown that SOD1 can acquire copper via a conserved auxillary pathway that is

dependant on the presence of reduced gluathione (GSH) (Carroll et al., 2004). Wang et al., (2002), generated transgenic mice that express SOD1 carrying disease linked-mutations which disrupt 2 of the 4 histidine residues which are crucial for copper binding; H46R and H48Q. These mice stil develop motor neurone disease, showing that disruption of copper binding does not eliminate toxicity.

The role of zinc in disease pathogenesis

Like copper, zinc acts as a co-factor for enzymatically active SOD1. Is it possible that zinc may also have some role in ALS? It has been shown that, compared to wt SOD1, FALS-associated SOD1 mutants have dramatically different metal binding and redox behaviour, (Lyons et al., 1996). A subsequent study demonstrated that the zinc affinity of four FALS-associated SOD1 mutants is decreased by approximately 30-fold, compared to wt. Such a loss of zinc resulted in an increased efficiency of peroxynitrite-mediated tyrosine nitration (Crow et al., 1997).

This decreased affinity of mutant SOD1 for zinc and the associated increase in tyrosine nitration induced MN death via apoptosis (Estevez et al., 1999). As NO is required for peroxynitrite production (Beckman, 1993), NO synthase (NOS) inhibitors, as well as peroxynitrite scavengers, prevent this zinc deficient SOD1-mediated apoptosis. Estevez et al., (1999) also showed that copper must be associated with zinc-deficient SOD1 in order for the induction of apoptosis to occur. Therefore, the authors propose that inactivation of zinc-deficient SOD1 by means of copper chelating compounds may be of therapeutic significance in treatment of ALS.

Mutations in SOD1 account for approximately 20% of inherited FALS cases. A possible mechanism for toxicity of mutant SOD1 have been discussed above, namely aberrant catalysis. It is also possible that mutant SOD1 mediates its toxicity by incorrect protein folding and the subsequent downstream effects of this. This will be discussed in a later section: Protein aggregation. But this aside, what is happening to cause disease in the majority of other cases of ALS? So far, studies suggest that ALS is a multi-factorial disease with a number of contributing factors, some of which are outlined below. However, how all these different factors are linked together and give rise to a remarkably similar disease pathogenesis remains unclear and is the subject of ongoing investigation.

Cytoskeletal involvement in ALS: Neurofilaments

Neurofilaments are the major intermediate filaments (IFs) in MNs. They are formed by co-polymerisation of three different subunits: NF-light (NF-L), 61kD; NF-medium (NF-M), 90kD and NF-heavy (NF-H), 115kD. Both the accumulation and abnormal assembly of NFs are pathological hallmarks of several neurodegenerative diseases, including ALS (Carpenter 1968). Two reports in 1993, (Xu et al., and Cote et al.), showed that over-expression of NF subunits can cause death and degeneration of MNs and these observations led to the proposal that the pathogenesis of ALS is linked to damage of NFs. Indeed, both the content and organisation of NFs influence the disease in mutant SOD1 transgenic mice: deletion of NF-L increases the lifespan of G85R mutant SOD1 transgenic mice (Williamson et al., 1998) and similar results were obtained by increasing the expression of NF-H in G37R mutant SOD1 transgenic mice (Couillard-Despres et al., 1998) and either NF-L or –H in G93A mutant SOD1

transgenic mice (Kong and Xu, 2000). These genetic manipulations have the overall effect of increasing the amount of NFs in the perikarya and decreasing NFs in the axons of MNs. However, as to how this increases longevity is as yet not known. It has been suggested that elevated levels of NFs in the cell body may act as a phosphorylation sink for deregulated cyclin dependent kinase 5 (CDK5) activity (Nguyen et al., 2001). CDK5 activity is abnormally increased in the spinal cord of G37R mutant SOD1 transgenic mice and this is associated with hyperphosphorylation of NFs. The authors propose that in these mice the NF accumulations act as a phosphorylaion sink for the deregulated CDK5 activity, thereby decreasing the potential hyperphosphorylation of other cellular substrates.

Neurofilament accumulations, which are hallmarks of ALS (Carpenter, 1968), can be phosphorylated, as shown by labelling with phosphorylation specific antibodies (Sobue et al., 1990). A recent report (Ackerley et al., 2004), has shown that a major stress-activated kinase in the nervous system; p38α, is also able to phosphorylate NFs. The precise role of NF phosphorylation is not clear at present, but it has been associated with slowing of axonal transport (Jung et al., 2000). Such retardation of axonal transport is an early pathological feature in mutant SOD1 transgenic mice (Zhang et al., 1997, Williamson and Cleveland, 1999), so it is possible that aberrant activation of p38α may have a role in this aspect of the disease. Indeed, p38α is associated with aberrantly phosphorylated NFs in human ALS cases (Ackerley et al., 2004). There is other evidence supporting such a role for p38α. Tortarolo et al., (2003), demonstrated increased p38α activity in the spinal cords of G93A mutant SOD1 transgenic mice and minocycline, an anti-inflammatory drug which delays onset and slows

disease progression in G37R mutant SOD1 mice, inhibits p38α (Kriz et al., 2002).

It has been shown previously that a mutation in NF-L is a primary cause of CMT disease type II (Mersiyanova et al., 2000, De Jonghe et al., 2001), a related neurodegenerative disease, and Al-Chalabi et al. (1999) have identified a set of inframe deletions or insertions in the NF-H tail domain in a small proportion of SALS cases. Therefore, it seems that both NF content and organisation are important risk factors and contributors in ALS but do not, by themselves, have a direct role in the cause of disease.

Cytoskeletal involvement in ALS: Peripherin

Peripherin is another neuronal IF, of 57kDa. It is expressed mainly in the peripheral nervous system (PNS) but it is also seen at low levels in defined populations of neurons in the central nervous system (CNS). It has been proposed that peripherin may have a role in neuronal regeneration, as its expression is upregulated following neuronal injury (Troy et al., 1990). In 1992, Corbo and Hays reported that peripherin co-localised with NF protein in axonal inclusions in MNs of ALS patients, thus suggesting a possible involvement of peripherin in ALS. It has since been shown that over-expression of a peripherin transgene in mice led to late onset motor neuron disease, characterised by formation of ALS-like IF inclusions (Beaulieu et al., 1999) and that over-expression of peripherin in cultured neurons causes apoptotic death in synergy with tumour necrosis factor-α (TNF-α) (Robertson et al., 2001). This may account for selective neuronal death in ALS. The report by Beaulieu also showed that a deficiency in NF-L accelerates the effects of wt peripherin over-expression. It has been shown that a neurotoxic peripherin isoform, peripherin

61, is expressed in G37R mutant SOD1 transgenic mice but not control or peripherin transgenic mice, (Robertson et al., 2003). This suggests that expression of a neurotoxic splice variant of peripherin is part of the mutant SOD1 disease mechanism. Peripherin 61 immunoreactivity was also detected in spinal cord MNs from ALS patients. However, notwithstanding all these reports, the role of peripherin involvement in ALS was called into question when a report (Lariviere et al., 2003) demonstrated that either elimination of all peripherin isoforms or over-expression of peripherin had no effect on survival in mutant SOD1 transgenic mice.

Excitotoxicity

Glutamate mediated excitotoxicity is another potential contributor to ALS. Glutamate is a neurotransmitter which activates glutamate receptors, leading to depolarisation of neuronal membranes and activation of voltage gated calcium (Ca^{2+}) channels (VGCCs). Abnormalities in this pathway can lead to dysfunctional Ca^{2+} homeostasis and cell death. Evidence for glutamate mediated excitotoxicity in ALS comes from several reports of elevated levels of glutamate in cerebrospinal fluid from ALS patients (Rothstein et al., 1990, Rothstein et al., 1991, Shaw et al., 1995). This same finding has now been reported in 40% of SALS cases. Synaptic actions of glutamate are terminated via glutamate transporters that surround the synaptic cleft. This action protects neurons from glutamate mediated toxicity. This is supported by evidence from the anti-sense knockdown of astroglial glutamate receptors which causes excitotoxic neuronal degeneration (Rothstein et al., 1996). Abnormal glutamate transport has been reported in ALS (Rothstein et al., 1992, Shaw et al., 1994). Different glutamate transporters have been identified and a subsequent study

demonstrated that it is loss of the astroglial transporter, excitatory amino acid transporter 2 (EAAT2) that is responsible for the abnormal glutamate transport seen in ALS (Rothstein et al., 1995). It has been proposed that aberrant RNA processing may account for this decrease in EAAT2 levels (Lin et al., 1998) but this remains controversial as another report (Meyer et al., 1999) showed that aberrant transcripts are present in both ALS cases and control patients. Mutations in EAAT2 have been reported (Aoki et al., 1998); N206S in a SALS patient, and a mutation in the 5' end of exon 7 and a silent G to A transition at codon 234 at exon 5 in two FALS patients. The N206S mutation occurs at an N-linked glycosylation site and causes aberrant targeting of the receptor and decreased uptake of glutamate by glial cells (Trotti et al., 2001). Glutamate mediated excitotoxicity has also been implicated in other neurological diseases that resemble ALS (Spencer et al., 1993). In this report, amyotrophic lateral sclerosis-Parkinsonism dementia complex (ALS-PDC) has been linked to a chronic reliance on native foodstuffs rich in glutamate receptor agonists in Guam.

Other evidence supporting an excitotoxic component in disease pathogenesis is the demonstration of reduced Ca^{2+} binding proteins, for example parvalbumin and calbindin D28k, in MNs that are at risk compared to those that are spared during the disease. (Alexianu et al., 1994, Ince et al., 1993).

Glutamate mediated excitotoxicity has also provided a mechanistic link between SALS and FALS; such links are very rare. A4V and I113T mutant, but not wt SOD1 cause inactivation of EAAT2 (Trotti et al., 1999) and decreased levels of EAAT2 are observed in a mutant SOD1 transgenic rat model of ALS (Howland et al., 2002). Although SOD1 has been implicated in glutamate

mediated excitotoxicity, its primary effects are in the MNs: astrogliosis occurs in mutant SOD1 transgenic mice after the first clinical symptoms of disease appear (Levine et al., 1999) and targeted expression of mutant SOD1 in glial cells does not result in disease in mice (Gong et al., 2000).

From the results described above it can be concluded that glutamate mediated excitotoxicity is an important contributor to neuronal death and ALS. Furthermore, Riluzole, a drug that acts by decreasing glutamate toxicity, is the only FDA (Food and Drug Administration) approved therapy for ALS.

Mitochondrial defects

In 1998 Kong and Xu demonstrated that abundant mitochondrial abnormalities can be detected very early on in disease progression in G93A mutant SOD1 transgenic mice. The onset of muscle weakness correlates with a massive vacuolation of mitochondria, suggesting a possible contribution of mutant SOD1 to disease pathology via mitochondrial degeneration. This vacuolation is associated with translocation of mutant SOD1 into the inter-membrane space of the mitochondria (Jaarsma et al., 2001). Another study has also reported the presence of mutant SOD1 in CNS mitochondria in G93A mutant SOD1 transgenic mice (Higgins et al., 2002). Other evidence supporting a role for mitochondrial involvement in ALS includes functional inhibition of mitochondria in *in vitro* cultured MNs inducing cell death (Kaal et al., 2000). Furthermore, a partial deficiency of the mitochondrial form of SOD, Mn SOD, exacerbates the clinical phenotype and disease progression in G93A mutant SOD1 transgenic mice (Andreassen et al., 2000). Also, a report by Borthwick et al., (1999), showed a selective decrease in cytochrome c oxidase; a mitochondrial enzyme, in spinal cord MNs from ALS patients. Cytochrome c oxidase is encoded by

mitochondrial DNA; it may, therefore, be the case that damage to mitochondrial DNA is implicated in ALS.

Two drugs, creatine and minocycline, which target mitochondria have been shown to be beneficial in mouse models of ALS. Creatine buffers intracellular energy stores and inhibits opening of the mitochondrial transition pore. Administration of this to G93A mutant SOD1 transgenic mice improves motor performance and protects them from loss of MNs (Klivenyi et al., 1999). Similarly, minocycline improves motor performance and also extends survival in G93A mutant SOD1 transgenic mice (Zhu et al., 2002). Minocycline has neuroprotective properties in other neurodegenerative conditions (e.g. Huntingdon's and Parkinson's diseases) and consequently was tested in this ALS disease model. This report demonstrated that minocycline exerted its effects via inhibition of permeability transition-mediated cyctochrome c release in mitochondria. The above reports also present data which implicate mitochondrial dysfunction in ALS. However, there is some conflicting evidence in that morphologically abnormal mitochondria were not observed in G85R mutant SOD1 transgenic mice (Bruijn et al., 1997b)

Activation of apoptosis

Bcl2 is an anti-apoptotic protein that has been shown to reduce MN loss in mice; it protects against axotomy-induced MN loss after transection of the facial nerve (Dubois-Dauphin et al., 1994). This led to a report by (Kostic et al., 1997), which demonstrated that over-expression of Bcl2 in G93A mutant SOD1 transgenic mice delays disease onset by decreasing loss of myelinated nerve fibres and death of spinal cord MNs, thereby prolonging survival. This is one of many publications linking ALS and increased levels of apoptosis.

Using an *in vitro* neuroblastoma cell model together with mutant SOD1 transgenic mice (G37R and G85R), (Pasinelli et al., 1998), demonstrated that neural cells and tissue expressing mutant SOD1 show cleavage of caspase-1/interleukin-β-converting enzyme (ICE). Complete cell death, however, requires additional stimuli such as oxidative stress. Caspase-1 and -3 are sequentially activated in the spinal cord of G93A mutant SOD1 transgenic mice with caspase-3 localised in those neurones which exhibit apoptotic features, and over-expression of Bcl2 delays this caspase activation (Vukosavic et al., 2000). Furthermore, mitochondrial-dependent apoptosis is activated in ALS: Bax and cytochrome C translocation occurs in the spinal cord of G93A mutant SOD1 transgenic mice. Cytochrome C is translocated out of the mitochondria, activating caspase-9, which then leads to activation of downstream effector caspases; caspase-3 and -7. In this study (Guegan et al., 2001), the authors also demonstrated that X-chromosome linked inhibitor of apoptosis protein (XIAP) is cleaved and consequently inactivated.

This link with apoptosis is also implicated in two studies which both demonstrate that inhibitors of apoptotic proteins have beneficial effects in mouse models of the disease. Expression of a dominant negative form of ICE in G93R mutant SOD1 transgenic mice slows disease progression (Friedlander et al., 1997), and pharmacological inhibition of caspase activity using N-benzyloxycarbonyl-Val-Asp-fluoromethylketone (zVAD-fmk), a broad range caspase inhibitor, delays disease onset and prolongs lifespan in G93A mutant SOD1 transgenic mice (Li et al., 2000).

Activation of apoptosis has been demonstrated in ALS patients as well as in mutant SOD1 transgenic mice. One of the hallmarks of apoptosis, DNA fragmentation, has been observed in CNS regions of ALS cases, together with

increases in both caspase-3 and the pro-apoptotic Bax and Bak in the mitochondria (Martin, 1999). Prostate apoptosis response-4 (Par-4), a protein induced in prostate cancer cells and neuronal apoptosis, is also increased in the spinal cord MNs of ALS patients (Pedersen et al., 2000).

Despite this huge body of evidence, which together demonstrates that the apoptotic process is activated in ALS, a report by (Migheli et al., 1999) demonstrated a lack of apoptosis in G93A mutant SOD1 transgenic mice. No DNA fragmentation has been observed in the MNs of these mice and immunohistochemical studies revealed no neuronal staining with antibodies specific for apoptosis-related proteins, e.g. activated caspase-3.

Axonal transport and motor proteins

Axonal transport has been implicated in ALS and related neurodegenerative diseases. The slowing of axonal transport is an early pathological feature in both G37R and G85R mutant SOD1 transgenic mice (Williamson and Cleveland, 1999). In CMT disease type II mutant NFs inhibit axonal transport of both NFs and mitochondria in cultured cortical and dorsal root ganglion neurones (Brownlees et al., 2002).

More recently, dynein, a specific component of axonal transport, has been linked to ALS (LaMonte et al., 2002, Hafezparast et al., 2003, Puls et al., 2003). Dynein, a motor protein responsible for retrograde transport along microtubules (MTs), has multiple cellular functions, including endoplasmic reticulum (ER) to Golgi trafficking and mitotic spindle assembly, but as yet is the only known motor protein which has been shown to play a role in retrograde transport in neurones. Dynein is activated by a multiprotein complex called dynactin and in mice over-expression of the dynamitin subunit of dynactin

renders dynactin non-functional, thereby reducing retrograde axonal transport. This leads to degeneration of MNs and development of an ALS-like phenotype in these mice (LaMonte et al., 2002). Mutations in dynein and related proteins have now been reported to cause MN disorders. Hafezparast et al. (2003) reported that mutations in the heavy chain of dynein perturb its neuron-specific functions and lead to progressive MN degeneration in mice. Puls et al. (2003) have identified a mutation in the gene encoding a subunit of dynactin in a family with slow progressing autosomal-dominant lower motor neuron disease. It is also possible that NF accumulations, a common feature of ALS pathogenesis (Carpenter, 1968), may be linked to disruptions in the axonal retrograde transport machinery.

Growth factor involvement in ALS: vascular endothelial growth factor

Given that vascular endothelial growth factor (VEGF) controls the growth and permeability of blood vessels, it is somewhat surprising that a link between VEGF and ALS has been observed. VEGF is rapidly up-regulated in response to changes in oxygen levels. Through their binding to the hypoxia response element in the VEGF promoter, hypoxia-inducible factors are essential in this response. Impaired hypoxic regulation of VEGF has been shown to be a risk factor for ischemic heart disease (Schultz et al., 1999). Following on from this, Oosthuyse et al., (2001), created mice with targeted deletion of the hypoxia response element; decreasing baseline and hypoxic induction of VEGF, in order to study the relevance of hypoxic regulation of this growth factor in ALS. These mice developed severe adult onset muscle weakness due to degeneration of lower MNs; symptoms which resemble ALS.

To determine whether VEGF has a role in MN degeneration, a large European study was carried out (Lambrechts et al., 2003). Although they did not find any sequence variations in the hypoxia response element of the VEGF gene, they identified three single nucleotide polymorphisms in the promoter region, which conferred a greater susceptibility to ALS. These 'at-risk' haplotypes were associated with both reduced VEGF expression and levels of circulating VEGF. Lambrechts et al., (2003), also demonstrated that reduced levels of VEGF in G93A mutant SOD1 transgenic mice exacerbate disease progression and furthermore, that VEGF protects mice against ischemic MN death.

These results strongly implicate VEGF as an 'at-risk' factor in ALS. However, it still remains to be determined whether chronic vascular insufficiency is a general contributor to ALS, whether VEGF acts as a neurotrophic factor for MNs and whether other hypoxia-inducible neurotrophic factors are involved in MN survival. It is also possible that VEGF could be used therapeutically to slow the onset and progression of MN degeneration in ALS. Indeed, a recent study has shown that retrograde viral delivery of VEGF in G93A mutant SOD1 transgenic mice delays both disease onset and progression (Azzouz et al., 2004). This effect was seen even when VEGF treatment was initiated at the time of disease onset. These results are extremely promising as disease onset occurs prior to the appearance of clinical symptoms and this approach has great potential in the treatment of human ALS.

Growth factor involvement in ALS: neurotrophic factors

Ciliary neurotrophic factor (CNTF) is an important survival factor for MNs. Disruption of the CNTF gene causes MN degeneration (Masu et al., 1993) and

reduced levels of CNTF have been reported in post-mortem ALS patient tissue (Anand et al., 1995). Furthermore, it was reported that a 25 year-old patient, who died from FALS carried a null mutation in the CNTF gene as well as a V148G mutation in the SOD1 gene (Giess et al., 2002). When G93A mutant SOD1 transgenic mice were crossed with CNTF deficient mice the resultant progeny, carrying mutations in both the SOD1 and CNTF genes, exhibited earlier disease onset and increased MN loss, compared to mice carrying only the mutant SOD1 gene (Giess et al., 2002). Based on these findings, it has been hypothesised that CNTF is a modifier gene in mutant SOD1 linked FALS.

However, Takahashi et al., (1994), reported that null mutations in CNTF are observed in healthy individuals as well as those with neurological disorders. A similar result was presented by Al-Chalabi et al., (2003). Two groups of patients with SALS and a group with mutant SOD1-linked FALS were studied and no difference in either disease onset or progression was noted for three CNTF phenotypes. Collectively these data suggest that CNTF does not influence ALS.

In addition to CNTF, there are other trophic factors which support MNs and may be involved in ALS pathogenesis. One of these is insulin growth factor-1 (IGF-1); retrograde viral delivery of IGF-1 has been shown to be beneficial in a mouse model of ALS (Kaspar et al., 2003). Glial cell line-derived neurotrophic factor (GDNF) was also tested using this method, but was less effective than IGF-1. The latter growth factor delays MN death, decline of motor function and prolongs survival, whether delivered prior to or at the time of disease onset. This study not only provides evidence of the beneficial effect of IGF-1, but also that specific targeting of MNs via this method could be utilised further in the treatment of the disease.

Microglia and inflammation

In ALS patients, microglia activation and proliferation occurs in regions of MN loss (Kawamata et al., 1992). Microglia mediate neuroinflammation and are activated in response to CNS injury. This affects neurons and macroglia (astrocytes and oligodendrocytes) via the release of cytokines and pro-inflammatory factors. Compared to non-diseased controls, increased levels of pro-inflammatory prostaglandin PGE2 have been reported in ALS cerebrospinal fluid, (Almer et al., 2002). Cyclo-oxygenase-2 (COX-2); a pro-inflammatory enzyme, and the number of activated microglia are also up-regulated in the spinal cord of ALS patients, compared to control samples (Yasojima et al., 2001).

Similar findings have been reported in mutant SOD1 transgenic mice. In 2001, Alexianu et al. demonstrated up-regulation of intercellular cell adhesion molecule-1 (ICAM-1), neuronal immunoglobulin G (IgG) deposits and microglial and astrocytic activation occur sequentially during disease progression of G93A mutant SOD1 transgenic mice. This suggests that up-regulation of pro-inflammatory factors occurs during the pre-symptomatic stages of the disease and is followed by expansion of immune activation; mechanisms which may contribute to disease progression. Cytokines are secreted by activated microglia and astrocytes and may have a role in MN dysfunction. Some cytokines, including TNF-α, are also up-regulated in G93A mutant SOD1 transgenic mice, while others, including interleukins-3 and –6 (IL-3 and –6), are not (Elliott, 2001). Furthermore, TNF-α, in concert with peripherin over-expression is required in order to cause death of cultured MNs (Robertson et al., 2001). Increased COX-2 immunoreactivity is seen in G93A mutant SOD1 transgenic mice (Almer et al., 2001), in both early symptomatic and end stage of the

disease, and a DNA microarray study (Olsen et al., 2001), following gene expression over disease course in G93A mutant SOD1 transgenic mice, has shown that microglia and astrocytic activation are coincident with disease onset.

So although the precise mechanisms and pathways involved remain to be determined, there is strong evidence suggesting an inflammatory role in ALS pathogenesis. This is further strengthened by the use of COX-2 as a therapeutic target. Inhibition of COX-2 has been shown to delay onset of motor dysfunction in G93A mutant SOD1 transgenic mice (Pompl et al., 2003). Also, minocycline, which inhibits microglial activation and reduces inflammation, delays the onset and slows progression of disease in G37R mutant SOD1 transgenic mice (Kriz et al., 2002).

Protein aggregation

Proteinaceous aggregates, or inclusions, are a common neuropathological feature of many neurodegenerative diseases, including ALS, Parkinson's, polyglutamine diseases, such as Huntington's, SBMA, and Alzheimer's. A report by Johnston et al., (1998), characterised aggregate/inclusion formation. Aggregation of protein occurs when the capacity of the proteasomal degradation machinery is saturated; either by increased expression of substrates or decreased proteasomal activity. They suggest that, once formed, these aggregates (or inclusions) are delivered, via retrograde transport on microtubules (MTs), to a Ub-containing structure at the MT organising centre (MTOC). Here, they are ensheathed in IF protein, this structure being termed an aggresome. Johnston et al., (1998), propose that aggresome formation is a general cellular response to the accumulation of un-degraded and aggregated protein. However, it is not known whether these aggregates/inclusions

themselves are either toxic, thus contributing to neurodegeneration in these diseases, or whether they comprise a cellular defence mechanism; acting as a 'sink' where potentially toxic molecules are sequestered. This is discussed by (Tran and Miller, 1999), and appears to be dependent on the disease in question. Lewy bodies in Parkinson's disease (intracytoplasmic inclusions with a dense eosinophilic core and pale surrounding halo) are thought to have a causative role in the disease, whereas the nuclear inclusions observed in the polyglutamine diseases are thought to have a protective role (Arrasate et al., 2004).

In ALS, inclusions are generally considered to contribute to neurodegeneration. Another possible mechanism for mutant SOD1-mediated toxicity is that mutant SOD1 is mis-folded and consequently more prone to aggregation, resulting in the formation of toxic inclusions. Mutations in SOD1 occur throughout all 5 exons, suggestive of altered protein conformation; X-ray crystallography has shown that conformation of the active site is indeed altered in mutant SOD1 (Deng et al., 1993). Over-expression of mutant but not wt SOD1 in primary neuronal cultures leads to inclusion formation and such inclusions are toxic, resulting in cell death (Durham et al., 1997). Intracytoplasmic, SOD1-containing inclusions are observed in MNs and astrocytes of G85R mutant SOD1 transgenic mice (Bruijn et al., 1998), and in spinal cord samples from FALS patients (Shibata et al., 1996). If these inclusions are themselves toxic, this could be exerted in a variety of ways: firstly, they could co-aggregate with other proteins, depleting the cell of essential components; secondly, they could burden the ubiquitin proteasome system (UPS), (as shown by Bence et al., 2001), preventing degradation of other proteins (of particular importance in this case are regulatory proteins, for

example cyclins and transcription factors), and thirdly, they could also disrupt axonal dependent MT transport.

Chaperone proteins facilitate in the refolding of proteins, and this may be a key factor in the ability of cells to defend themselves against aggregation of mutant SOD1. In a report by Bruening et al., (1999), chaperone proteins were shown to be up-regulated in cells and tissues containing mutant, but not wt, SOD1. However, this up-regulation was not observed in the spinal cord of mutant SOD1 transgenic mice. This led to the hypothesis that mutant, mis-folded SOD1, present within a cell is likely to divert chaperone proteins towards trying to refold it. This could have a detrimental affect on the cell, as the chaperones are diverted away from the refolding of other proteins, leading to more aggregation, thus rendering the cell more susceptible to other stresses, both physiological and environmental. Such stress could contribute to dysfunction and death. Most cells are able to up-regulate chaperones, so the mutant SOD1 would not create such a problem. However, it may be the case that MNs are deficient in the ability to up-regulate chaperones in response to stress. They are also already exposed to the physiological stress of a high excitatory input, due to their role in relaying electrical impulses and effecting muscle movement, and this adds to the overall burden. This hypothesis also goes some way to explaining the selective vulnerability of MNs in ALS. In order to test this hypothesis, Bruening et al., (1999), co-injected heat shock protein (HSP) 70 and mutant SOD1 into cultured primary MNs. This resulted in a decrease in the number of cells containing mutant SOD1 inclusions and prolonged cell survival.

Mutant SOD1 from NIH3T3 cell extracts and G93A mutant SOD1 transgenic mice spinal cord extract is detergent insoluble, and chaperone

proteins, namely HSPs 70, 40 and αB-crystallin, co-immunoprecipitate with mutant SOD1 from NIH3T3 cells (Shinder et al., 2001). Again, it has been suggested that mutant SOD1 inclusions may result from an inadequate stress response. Indeed, MNs have a high threshold for induction of the stress response, (an overview of this follows in a later section, The heat shock response). Takeuchi et al., (2002), have shown that mutant, but not wt, SOD1 induces inclusion formation, fewer neurites and cell death in a neuroblastoma (Neuro2a) cell line. This supports the hypothesis that inclusion formation contributes to cellular dysfunction in neurodegenerative disease. Over-expression of HSPs 70 and 40 suppresses aggregation of mutant SOD1, promotes neurite outgrowth and suppresses cell death in this same cell line.

More recently, Kieran et al., (2004), reported that up-regulation of HSPs in a mouse model of ALS increases the life expectancy of these animals. Here, arimoclomol, a drug which acts as a co-inducer of HSPs, was used to treat G93A mutant SOD1 transgenic mice. This treatment resulted in a 22% increase in lifespan, due to an improvement in muscle function and increased MN survival. HSPs have also been shown to be protective in other neurodegenerative diseases. Using a *Drosophila melanogaster* model of polyglutamine disease, (Warrick et al., 1999), showed that directed expression of HSP 70 suppressed polyglutamine mediated neurodegeneration. Over-expression of HSPs 70 and 40 reduced aggregate formation and suppressed apoptosis in a neuronal cell model of SBMA (Kobayashi et al., 2000). Spinocerebellar ataxia type 1 (SCA1) is another example of a polyglutamine disease. High levels of HSP 70 in SCA1 transgenic mice were shown to suppress neuropathology and improve motor function (Cummings et al., 2001).

The data discussed above show that chaperone proteins play an important role in protein aggregation in neurodegenerative diseases. Up-regulation of chaperone proteins suppresses aggregate formation in both cell and animal disease models. Also, it has recently been shown that mutations in some chaperone proteins, namely HSP 27 (Evgrafov et al., 2004) and HSP 22 (Irobi et al., 2004), are linked to neurodegenerative diseases, namely CMT disease and distal hereditary motor neuropathy.

Chaperone proteins

All cells and organelles possess chaperone proteins whose function is to support the correct folding of proteins during translation, translocation and periods of stress (Buchner, 1996, Hartl and Hayer-Hartl, 2002). In order to perform this role, chaperones differentiate between native and non-native (i.e. mis-folded) forms of the target protein. They act by binding un- and mis-folded polypeptides, decreasing the probability of irreversible interactions of exposed hydrophobic regions and consequently allowing the folding and maintenance of protein structure under non-permissive conditions. Such binding is regulated by adenosine triphosphate (ATP)-induced conformational changes in the substrate-binding domain. Chaperones themselves do not convey specific information for the folding of the target protein, but instead support correct structure by the prevention of aberrant interactions with un- or mis-folded proteins within the cell which, in the absence of this surveillance mechanism, may lead to aggregation and inclusion formation (Buchner, 1996, Hartl and Hayer-Hartl, 2002). As well as this role in maintaining the correct folding of protein during translation, translocation and stress, chaperones have other cellular functions, including: (a) translocation of proteins across membranes (b)

macromolecular assembly and disassembly (c) transfer of un- and mis-folded protein to the proteasome for degradation (d) acting as important components of signal transduction pathways involved in the stress response. These proteins also influence the cell's cytoskeleton, facilitating the formation of cytoskeletal elements and performing different, but co-operative roles in regulation of cytoskeletal function (Perng et al., 1999a).

In recent years, most classes of HSPs have been identified as molecular chaperones (Buchner, 1996). HSPs are divided into the following families, according to their function, structure and size: small HSPs (sHSPs); HSP60; HSP70; HSP90 and HSP100. sHSPs are an abundant and ubiquitous family of proteins involved in the stress response. They have molecular weights of between 12 and 40kDa and mammalian sHSPs form oligomeric structures of approximately 32 subunits, corresponding to a molecular weight 800kDa (Arrigo et al., 1988). All sHSPs are characterised by a conserved core α-crystallin domain of between 80 and 100 amino acids, in the C-terminal region of the protein (deJong et al., 1988). The expression of these proteins is increased under heat shock conditions, and like other chaperones, sHSPs recognise and bind denatured protein, thus preventing the formation of aggregates independently of ATP (Jakob et al., 1993). A report by Lee et al., (1997), proposed that other molecular chaperones recognize sHSP-substrate complexes and then actively participate in the refolding of the substrate: energy-independent sHSPs trap non-native proteins during stress conditions, thus protecting them from aggregation. Under permissive conditions, these energy-dependent chaperones can then complete the refolding of this reservoir of folding-competent protein. Thus, sHSPs prevent rapid protein aggregation by the initiation of binding events while other chaperones primarily refold non-

native protein. sHSPs also undergo specific interactions with the cytoskeleton, preserving cell shape and integrity (Perng et al., 1999a)

Mutations in sHSPs affect their function and these have been linked to various diseases (Clark and Muchowski, 2000). The R120G mutation in the sHSP αB-crystallin causes structural alteration, which leads, indirectly to limited functioning (Bova et al., 1999, Perng et al., 1999b, Chavez Zobel et al., 2003), and this has in turn been linked to the cardiovascular disorder, desmin-related myopathy (DRM) (Perng et al., 1999b). Recently, two reports have linked mutations in sHSPs to neurodegenerative diseases (Irobi et al., 2004, Evgrafov et al., 2004). Both mutation of K141 in HSP 22 (Irobi et al., 2004), and S135 in HSP 27 (Evgrafov et al., 2004) lead to structural instability, as these residues are located in the core α-crystallin domain.

The heat shock response

An evolutionarily conserved and cytoprotective mechanism – the heat shock response – is mediated in response to stress by increasing levels of transcription of genes encoding HSPs. (For a review, see Morimoto et al., 1997). As a type of chaperone protein, both stress induced and constitutively expressed HSPs facilitate nascent protein folding, and re-folding or degradation of un- or mis-folded protein. In eukaryotic systems, the action of HSPs is mediated by binding of heat shock transcription factors (HSFs) to heat shock elements (HSEs), on the promoters of HSPs. Up-regulation of HSPs, due to environmental and physiological stresses, occurs primarily via the action of heat shock factor 1 (HSF1) (Morimoto et al., 1998). In neural cells, HSPs protect against hyperthermia, oxidative stress, ischemia and excitotoxicity (Rordorf et al., 1991, Uney et al., 1993, Yenari et al., 1998).

As previously discussed, one proposed mechanism for disease pathogenesis in ALS is structural changes arising in SOD1 resulting from mutations, which lead to altered solubility and aggregation. Gene transfer of HSP 70 in a cell culture model of ALS protects against mutant SOD1 aggregation (Bruening et al., 1999). This raised the question as to whether MNs are able to initiate a sufficient heat shock response in response to stresses such as protein aggregation. A study carried out by the same research group, (Batulan et al., 2003), investigated the endogenous heat shock response in MNs and showed that these cells do in fact have a high threshold for response. Glia, but not MNs, from spinal cord cultures, up-regulate HSP 70 in response to heat shock. MNs also failed to up-regulate HSP 70 in response to other stresses, including glutamate excitotoxicity and mutant SOD1. Similar findings were observed in mutant SOD1 transgenic mice and ALS patients. Like HSP 70, αB-crystallin and HSP 27, although present in the cytoplasm of MNs, are not up-regulated after subjection to stress treatments *in vitro*, in either mutant SOD1 transgenic mice or in spinal cord extracts from ALS patients.

Exposure of MNs to heat shock would be expected to activate heat shock gene expression via HSF1 (Morimoto, 1998). Inactive HSF1 is either a cytoplasmic monomer (Morimoto and Santoro, 1998), or present in nuclear granules (Jolly et al., 2002). In stressed cells, containing insufficient levels of HSPs, HSF1 trimerises and binds HSEs. Multiple phosphorylation then causes conformational changes, finally resulting in the recruitment of transcription machinery and transcription of heat shock genes (Morimoto and Santoro, 1998). Therefore, deficiency of HSP induction in MNs could occur at any of these levels. MNs have been shown to express both of the major HSFs: HSF 1 and 2 (Batulan et al., 2003). It may be that the levels of these are insufficient to mount

a heat shock response. However, even after micro-injection of a plasmid encoding HSF1, no increase in HSP 70 expression was detected after heat shock. This implies that this impaired ability of MNs may be due to an inability to activate HSF1 (Batulan et al., 2003).

Recently it has been shown that treatment of G93A mutant SOD1 transgenic mice with a co-inducer of HSPs delays disease progression (Kieran et al., 2004). Arimoclomol is a hydroxylamine derivative of bimoclomol, which acts as a co-inducer of HSP expression (Vigh et al., 1997). Treatment of these G93A mutant SOD1 transgenic mice with this drug resulted in improved muscle function and elevated MN survival, giving rise to a 22% increase in lifespan. This family of molecules, of which arimoclomol and bimoclomol are members, has been shown to mediate their affects by prolonging activation of HSF1 (Hargitai et al., 2003). So, although MNs have an impaired ability to activate HSF1 (Batulan et al., 2003), therapeutic intervention with a drug that activates the heat shock response and subsequent up-regulation of HSPs, via prolonging activation of HSF1, may allow this deficiency of MNs to be overcome.

The ubiquitin proteasome system

The UPS is a highly complex and tightly regulated protein degradation system. It consists of a 26S proteasome complex: a large, multi-catalytic protease made up of 2 sub-complexes: a 20S core catalytic particle and a 19S regulatory particle. The proteasome not only serves as a mechanism for the degradation of mis-folded, unassembled or damaged proteins, but it is also able to carry out limited proteolysis and post-translational processing (e.g. the proteasome processes major histocompatibilty (MHC) class I antigens and generates active

subunits of the transcriptional regulator NF-κB from larger, inactive precursors (Ciechanover and Brundin, 2003).

Polyubiquitin acts as a degradation signal in the UPS. The process of polyubiquitination occurs as follows, via a system of different enzymes: firstly, Ub activating enzyme; E1, activates Ub. Secondly, Ub conjugating enzyme; E2, transfers the activated Ub to the substrate protein, which itself may be bound by Ub-protein ligase; E3. E3s are the specific substrate recognition factors of the UPS. Next, a poly-Ub chain is formed, via the processive transfer of Ub to the lysine 48 residue of the previous Ub moiety. This polyubiquitinated substrate protein is then recognised by the 19S regulatory particle which results in the protein being unfolded prior to degradation by the proteasome. This process requires ATP and releases free, reusable Ub (Ciechanover and Brundin, 2003).

The UPS and ALS

The presence of Ub-containing inclusions is frequently observed in many neurodegenerative diseases. It may be that these inclusions arise as a result of failed attempts by the UPS to degrade damaged and abnormal proteins. However, it is also possible that they are formed as a protective mechanism, removing the soluble fraction of aggregated protein which may be toxic. It is probable that the reasons for the presence of these Ub-containing inclusions are disease specific. A report by Bence et al., (2001), demonstrated that aggregated proteins can inhibit the UPS. This complicates matters, as aggregated proteins are simultaneously inhibitors of the UPS and the products resulting from its inhibition. An increase in protein aggregation would inhibit UPS activity which in turn leads to further increases in protein aggregation, and so on. This positive feedback mechanism may have a role in the loss of

neuronal function which characterises the progression of many of these neurodegenerative diseases.

As already discussed, in FALS, 20% of patients have mutations in SOD1. Mutant SOD1, again, as already discussed, is more prone to mis-folding, leading to formation of inclusions. Mutant SOD1 inclusions in mouse models and human FALS patients have been shown to contain Ub (Bruijn et al., 1998). This implicates a role for the UPS in ALS disease pathogenesis. Mutant SOD1 is less soluble than wt SOD1 and forms high molecular weight complexes in non-neuronal cells. The amount of these non-native oligomers is further increased by inhibition of the UPS. Non-native oligomers are also observed in mutant SOD1 transgenic mice (Johnston et al., 2000).

Over-expression of an E3 ligase, dorfin, has been shown to prevent cell death induced by mutant protein, presumably by promoting its degradation via the UPS (Niwa et al., 2002). Furthermore, dorfin expression has been shown to be elevated in the spinal cord of ALS patients (Ishigaki et al., 2002) and is present in inclusions in cases of both FALS and SALS (Niwa et al., 2002).

The report by Bence et al., (2001), demonstrated UPS inhibition by aggregated protein and there is evidence for this also occurring in ALS. Urushitani et al., (2002), have shown that the presence of mutant mis-folded SOD1 reduces the catalytic activity of the UPS in a neuroblastoma cell line. Furthermore, this is not due to incorporation of proteasome components into inclusions, as occurs in some other neurodegenerative diseases (Cummings et al., 1998). Urushitani et al., (2002), also proposed a model of disease pathogenesis in ALS: mutant, mis-folded and polyubiquitinated SOD1 overloads the UPS, leading to its further accumulation. Such accumulation will have an affect on the normal functioning of SOD1 i.e. it will cause impairment of the

defence mechanisms that protect against oxidative stress. As a consequence of this, the increased stress may cause further mis-folding of proteins, including mutant SOD1, thereby exacerbating the substrate overload on the UPS even further. All this results in a self-perpetuating cycle occurring within the cell.

Is it possible that MNs are particularly vulnerable to UPS inhibition? It is MNs that are selectively affected in ALS, and, compared to non-neuronal cells, cultured MNs show a significant decrease in viability in the presence of the proteasome inhibitor lactacystin (Urushitani et al., 2002). However, despite the data discussed above, the role of protein aggregation and the UPS in ALS remain unclear.

Aims of the study

This chapter has discussed the wide range of contributing factors in the disease pathogenesis of ALS, both in mouse models of the disease and ALS patients. One of the major hypotheses for the cause of mutant SOD1-linked FALS, is protein aggregation. Mutant SOD1 is mis-folded and consequently prone to aggregation, leading to the formation of SOD1 positive inclusions that are observed in a number of mouse models and diseased human tissue. As discussed above, chaperone proteins, which are involved in protein folding, as well as the UPS, responsible for the degradation of mis-folded and damaged proteins, are both closely linked to protein aggregation in neurodegenerative diseases such as ALS. MNs, which are selectively affected in ALS, may be deficient in their ability to up-regulate chaperones and/or more susceptible to disruption of the UPS. I have chosen to investigate further the role of chaperone proteins, more specifically sHSPs, in mutant SOD1-linked FALS. A model cell system of mutant SOD1 inclusion formation has been established, whereby over-expression of G85R mutant SOD1 and subsequent treatment with proteasome inhibitor in HEK293 cells leads to inclusion formation. These inclusions have been shown, by IMF microscopy, to contain both components of the UPS and chaperone proteins. The results are presented in chapter 3. Co-expression of sHSPs in this model system have been shown to influence G85R mutant SOD1 inclusion formation: co-expression of wt sHSPs decreases the amount of insoluble mutant SOD1, whereas mutant sHSPs further increase the amount of insoluble mutant SOD1. Co-expression of mutant sHSPs increases the insolubility of wt SOD1, which, in this system is soluble under normal conditions. The increase in insoluble mutant SOD1 appears to increase the viability of these cells. These data are presented and discussed in chapter 4.

Chapter 5 addresses the *in vitro* interactions of SOD1 with sHSPs. Three different methods have all shown that there is no such interaction. Chapter 6 addresses parallel studies carried out in a neuronal cell line, Neuro 2a (N2a) cells. Such a model cell system is better suited to these studies, as MNs undergo selective degeneration in ALS. However, the transfection rate in this cell line is very low, making studies difficult and at present the results obtained remain inconclusive.

CHAPTER 2
MATERIALS AND METHODS

Chemicals

All chemicals used were of analytical grade and, unless otherwise stated, purchased from either VWR (Lutterworth, UK) or Sigma Aldrich (Poole, UK).

Cell Culture

The following cell lines were used: human embryonic kidney (HEK293) cells, human lens epithelial (H36CEI) cells, breast cancer (MCF7) cells, human astrocytoma (U373MG) cells, mutant H36CEI (mH36) cells, neuroblastoma x spinal cord hybrid (NSC34) cells and mouse neuroblastoma Neuro2A cells.

HEK293, H36, MCF7, U373MG and Neuro 2A cells were obtained from the European Collection of Cell Cultures (ECACC, Porton Down, UK). mH36 cells were obtained from a cataract patient. NSC34 cells were a gift from Professor Pam Shaw (University of Sheffield). All cell lines, excluding NSC34 and n2a cells, were cultured in Dulbecco's Modified Eagle Medium (DMEM) supplemented with 10%(v/v) foetal calf serum (FCS) 2mM L-glutamine and antibiotics ($100Uml^{-1}$ penicillin and $100\mu gml^{-1}$ streptomycin), at 37°C in a humidified atmosphere of 5%(v/v) CO_2. In general, cells were grown in 75 cm^2 flasks, 9cm diameter culture dishes or 6-well plates (Greiner Bio-One). The cells were grown to 80-90% confluence, prior to subculture. Cells were washed twice with phosphate buffered saline (PBS) and then 2 ml trypsin-EDTA solution (0.05% (w/v) trypsin, 0.02% (w/v) EDTA) was added and the cells incubated until they had detatched and rounded up; this normally takes approximately 5 min. The cell suspension was diluted 1:10 with pre-warmed medium, which was supplemented with more media so as to cover the bottom of the culture vessel.

NSC34 cells were grown as above but were subcultured at 60-70% confluence by trituration with 10ml pre-warmed medium and then seeding new 75 cm^2 flasks with $1.5x10^5$ cells and adding sufficient pre-warmed media to cover the bottom of the flask. Neuro 2A cells were grown as above but cultured in Modified Eagle Medium (MEM) supplemented with 10%(v/v) FCS, 2mM L-glutamine, ImM sodium pyruvate and antibiotics ($100Uml^{-1}$ penicillin and $100\mu gml^{-1}$ streptomycin),

Cell Transfections

For transient transfections, plasmid DNA was prepared using MaxiPrep kits (Qiagen). Samples were then run on agarose gels to check the quality of the DNA (see below for an example).

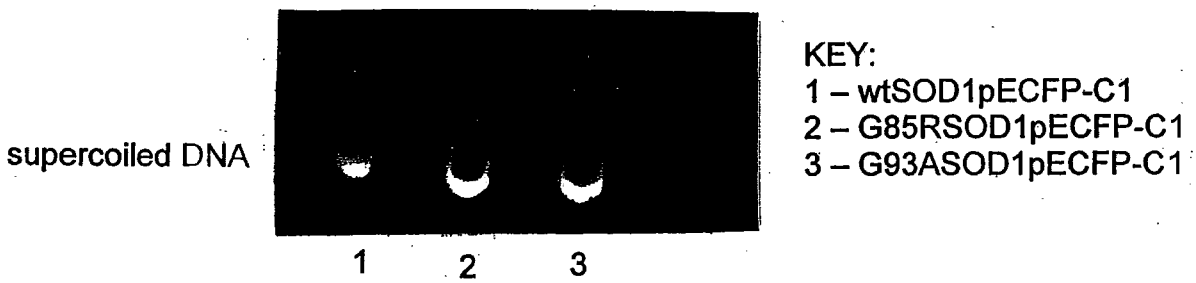

Cells were seeded onto either 6-well plates or 9 cm diameter culture dishes, and at a confluence of ≥50%, were transfected with GeneJuice (Novagen), a lipid based system. This method involved combining 3µl GeneJuice with 100µl serum-free (DMEM). This was allowed to stand for 5 min before the adding dropwise to 1.5µg maxiprep DNA. This solution was incubated at room temperature for 15 min and then added dropwise to the cells.

Cells were then grown as described previously for up to 48 hr prior to further processing. In the case of proteasome inhibitor treatment, ALLN (N-Acetyl-Leu-

Leu-Nle-CHO) (Calbiochem), was added to a final concentration of 6.25μgml^{-1} at specific time intervals following transfection.

Cell Viability Assays

Cell viability assays were carried out using CellTiter96 AQ_{ueous}One Solution Cell Proliferation Assay (Promega), according to the manufacturers instructions. This colourmetric assay measures the quantity of formazan, which is directly proportional to the number of living cells.

Cell Extractions

Cells were washed twice with phosphate buffered PBS.To obtain a total protein cell extract, cells were taken up into cell extraction buffer (0.5M Tris-HCl pH8, 0.5M EDTA, 10%(w/v) SDS, 1%(v/v) protease inhibitor cocktail). The lysate was then boiled for 5 min and dissolved in 2x Laemmli's sample buffer (2x LSB) (Laemmli, 1970).

To obtain soluble and insoluble cell fractions, cells were taken up into cell homogenisation buffer (3M KCl, 0.01%(v/v) Triton X-100 and 1%(v/v) protease inhibitor cocktail in Tris buffered saline (TBS)). Cell lysates were homogenised using a Dounce homogeniser, before centrifugation at 10000 rpm (g_{av} – 10600g), for 15 min at 4°C. The pellet fraction (P1) was washed once in TBS containing 5mM EDTA before dissolving in 2x LSB. A sample of the supernatant (SN) fraction (SN1) was added to an equal volume of 2x LSB and the remainder subjected to high speed centrifugation; 40000 rpm (g_{av} – 106000g) 30 min at 4°C in a Beckman TLS55 rotor. This resulted in SN2 and P2; SN2 was added to an equal volume of and P2 dissolved in 2x LSB.

Prior to addition of 2x LSB, protein concentrations were determined using the BCA Protein Assay (Pierce), according to the manufacturers instructions.

Electrophoresis

Proteins (between 10 and 50µg) were separated by SDS-PAGE under reducing conditions, essentially as described previously (Laemmli, 1970), using Mini Gel equipment (BioRad Mini Protean II). Protein samples were loaded onto 12%(w/v) bis-acrylamide gels and run at 200V for approximately 45 min until the dye front had reached the bottom. After electrophoresis gels were either stained or blotted (see below).

Coomassie staining: gels were stained for 5-10 min in Coomassie stain (0.5%(w/v) R250 Coomassie brilliant blue, 50%(v/v) methanol, 10%(v/v) acetic acid), destained by several changes of destain (10%(v/v) methanol, 5%(v/v) acetic acid) and the protein bands visualised and recorded, using a Fujifilm LAS-1000 Intelligent Dark Box II running IR LAS-1000 Pro version 2.11 software.

Sypro staining: gels were fixed for 30 min (50%(v/v) ethanol, 10%(v/v) acetic acid), stained overnight with Sypro Ruby (Molecular Probes) and then destained for 30 min (10% methanol, 7% acetic acid). Gels were then viewed under UV light for visualisation and recording (see previous paragraph).

Western Blotting

Western blotting was performed using the semi-dry method as described by Kyhse-Anderson, (1984), using a BioRad Trans Blot SD Semi Dry Transfer Cell. 12%(w/v) polyacrylamide mini-gels (see section 2.6) were transferred to nitrocellulose membranes for 1 hr at $0.8mAcm^{-2}$. Membranes were washed in

deionised water, stained with Ponceau S for 5 min and destained with TBS after visualisation and recording if necessary. Membranes were then blocked and stained using either the BSA or milk method (see below).

The BSA method: membranes were blocked overnight at 4°C in blocking buffer (5% (w/v) BSA in TTBS (TBS containing 0.2% (v/v) Tween)). Primary and secondary antibodies were diluted in 1% (w/v) BSA in 1:1 TTBS:TBS and incubated for 1 hr at room temperature on a shaking platform. Membranes were washed five times, each for 5 min, in TTBS following the primary and TBS following the secondary antibody incubation. Antibodies were detected by enhanced chemiluminescence (ECL) (Amersham) using a Fujifilm LAS-1000 Intelligent Dark Box II running IR LAS-1000 Pro version 2.11 software.The milk method: membranes were blocked overnight at 4°C in blocking buffer (5% (w/v) milk powder (Tesco) in TTBS). Antibodies were diluted in washing/staining buffer (3% (w/v) milk powder in TBS/TTBS (1:1); primary antibodies for 2 hr and secondary antibodies for 1 hr, all at 37°C with agitation. After each incubation, membranes were washed five times, each for 5 min, in washing/staining buffer and antibodies were detected by ECL. Details of the primary antibodies used are shown in Table 2.1. Appropriate horseradish peroxidase (HRP) conjugated secondary antibodies (Dako) were diluted 1:1000.

Immunofluoresence Microscopy

Cells to be used for IMF microscopy were seeded onto 13 mm glass coverslips in 6-well plates or LabTek chamber slides (Nunc). Cells were washed twice with PBS and fixed with 4%(w/v) paraformaldehyde in PBS for 15 min, washed twice with PBS containing 0.02%(w/v) BSA and 0.02%(w/v) sodium azide

(PBS/BSA/NaAz). They were then permeabilised with 0.5%(v/v) Triton X-100 in PBS for 5 min at 4°C. After washing twice with PBS/BSA/NaAz, cells were incubated with normal goat serum diluted 1:10 in PBS/BSA/NaAz for 20 min. Cells were then incubated with primary antibody for 1 hr, washed twice (PBS/BSA/NaAz), incubated with secondary antibody and 25ngml^{-1} DAPI (4',6-diamidino-2-phenylindole, dihydrochloride) for 1 hr and washed again PBS/BSA/NaAz). All antibodies were diluted in PBS/BSA/NaAz and incubations carried out in the dark to prevent bleaching. Primary antibodies (see Table 2.1) were detected using either Alexa Fluor594-labelled goat anti-rabbit IgG, Alexa Fluor488-labelled goat anti-mouse IgG (appropriately diluted, Molecular Probes) or TRITC (tetramethylrhodamine isothiocyanate)-labelled anti-mouse IgG. Coverslips were mounted on slides with Citifluor (Citifluor Labs), a fluorescent protective reagent and the coverslip, was sealed with clear nail varnish.

Cells were observed with a Zeiss Axioplan fluorescent microscope using 63X Plan-Apochromat 1.4N objective lens or Zeiss Axiovert 200M confocal microscope (both Carl Zeiss). Images were obtained via a cooled CCD camera (Digital Pixel Ltd) running IP Lab software for the fluorescent microscope and LSM 510 META software for the confocal microscope, and processed using Adobe Photoshop 8.

Table 2.1 Antibody Information

Human Antigen Detected	Antibody: Host Animal	Isotype	Clone	Dilution: WB	IMF	Supplier/ Reference
Vimentin	Mouse Mouse	IgG_1	V9 3052	1:1000 1:500	1:100 1:50	Sigma Quinlan (Durham)
Hsp70	Mouse	IgG_{2a}	MBH1	1:1000	1:100	(Hopwood et al., 1997)
Hsp27	Mouse Mouse	IgG_1	ERD5 G3.1	1:1000 1:500	1:100 1:50	(King et al., 1987) ID Labs
αB-crystallin	Mouse Rabbit		2D2B6 3148	1:10 1:400	1:1 1:40	(Sawada et al., 1993) Quinlan (Durham)
SOD1	Mouse Rabbit	IgG_1	30F11	1:500 1:1000	1:50 1:100	Novocastra The Binding Site
SC35	Mouse				1:1000	Sigma
SP10	Mouse				1:1000	Prescott (Duncee)
Dorfin	Rabbit				1:100	(Niwa et al., 2001)
Ubiquitin	Mouse	IgG_1	P4D1		1:100	Cell Signalling Technology

WB – Western Blotting, IMF – immunofluorescence

Molecular Cloning

Cloning SOD1 into pET23b (CN Biosciences):

SOD1pBSKS(-) was used as a template in a PCR reaction (see Table 2.2) with the following primers: forward primer – 5'-GTACATATGGCCACGAAGGCCGTGTGCGTGC-3'; reverse primer – 5'-GAATTCTTATTGGGCGATCCCAATTACACC-3', in order to introduce an NdeI site into the SOD1 construct. The resultant PCR fragment was directly ligated into the pTOPO vector system (Promega) according to the manufacturers instructions. This system allows blue white selection for insert containing colonies. DNA from positive clones was prepared using a Miniprep kit (Qiagen). The DNA was digested with NdeI and EcoRI (NEB) and the DNA run on a 1% agarose gel at 90mA for approximately 30 min. The 500bp insert band was cut

out under UV transillumination and purified using a QIAquick gel extraction kit (Qiagen). This purified insert band was then ligated into pET23b pre-digested with the same restriction enzymes (REs) using T4 DNA ligase (Roche). The ligation reactions were then transformed into the DH5α strain of *E.coli.* DNA was prepared by miniprep (Qiagen) and restriction analysis with NdeI and EcoRI used to confirm the presence of the 500bp insert prior to sending samples for full sequencing (University of Durham Sequencing Facility).

Cloning into pBUD (Invitrogen):

SOD1pECFP-C1 (prepared previously by Vilius Pigaga, University of Durham) was digested with NheI, blunted by incubation with T4 DNA polymerase (BioLine), digested with BamHI and the resultant fragment gel purified. pBUD vectors, containing wt or mutant (R120G) αB-crystalllin in the CMV site (cloned previously by Terry Gibbons, University of Durham) were digested with NotI, blunted by incubation with T4 DNA polymerase (Bioline), digested with BglII and the resultant vector band gel purified. The purified cut vector was then dephosphorylated with alkaline phosphatase (Roche) and used in a ligation reaction with the SOD1 fragment prior to transformation into the DH5α strain of *E.coli.* DNA was prepared by miniprep (Qiagen) and restriction analysis with StuI used to confirm the presence of the 500bp insert prior to sending samples for sequencing.

Table 2.2 PCR Reaction Conditions

Initial melting	94°C for 2 min
Strand separation	94°C for 1 min
Primer annealing	66°C for 1 min
Extension	72°C for 2min 30s
Number of cycles	30
Final Extension	72°C for 5 min

Map of pET23b (CN Biosciences)

pET-23a(+) sequence landmarks	
T7 promoter	303-319
T7 transcription start	302
T7•Tag coding sequence	207-239
Multiple cloning sites (*Bam*H I - *Xho* I)	158-203
His•Tag coding sequence	140-157
T7 terminator	26-72
pBR322 origin	1450
bla coding sequence	2211-3068
f1 origin	3200-3655

The maps for pET-23b(+), pET-23c(+) and pET-23d(+) are the same as pET-23a(+) (shown) with the following exceptions: pET-23b(+) is a 3665bp plasmid; subtract 1bp from each site beyond *Bam*H I at 198. pET-23c(+) is a 3664bp plasmid; subtract 2bp from each site beyond *Bam*H I at 198. pET-23d(+) is a 3663bp plasmid; the *Bam*H I site is in the same reading frame as in pET-23c(+). An *Nco* I site is substituted for the *Nde* I site with a net 1bp deletion at position 238 of pET-23c(+). As a result, *Nco* I cuts pET-23d(+) at 234, and *Nhe* I cuts at 229. For the rest of the sites, subtract 3bp from each site beyond position 239 in pET-23a(+). *Nde* I does not cut pET-23d(+). Note also that *Sty* I is not unique in pET-23d(+).

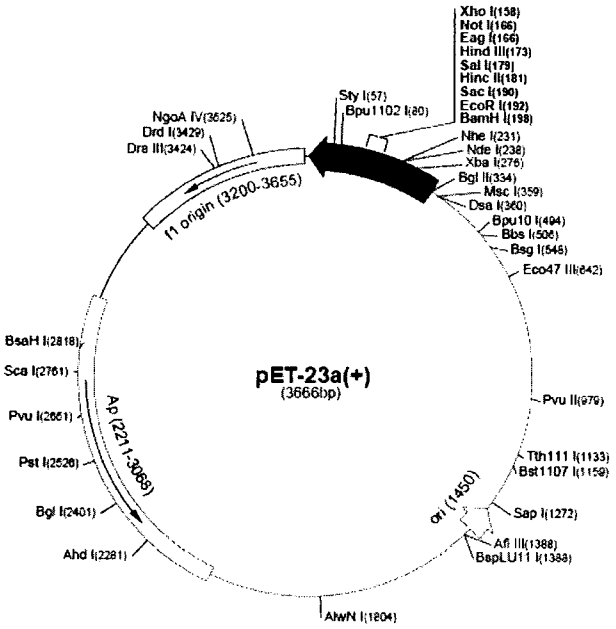

Map of pBUD (Invitrogen)

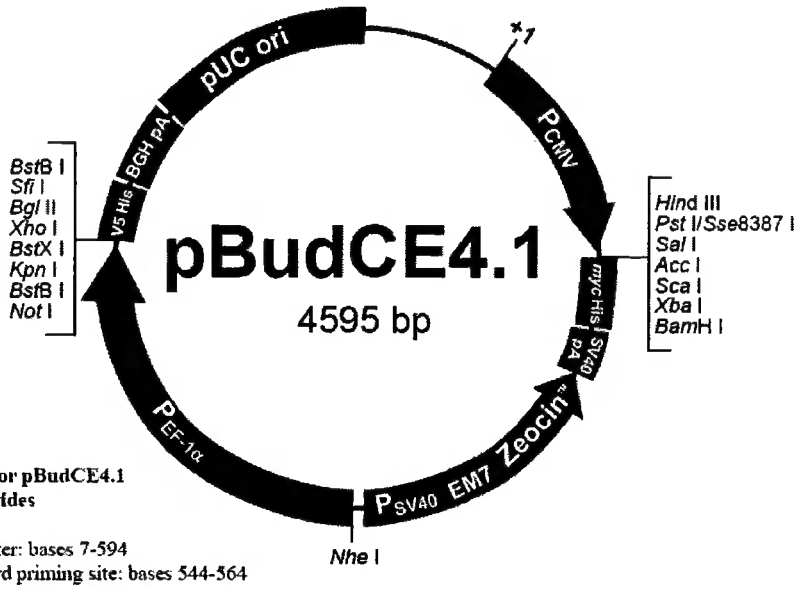

Comments for pBudCE4.1
4595 nucleotides

CMV promoter: bases 7-594
CMV Forward priming site: bases 544-564
T7 promoter/priming site: bases 638-657
CMV multiple cloning site: bases 664-713
myc epitope: bases 719-748
6xHis tag: bases 764-782
SV40 polyadenylation sequence: bases 803-933
Zeocin™ resistance gene: bases 1063-1437 (complementary strand)
EM7 promoter: bases 1456-1510 (complementary strand)
SV40 early promoter: bases 1547-1869 (complementary strand)
EF-1α promoter: bases 1885-3051
EF-1α Forward priming site: bases 2999-3019
EF-1α multiple cloning site: bases 3062-3126
V5 epitope: bases 3127-3168
6xHis tag: bases 3178-3195
BGH Reverse priming site: bases 3218-3235 (complementary strand)
BGH polyadenylation sequence: bases 3224-3447
pUC origin: bases 3521-4194

Expression of Recombinant SOD1

SOD1pET23b vectors were transformed into the BL21(DE3)plysS strain of *E.coli* . Single colonies were picked and grown overnight at 37°C with vigorous shaking at 225 rpm in a starter culture of 10ml LB broth containing 2μM $CuCl_2$ and $ZnCl_2$ and antibiotics (50μgml^{-1} ampicilin and 34μgml^{-1} chloramphenicol). The starter culture was diluted 1:100 in a 1 l culture and this was grown at 37°C with vigorous shaking at 225 rpm until the absorbance at 600nm (A_{600}) reached 0.25-0.5. Plasmid expression was then induced with 0.5mM IPTG

(isopropylthio-β-D-galactosidase) and the culture grown for a further 4 hr at 37°C with vigorous shaking. Cells were then harvested by centrifugation at 5000 rpm (g_{av} – 6000g), for 15 min at 4°C in a Beckman JLA8.1000 rotor. The supernatant (SN) was removed and the pellet stored at -20°C for subsequent purification.

Purification of Recombinant SOD1

For purification of soluble SOD1, the pellet was freeze-thawed (-20°C and room temperature) two to three times, resuspended in 20ml TEN buffer (50mM TrisHCl pH8, 1mM EDTA, 100mM NaCl, 1mM $MgCl_2$,, 0.2M PMSF) containing Complete protease inhibitor cocktail tablet (Roche) and homogenised in a Dounce homogeniser. Benzonase nuclease (Novagen) was added at a concentration of $10Uml^{-1}$ to the lysate and incubated at room temperature for 30 min. This was then centrifuged at 15000 rpm (g_{av} – 27000g) in a Beckman JA-20 rotor for 30 min at 4°C. Polyethyleneimine (PEI) was added to form a 0.06% (v/v) solution, followed by incubation on ice for 5 min and centrifugation at 15000 rpm for 10 min in order to pellet the DNA. The SN was dialysed overnight against buffer A (20mM TrisHCl pH8.5, 20mM NaCl, 1mM $MgCl_2$,, 1mM EDTA, 1mM DTT, 0.2M PMSF), centrifuged at 50000 rpm (g_{av} – 128000g) for 30 min at 4°C in a Beckman MLA-80 rotor and loaded onto a TMAE-sepharose column (VWR), pre-equilibrated with buffer A. Protein was eluted with a linear gradient of 0-1M NaCl in buffer A. Fractions were collected and SOD1 positive fractions, as determined by SDS-PAGE and Coomassie staining, were pooled and stored at -20°C.

For purification of insoluble SOD1 from inclusion bodies, the bacterial pellet was resuspended in 10ml lysis buffer (0.75M sucrose, 50mM TrisHCl pH8,

1mM EDTA) and the solution homogenised using a Dounce homogeniser. 1 ml of lysozyme (1mgml $^{-1}$) was then added and the suspension incubated on ice for 30 min. 20 ml detergent buffer (1% (w/v) deoxycholic acid, 1% (v/v) Nonident P40, 20mM TrisHCl pH7.5, 2mM EDTA, 0.2M NaCl) was then added, the lysate homogenised using a Dounce homogeniser and centrifuged at 15000 rpm (g_{av} – 27000g) for 15 min at 4°C in a Beckman JA-20 rotor. The pellet was resuspended in 20 ml buffer AB (1% (v/v) Triton X-100, 5mM EDTA, 1.5M KCl, 10mM TrisHCl pH8) and centrifuged at 10000 rpm (g_{av} – 12000g) for 5 min at 4°C. The pellet was resuspended in 20 ml buffer AB and stirred for 10 min prior to centrifugation at 10000 rpm for 20 min at 4°C. The pellet was then resuspended in 20 ml buffer C (10mM TrisHCl pH8, 0.15M NaCl, 5mM EDTA) and centrifuged at 10000 rpm for 5 min at 4°C.

The pellet was then dissolved in chromatography buffer A (6M urea, 20mM TrisHCl pH8.5, 1mM DTT, 2mM EDTA), dialysed over night at 4°C against the same buffer and centrifuged at 50000 rpm (g_{av} – 128000g) for 30 min at 4°C in the Beckam MLA-80 rotor. The supernatant was loaded onto a TMAE-sepharose column pre-equilibrated with chromatography buffer A and eluted with a linear gradient of 0-1M NaCl in the same buffer. Fractions were collected and SOD1 positive fractions, as determined by SDS-PAGE and Coomassie staining, were pooled and stored at -20°C.

The anion-exchange chromatography system used was a Merck-Hitachi Biochromatography system, controlled by Chromeleon system (Dionex).

Immunoprecipitation

For IP experiments, 10μg of each protein was made up to 50μl with buffer A (150mM KCl, 20mM K_3PO_4). Proteins were mixed together (as appropriate)

and incubated at room temperature for 1 hr. 10µl of purified monoclonal αB-crystallin antibody was added and the mixture mixed continuously for 1-2 hr. 50µl of pre-cleaned and pre-blocked protein G-coupled beads was added and the mixture rotated end-over-end for 1 hr. The protein G slurry was washed 4 times with PBS, each time removing the SN with a syringe and 23 gauge needle. After the fourth wash, 50µl 2x LSB was added to the beads and the mixture boiled for 5 min. The SN was removed and samples analysed by SDS-PAGE and Western Blotting.

Size-Exclusion Chromatography

A Fractogel EMD BioSEC 650 column (VWR) pre-equilibrated with buffer A (100Mm NaCl, 20mM TrisHCl pH8, 2µM $CuCl_2$ and $ZnCl_2$, 1mM DTT) containing Complete protease inhibitor cocktail tablet (Roche). Protein samples were dialysed overnight at 4°C against the same buffer, centrifuged at 50000 rpm (g_{av} – 128000g) for 30 min at 4°C in a Beckman MLA-80 rotor, treated as appropriate and loaded onto the column. Fractions were collected and analysed by SDS-PAGE and Sypro staining.

The size-exclusion chromatography (SEC) system used was a Merck-Hitachi Biochromatography system, controlled by Chromeleon software (Dionex).

CHAPTER 3
ESTABLISHING A MODEL CELL SYSTEM OF MUTANT SOD INCLUSION FORMATION AND PROPERTIES OF INCLUSIONS FORMED

Mutant SOD inclusion formation in culture cells

In order to investigate the role of sHSPs in mutant SOD1 inclusion formation, we first had to establish a model cell system of mutant SOD1 inclusion formation. In order to do this, preliminary experiments were carried out in which HEK293 cells, and H36CEI cells carrying an αB-crystallin mutation (known as mH36 cells), were transiently transfected with mammalian expression vectors containing yellow fluorescent protein (YFP)-tagged and non-tagged wt and mutant SOD1 (see Materials and Methods for details of transfection protocol and construction of vectors). Cell extracts were taken from these cells and samples analysed by SDS-PAGE and Western Blotting. In mH36 cells, transient transfection of wt and G85R mutant SOD1 did not cause an increase in SOD1 levels, whereas transient transfection of the same constructs which were YFP-tagged, did give rise to increased SOD1 levels (Figure 3.1A). Similar results were seen with HEK293 cells after over-expression of 6 different mutant tagged and non-tagged constructs (Figure 3.1B). It was decided to continue the studies using the YFP-tagged constructs, as they resulted in over-expression of wt and mutant SOD1s. It may have been that the non-tagged SOD1 constructs did result in over-expression, but at levels which could not be detected by Western Blotting.

Since establishing that YFP-tagged SOD1 constructs could be successfully over-expressed in these cell lines, more studies were carried out in order to visualise and determine the appropriate conditions for mutant SOD1 aggregation and inclusion formation. Johnston et al., (2000), have previously

shown that over-expression of mutant SOD1 in HEK293 cells and subsequent treatment with proteasome inhibitor led to SOD aggregation and inclusion formation. HEK293 and mH36 cells were transiently transfected with mutant YFP-tagged SOD1s and grown in the presence of proteasome inhibitor (6.25μgml^{-1} ALLN), prior to processing for IMF microscopy studies (see Materials and Methods). Under these conditions, mutant, but not wt SOD1 formed inclusions in both cell types. The results are shown in Figure 3.2. These mutant SOD1 inclusions appeared as intense green juxtanuclear accumulations of protein. In HEK293 cells, 14% of transfected cells contained inclusions, in mH36 cells, 21% of transfected cells formed inclusions.

These preliminary studies have demonstrated that YFP-tagged SOD1 constructs can be successfully over-expressed in HEK293 and mH36 cells, and IMF microscopy has shown that this over-expression, in the presence of proteasome inhibitor, leads to mutant SOD1 inclusion formation in HEK293 and mH36 cells. During these studies, 6 different mutant SOD1 constructs were used and each showed similar successful over-expression and inclusion formation in culture cells. It was decided that for subsequent studies, one mutant construct, namely G85R, be used. G85R mutant SOD1 has decreased activity in humans compared to other FALS mutants (Borchelt et al., 1994, (Bowling et al., 1995). Bruijn et al., (1997b), report that G85R mutant SOD1 caused dominantly inherited, rapidly progressing disease in mice, in spite of low levels of accumulated protein. Also, due to good transfection rates (≥50%) in HEK cells, this cell line was used as our model cell system of G85R mutant SOD1 inclusion formation.

Endogenous chaperone levels affect mutant SOD1 inclusion formation

It was interesting to note, that compared to HEK293 cells, there was an increased proportion of G85R mutant SOD1-transfected mH36 cells which contained inclusions. 21% of transfected mH36 cells contained inclusions whereas 14% of HEK293 cells contained inclusions. In each experiment, two hundred transfected cells were counted, and scored for the presence/absence of an inclusion, and experiments were carried out in triplicate. Our criterion for the presence of an inclusion was an intense green juxtanuclear accumulation, rather than a small green spot (see Figure 3.2D for examples of each). This difference in inclusion frequency may have been due to the mutation in αB-crystallin this cell line carries. This suggests that mutant SOD1 inclusion formation is affected by levels of functional αB-crystallin. Chaperone proteins such as αB-crystallin help prevent mis-folded proteins from damaging cells, as described previously. It is possible that the mutation in αB-crystallin in this cell line renders the cells less efficient at processing mutant SOD and thus leading to increased inclusion formation. This led us to hypothesise that endogenous chaperone levels may affect mutant SOD1 inclusion formation. To study this further, U373 and MCF7 cells were transiently transfected with YFP-tagged mutant SOD1 and treated with proteasome inhibitor, as before. Subsequent IMF microscopy showed the incidence of aggregation and inclusion formation in these cell lines was lower than previously seen with HEK293 and mH36 cells: either no inclusions were observed or the beginnings of small aggregations were observed infrequently (Figure 3.3). The levels of chaperones in each cell type appear to relate to the number of inclusions: U373 cells contain high levels of both αB-crystallin and HSP 27, and MCF7 cells contain high levels of HSP 27, but no αB-crystallin (Figure 3.3). The high levels of these two chaperones in

the U373 cells could explain the lack of inclusions and in the case of MCF7 cells, the high levels of HSP 27 probably compensate for the lack of αB-crystallin, again explaining the lack of inclusions. HEK293 cells contain low levels of both of proteins and although mH36 cells contain slightly higher levels compared to the HEK293 cells, (Figure 3.3), some of the αB-crystallin is mutated and thus non-functional. These results support our hypothesis that endogenous chaperone levels influence mutant SOD1 inclusion formation.

Accumulation of protein folding and protein degradation machinery at mutant SOD1 inclusion sites

If endogenous chaperones influence mutant SOD1 inclusion formation, it is possible that they may be involved directly, and localise to the inclusions. G85R mutant SOD1 inclusions were formed in HEK293 cells as described previously, and IMF confocal microscopy shows that αB-crystallin, HSP 27 and HSP 70 all co-localise to these cytoplasmic inclusions (Figure 3.4).

The UPS acts to degrade un- or mis-folded and damaged proteins and dysfunction of the UPS is often seen in neurodegenerative diseases. The target for degradation of such proteins by the UPS is polyubiquitin and in ALS patients and mouse models, inclusions have been shown to contain Ub (Shibata et al., 1996 and Bruijn et al., 1998). With our model cell system of G85R mutant SOD1 inclusion formation, we have shown, using IMF confocal microscopy, that Ub is co-localised to these mutant SOD1 inclusions (Figure 3.5A). Dorfin, another component of the UPS, an E3 Ub ligase, has been shown to be up-regulated in ALS (Ishigaki et al., 2002), and its over-expression prevents cell death induced by mutant protein (Niwa et al., 2002). Again, using our HEK293 cell system and

IMF confocal microscopy, we show that dorfin co-localises to G85R mutant SOD1 inclusions (Figure 3.5B).

These studies confirm previous reports of accumulation of both chaperone proteins; the protein folding machinery, and UPS components; the protein degradation machinery, into mutant SOD1 inclusions.

Affects of mutant SOD1 on transcription

Although over-expression of mutant SOD1 in cultured MNs leads to inclusion formation and cell death (Durham et al., 1997), it is not certain how mutant SOD1 exerts its toxicity. In other neurodegenerative diseases, mutant protein has been shown to affect transcription, which may contribute to neurodegeneration. It is possible mutant SOD1 may have a similar role in ALS. We have antibodies to components of the speckle compartments, which have been used to see if transcription is altered in response to G85R mutant SOD1 over-expression. Huntingtin is the protein which causes Huntington's Disease when its polyglutamine tract is extended above thirty-seven glutamine residues. Truncated N-terminal mutant huntingtin represses transcription, whereas wt huntingtin does not (Kegel et al., 2002). These authors suggest that wt huntingtin has a function in the nucleus in the assembly of nuclear matrix bound protein complexes involved in transcriptional repression and pre-mRNA splicing, and that proteolysis of mutant huntingtin may inappropriately repress transcription in Huntington's Disease. β-amyloid precursor protein (APP), as its name suggests, is the precursor of the amyloid-β-peptide, which makes up the plaques seen in brains of Alzheimer's Disease patients. Muresan and Muresan, (2004), showed that a phosphorylated, C-terminal fragment of APP is present in the nucleus and localises to the splicing factor compartment, thus indicating that

APP may have a role in pre-mRNA splicing and/or transcription in Alzheimer's Disease.

Speckles, or interchromatin granules, are distinct nuclear structures involved in the processing and transcription of RNA (Wei et al., 1999). They can be detected using antibodies to components of the spliceosome, either small nuclear ribonucleoprotein (snRNP) components like Sm and UIA, or non-snRNP components like SC35 and TMG (Antoniou et al., 1993). By looking at the pattern of speckles obtained by staining with these antibodies, insights into the transcriptional activity of the cell can be gleaned. Using our HEK293 model cell system, we used antibodies to SC35 and Sm to look at speckle patterns. HEK293 cells were grown on coverslips, and transiently transfected, with appropriate SOD1 constructs, prior to fixing and staining with these antibodies, and IMF confocal microscopy. Results are shown in Figure 3.6. No differences in the speckle patterns were observed between control (mock transfected), wt, G85R SOD1 or proteasome inhibitor only treatments. These results suggest that mutant SOD1 does not have any affect on the transcriptional activity of the cell. Whether this is a general phenomenon or specific for the G85R mutant of SOD1 used here remains to be ascertained. However, there are disadvantages of using speckles as a measure of transcription, as speckles indicate gross transcriptional changes. It is possible that mutant SOD1 affects transcription on a smaller scale. An alternative method of investigating this affect would be to monitor differential gene expression in the presence and absence of mutant SOD1 using DNA microarrays, for example.

Conclusions

SOD1 inclusions are a histopathological feature of ALS: intracytoplasmic SOD1-containing inclusions are observed in mutant SOD1 transgenic mice (Bruijn et al., 1998), as well as ALS patients (Shibata et al., 1996). We have established a model cell system of G85R mutant SOD1 inclusion formation. Over-expression of YFP-tagged G85R mutant SOD1 in HEK293 cells and treatment with proteasome inhibitor, gives rise to mutant SOD1 inclusion formation. These inclusions contain both chaperone proteins and the UPS components dorfin and Ub, but do not appear to effect transcription. Previous studies have implicated chaperone proteins and the UPS in neurodegenerative diseases such as ALS. For example, Bruening et al., (1999), have shown that over-expression of HSP 70 decreased the number of cultured cells containing mutant SOD1 inclusions as well as prolonging cell survival and a report by Niwa et al., (2002), showed that over-expression of dorfin prevented cell death caused by mutant protein. Our results further support the role of chaperones, as we have shown endogenous chaperone levels influence inclusion formation. We shall use this model cell system to further study the role of chaperone proteins, or more specifically, small heat shock proteins (sHSPs), in mutant SOD1 inclusion formation.

Figure 3.1A and B Over-expression of SOD1 in mH36 and HEK293 cells

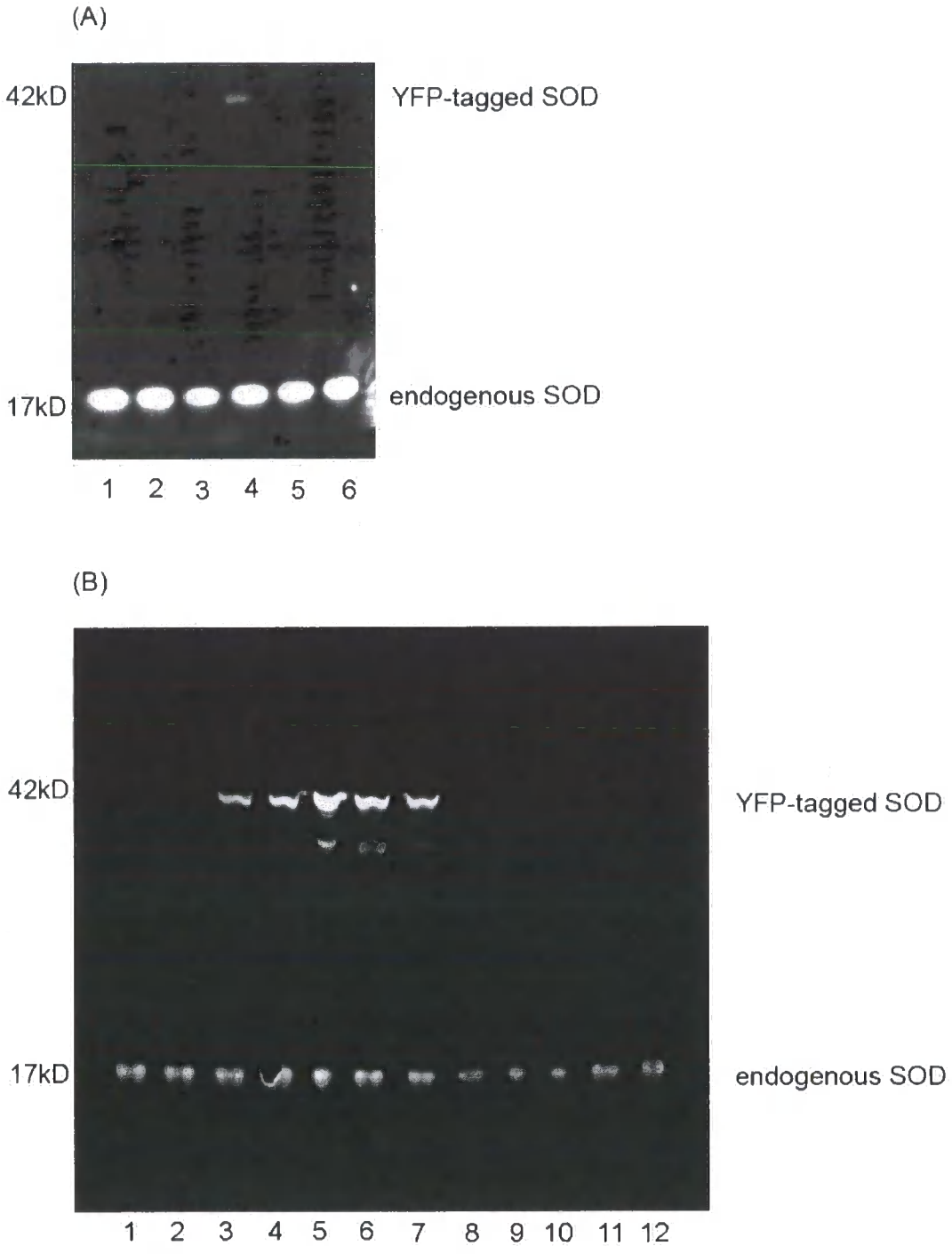

Figure 3.1A Over-expression of SOD1 in mH36 cells

The figure shows total protein extracts from mH36 cells over-expressing SOD1 constructs, run on a 12% (w/v) polyacrylamide gel, blotted and probed with a monoclonal anti-SOD1 antibody. Lanes 1 and 2 show controls: lane 1 - non-transfected cells, lane 2 - cells transfected with YFP-tag only. Lane 3 - cells transfected with wt YFP-tagged SOD1, lane 4 - cells transfected with G85R YFP-tagged SOD1, lane 5 - cells transfected with wt SOD1 and lane 6 - cells transfected with G85R SOD1. In lane 3 there is a faint band corresponding to over-expression of wt YFP-tagged SOD1. The fact that the wt construct appears to express less well than the mutant could be due to contamination of the DNA in that particular preparation. Alternatively, it could be the case that the amount of protein loaded onto the gel was inaccurate.

Figure 3.1B Over-expression of SOD1 in HEK293 cells

The figure shows total protein extracts from HEK293 cells over-expressing various SOD1 constructs, again run on a 12% (w/v) polyacrylamide gel, blotted and probed with an anti-SOD1 antibody. Lanes 1 and 2 are controls: lane 1 - non-transfected cells and lane 2 - YFP-tag only transfected cells. Lanes 3 to 7 show cells transfected with tagged constructs and lanes 8 to 12 show cells transfected with non-tagged constructs. Lanes 3 and 8 - A4V SOD1, lanes 4 and 9 - G37R SOD1, lanes 5 and 10 - G85R SOD1, lanes 6 and 11 - G93A SOD1 and lanes 7 and 12 - I113T SOD1. The lower molecular weight bands seen in lanes 4 to 7 could be proteolytic fragments. To confirm loading consistencies, a β-actin antibody stain could have been used.

Figure 3.2 Mutant SOD1 inclusion formation

Mutant, but not wt SOD1, forms inclusions in mH36 and HEK293 cells in response to over-expression and proteasome inhibition, achieved by addition of 6.25μgml^{-1} ALLN. Figure 3.2A shows over-expression of wt SOD1 in mH36 cells. Figure 3.2B shows over-expression of four different mutant SOD1s in mH36 cells. 1 - G37R, 2 - G85R, 3 - G93A and 4 - I113T. YFP-tagged SOD1 is green, vimentin is stained red. Figure 3.2C shows over-expression of wt SOD1 and figure 3.2D shows over-expression of G85R SOD1, our chosen mutant, in HEK293 cells. YFP-tagged SOD1 is shown in green. Non-transfected cells showed no green signal (data not shown). In Figure 3.2D, the arrows indicate intense green juxtanuclear accumulations of protein counted as inclusions as well as the small green spots not counted as inclusions.

Figure 3.2A

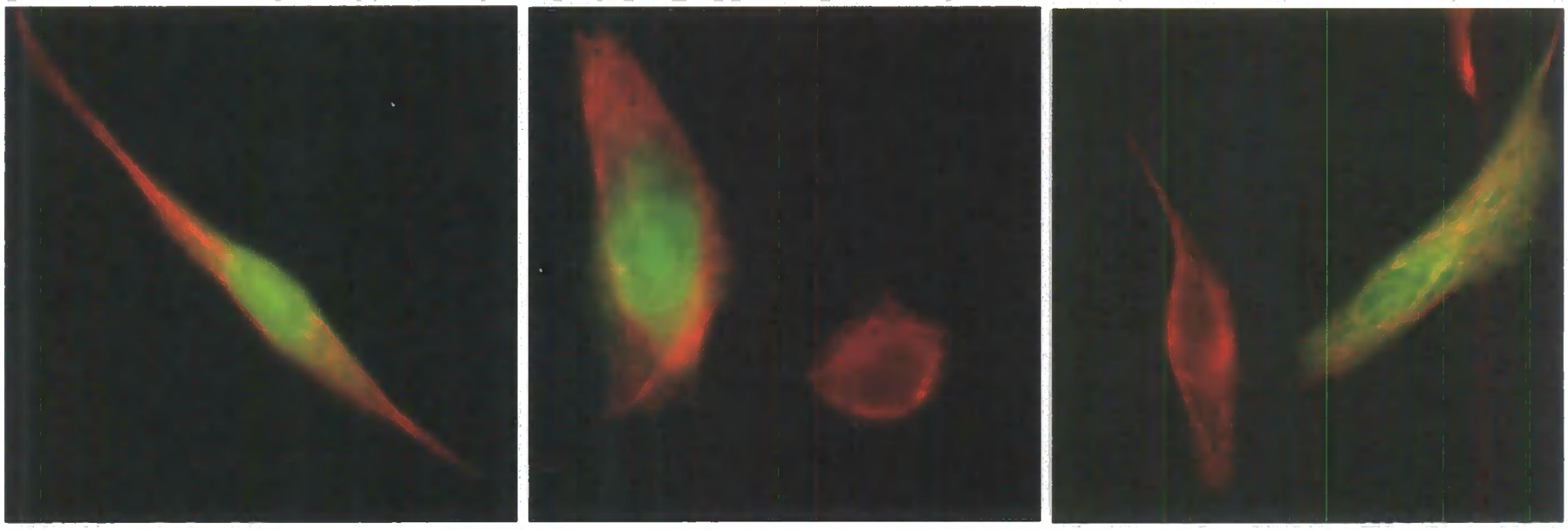

Figure 3.2B

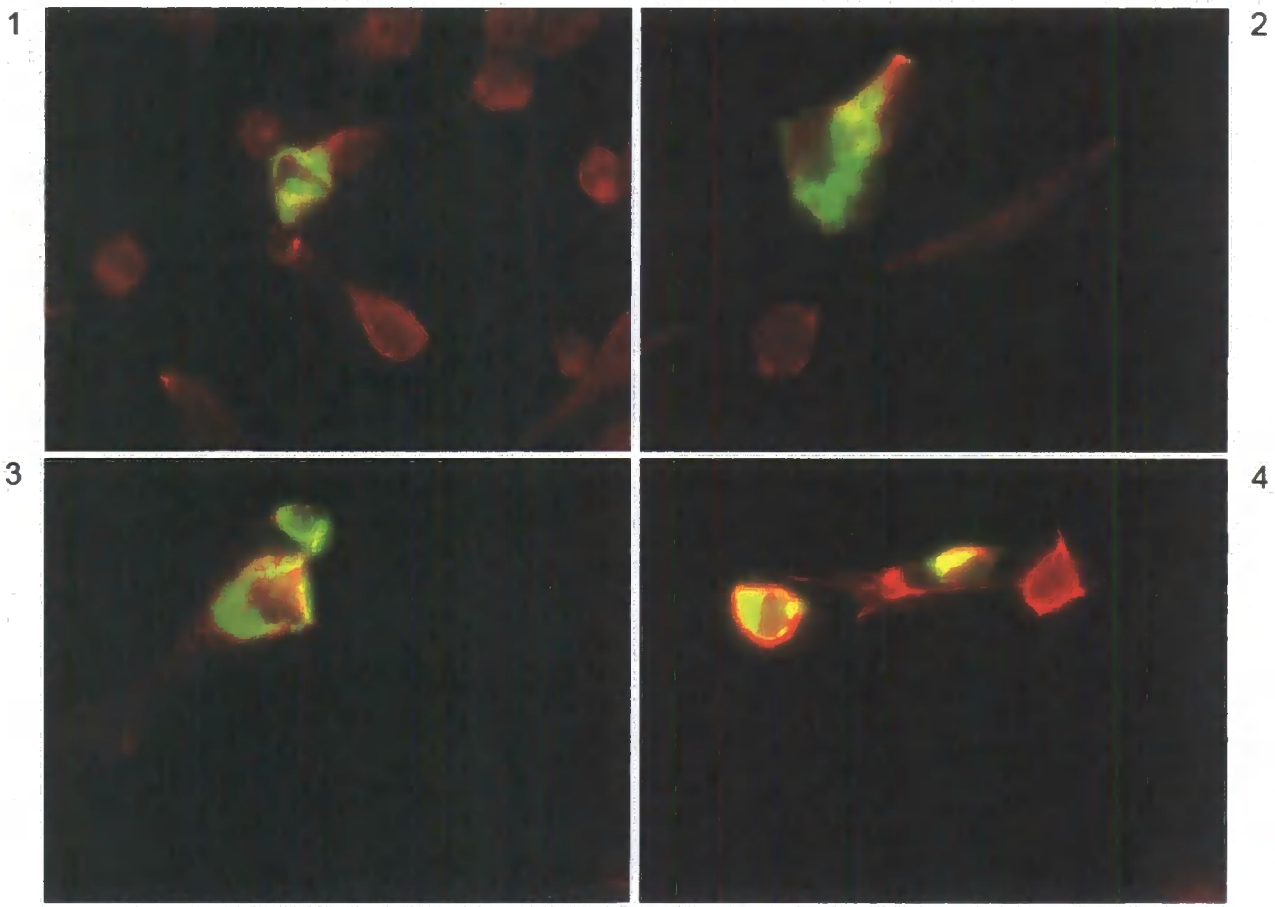

Figure 3.2C

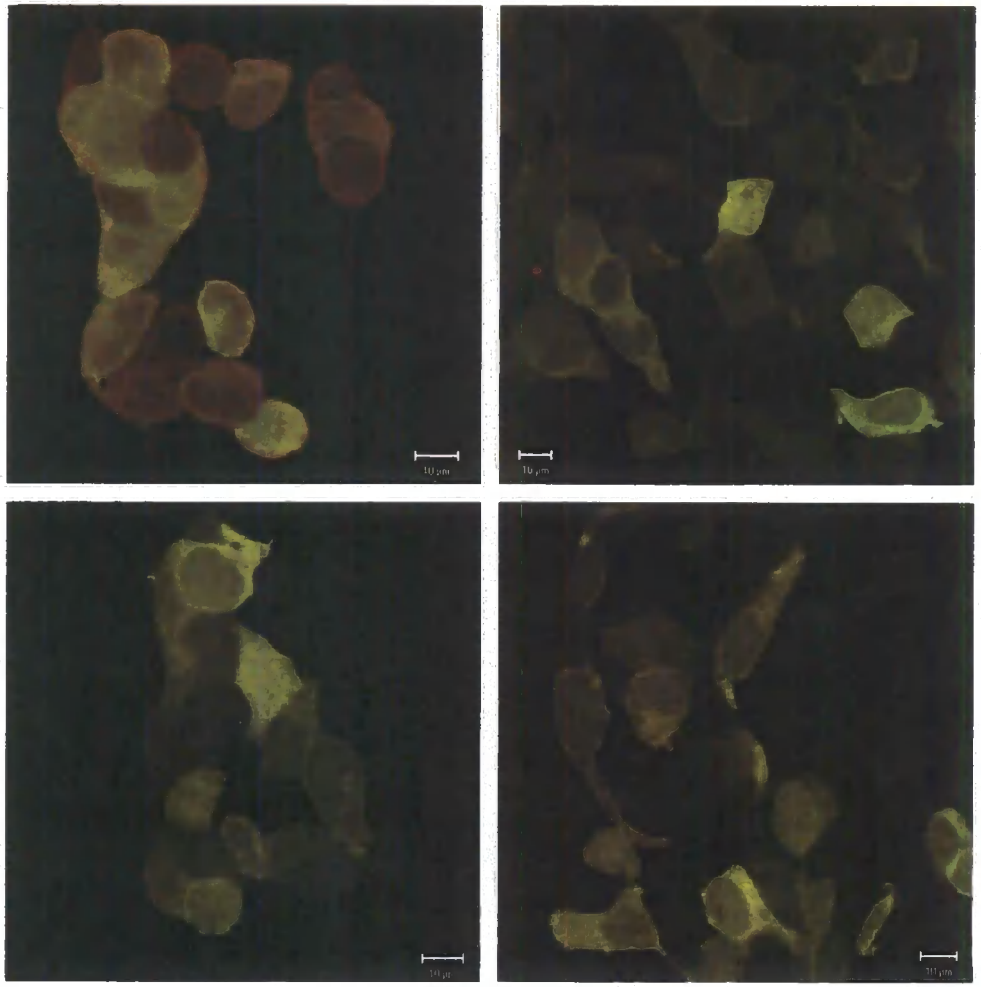

Figure 3.2D

small green spot

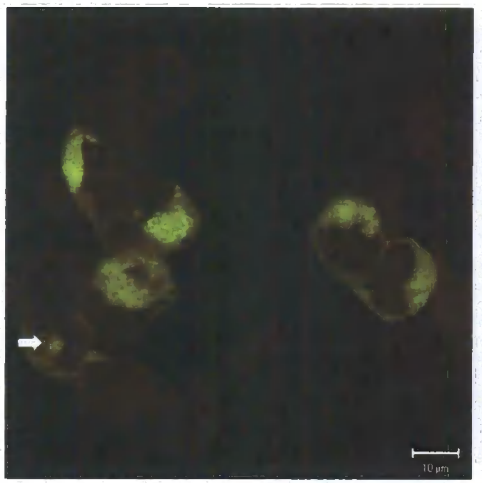

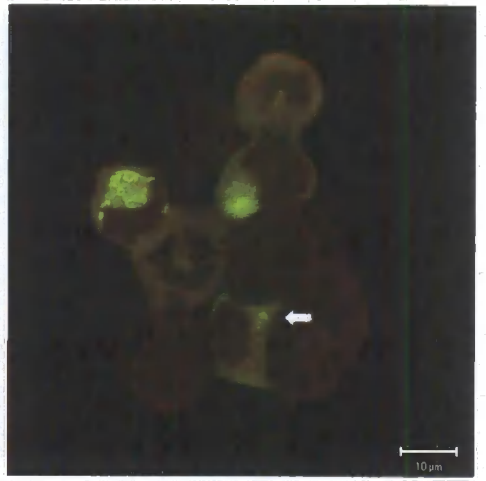

small green spot

intense greenjuxtanuclear inclusions

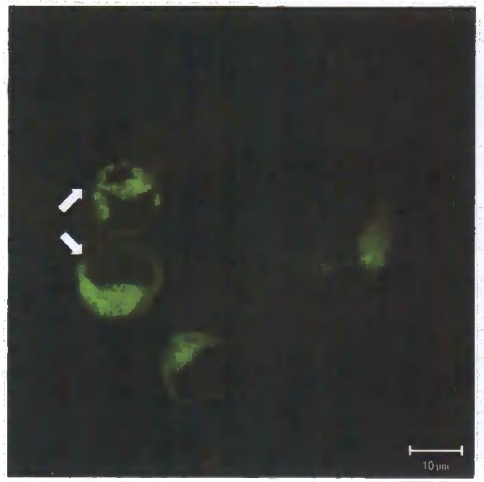

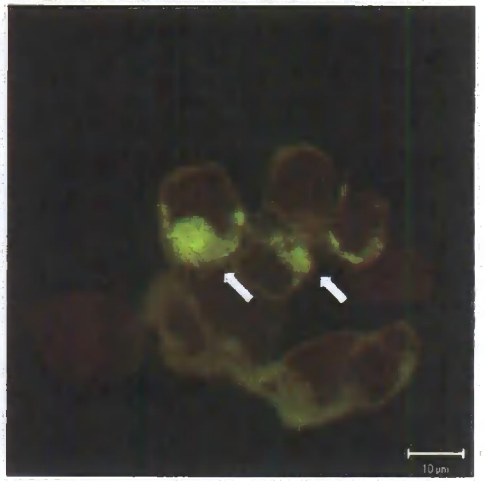

intense green juxtanuclear inclusions

Figure 3.3 Endogenous chaperone levels affect G85R mutant SOD inclusion formation

Cell type	%of transfected cells containing inclusions
HEK293	14 ± 2
MH36	21 ± 1.732
MCF7	0
U373	0

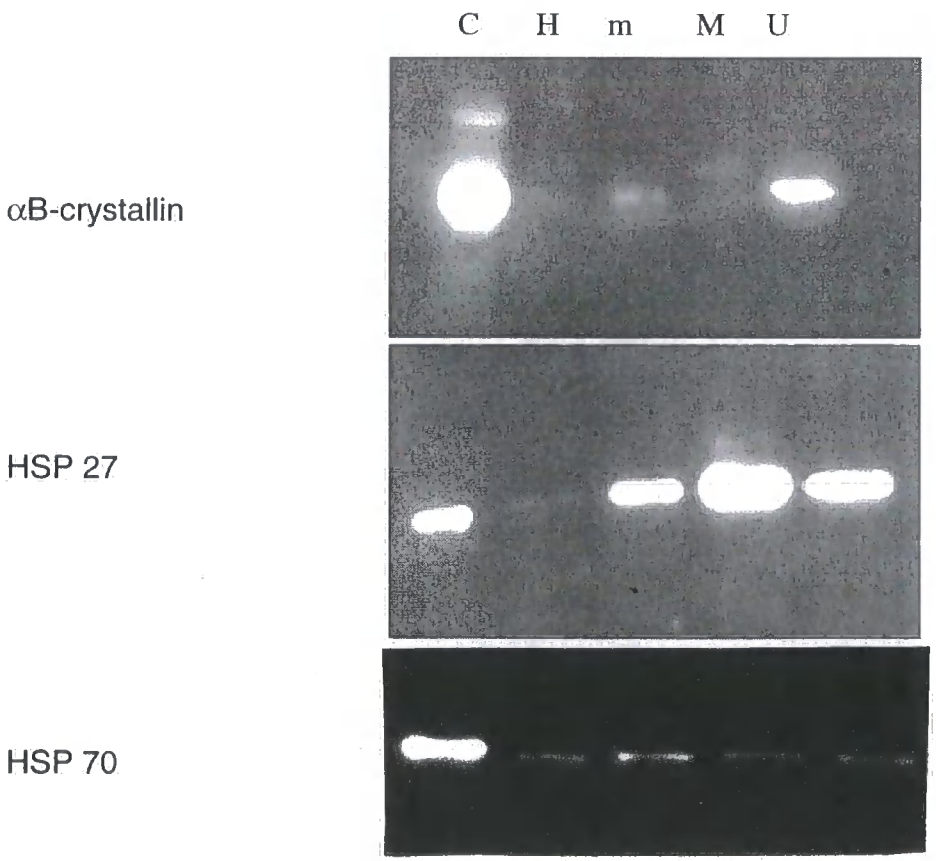

Figure 3.3 Endogenous chaperone levels affect G85R mutant SOD1 inclusion formation

The table shows the percentage of transfected cells containing inclusions for each cell type used. Cells were transiently transfected with G85R mutant SOD1, treated with proteasome inhibitor and processed for IMF microscopy studies. Two hundred transfected cells were counted and scored for the presence/absence of an inclusion in each experiment, and experiments were carried out in triplicate. Our criteria for the presence of an inclusion was an intense green juxtanuclear accumulation rather than a small green spot (see Figure 3.2D for examples of each).

The image shows the different levels of various chaperone proteins in the cell types used. Cells extracts were taken and protein concentrations measured using the BCA protein assay (see Materials and Methods). Equal amounts of each sample were loaded, subjected to SDS-PAGE on 12% (w/v) polyacrylamide gels and Western Blotted with the appropriate antibody. Key: C – antibody positive control; H – HEK293 cell extract; m – mH36 cell extract; M – MCF7 cell extract and U – U373 cell extract.

Figure 3.4 Heat shock proteins co-localise with G85R mutant SOD1 inclusions

HEK293 cells were seeded onto coverslips, transiently transfected with appropriate constructs, and treated with proteasome inhibitor to induce inclusion formation, prior to fixing and staining with appropriate antibodies for IMF confocal microscopy. A - αB-crystallin staining in red. B – HSP 27 staining in red. C – HSP 70 staining in red. In all cases mutant YFP-tagged SOD1 is green, but appears yellow due to co-localisation. The nuclei were visualised by staining with DAPI (bue).

Figure 3.4

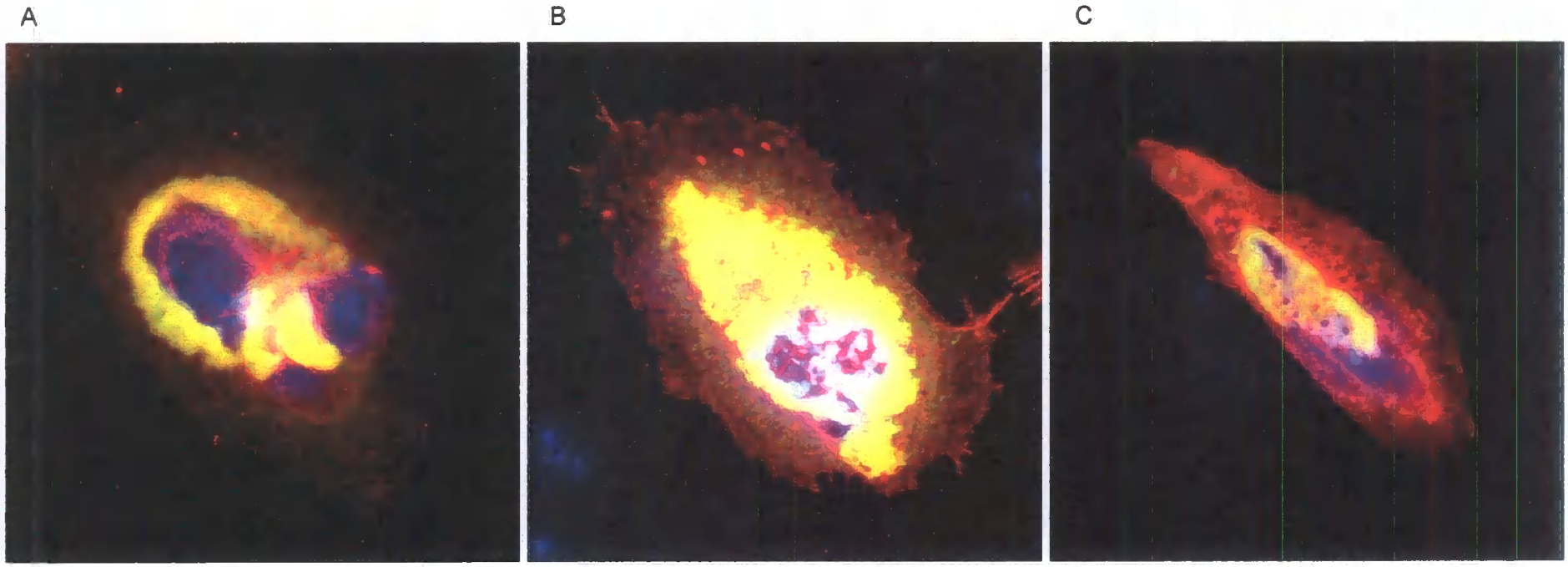

Figure 3.5 Accumulation of UPS components with G85R mutant SOD1 inclusions

HEK293 cells were seeded onto coverslips, transiently transfected with appropriate constructs, and treated with proteasome inhibitor (ALLN) to induce inclusion formation, prior to fixing and staining with appropriate antibodies for IMF confocal microscopy. Figure 3.5A – co-localisation of Ub to mutant SOD1 inclusions; 1 - 3 wt SOD, 4 - 6 G85R SOD1. Figure 3.5B – co-localisation of dorfin to mutant SOD inclusions; 1 - 3 wt SOD1, 4 - 6 G85R SOD1. YFP-tagged SOD1 is green and the UPS component is stained red.

Figure 3.5A

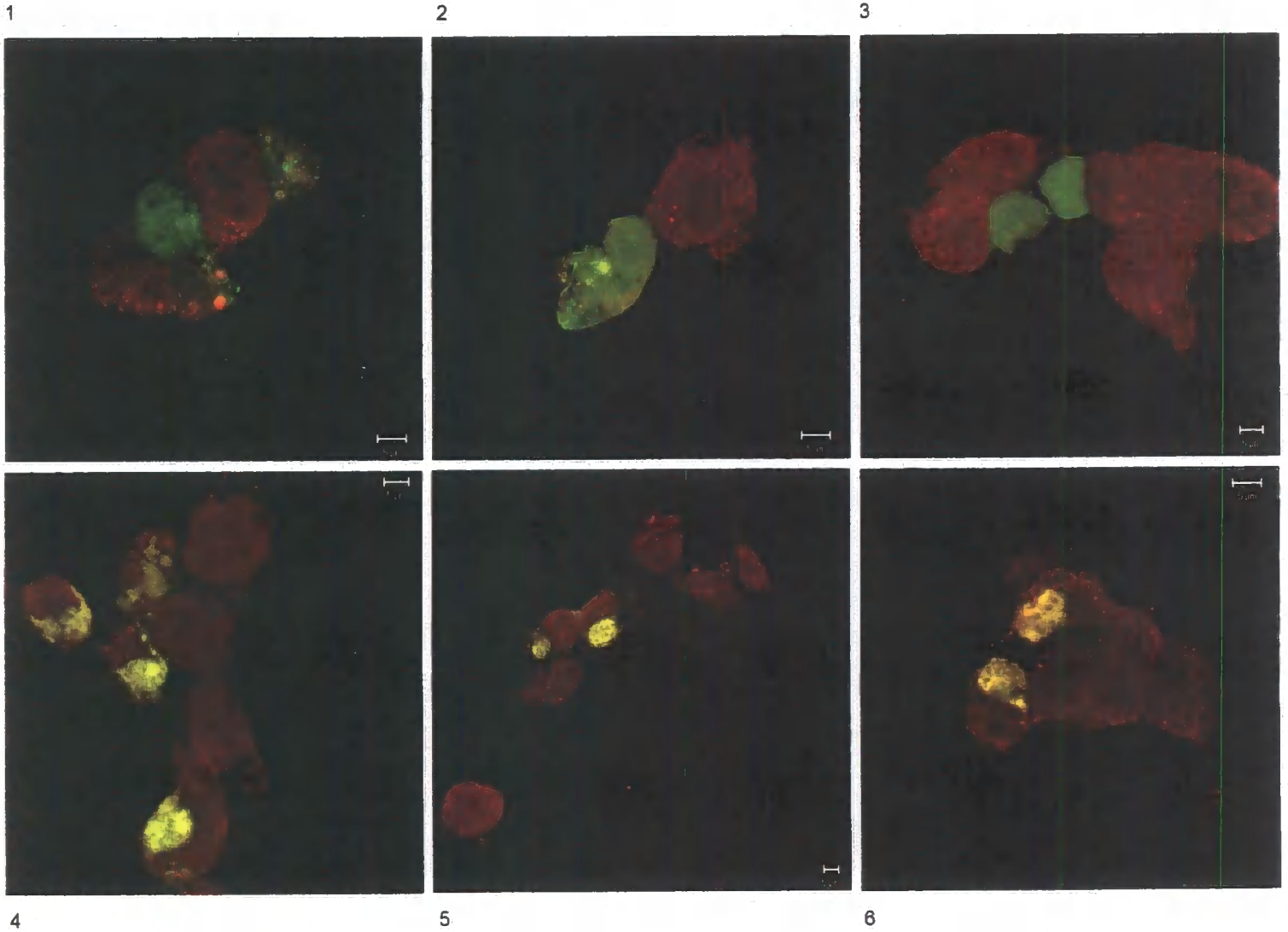

Figure 3.5B

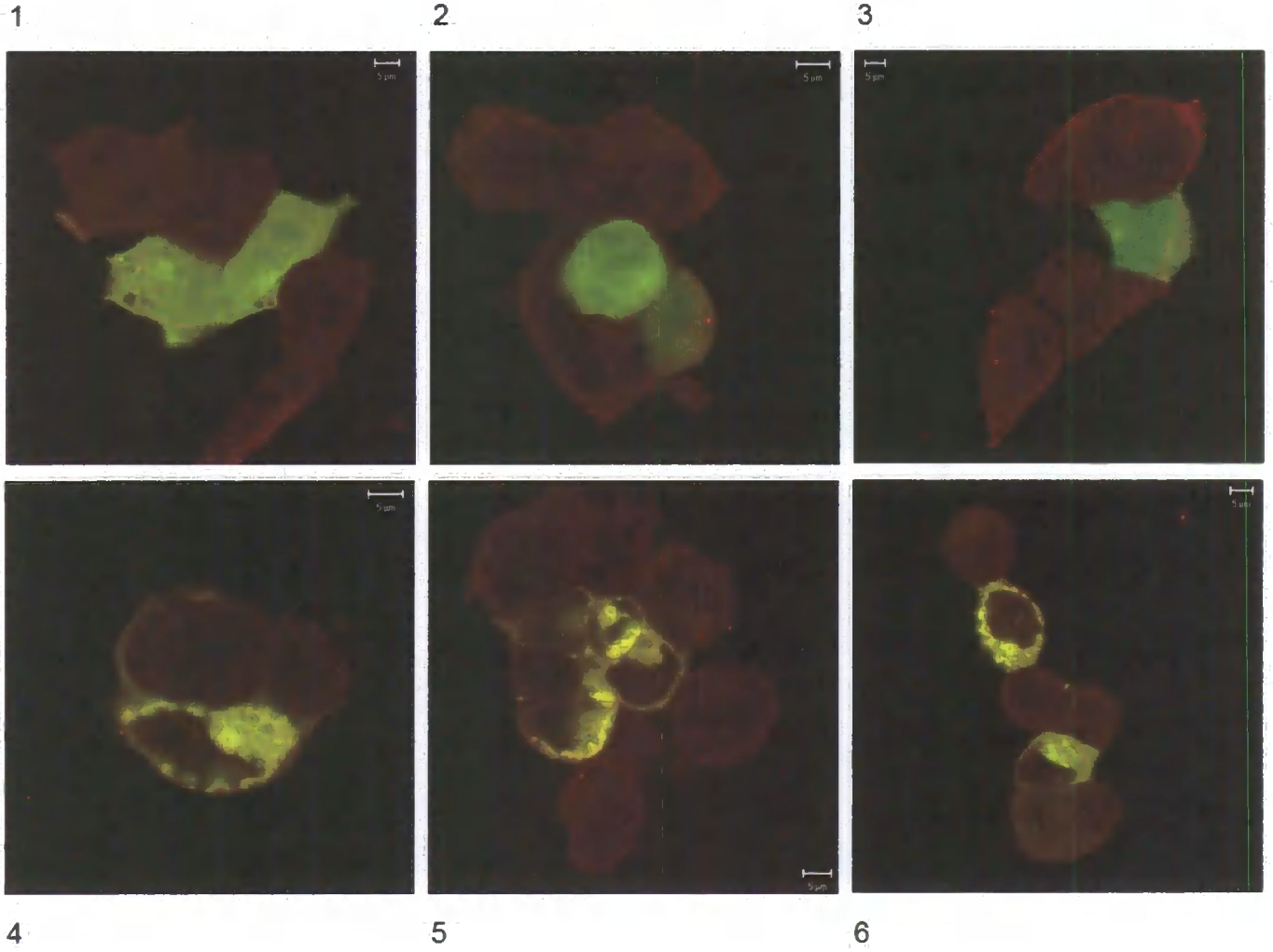

Figure 3.6 The speckle pattern in HEK293 cells is not affected by over-expression of mutant SOD1

HEK293 cells were seeded onto coverslips and transiently transfected with appropriate constructs, prior to fixing and staining with appropriate antibodies for IMF confocal microscopy. Figure 3.6A – SC35 antibody; 1 - untreated cells, 2 – ALLN only treated cells, 3 and 4 – wt SOD1, 5 and 6 – G85R SOD1. Figure 3.6B – Sm antibody; 1 - untreated cells, 2 – ALLN only treated cells, 3 and 4 – wt SOD1, 5 and 6 – G85R SOD1. YFP-tagged SOD1 is green, speckle compartment is stained red.

Figure 3.6A

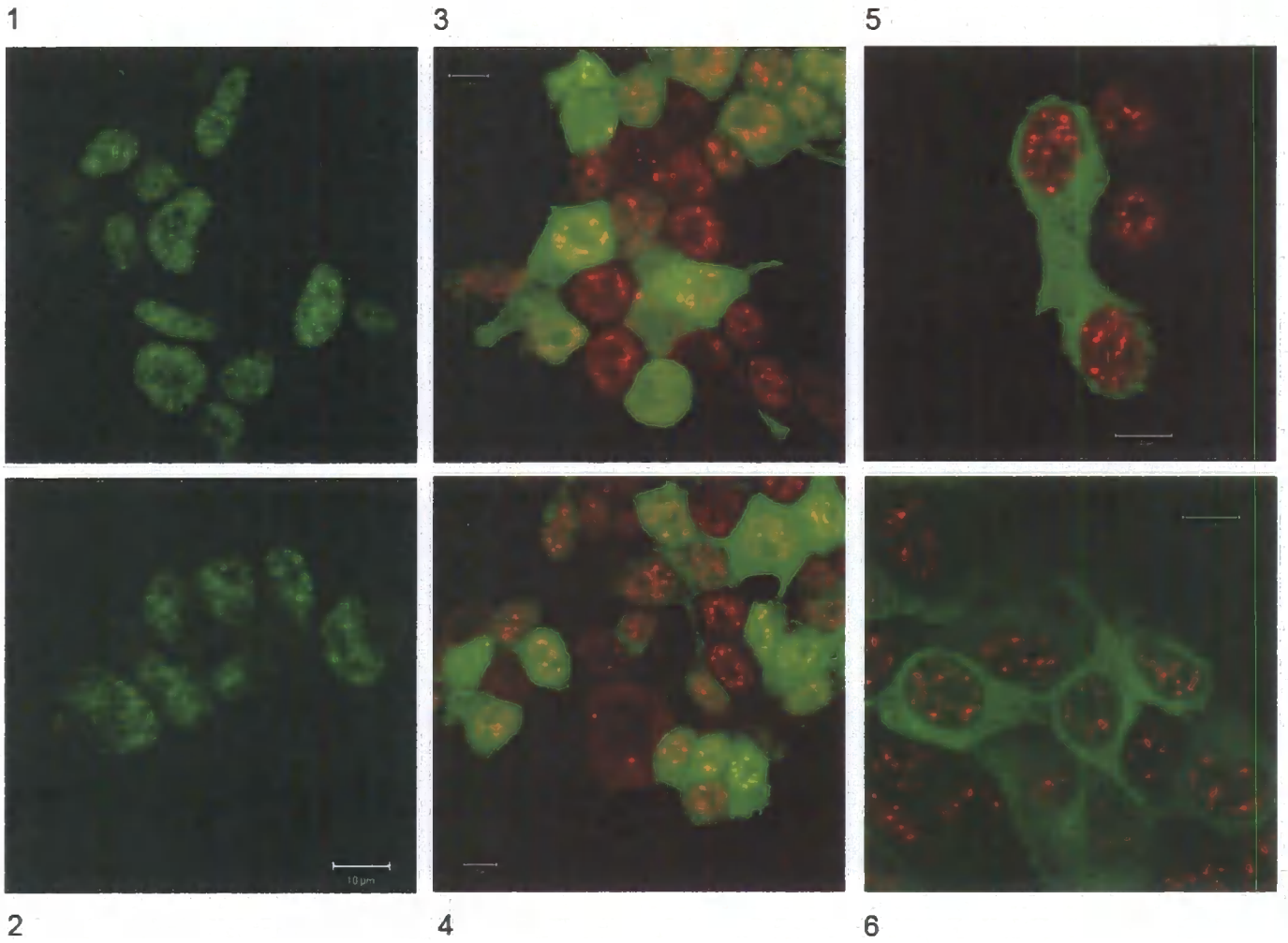

Figure 3.6B

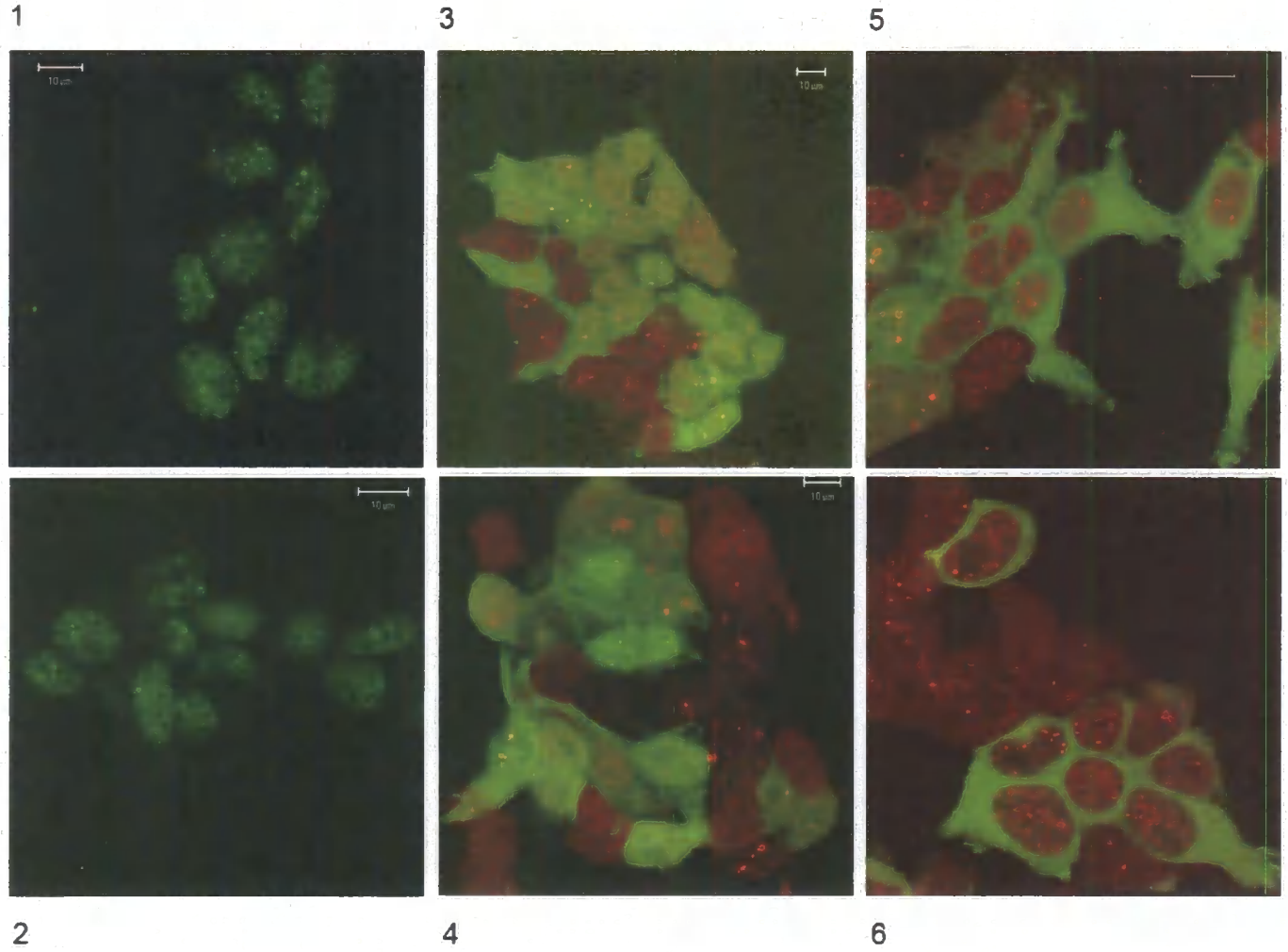

CHAPTER 4
CHAPERONE PROTEIN INVOLVEMENT IN MUTANT SOD1 INCLUSION FORMATION

The aim of this study was to investigate the involvement of chaperone proteins, specifically sHSPs, in mutant SOD1 inclusion formation. HSP 70 protects against mutant SOD1 inclusion formation and subsequent cell death in cultured primary MNs (Durham et al., 1997), and HSP 70 and 40 protect against mutant SOD1 inclusion formation and cell death in a neuroblastoma cell line, as well as improving neurite out-growth, this being diminished in cells containing mutant SOD1 inclusions (Takeuchi et al., 2002). Together with the demonstration that mutant SOD1 is co-immunoprecipitated with chaperone proteins, namely HSP 70, 40 and αB-crystallin, from NIH3T3 cell extracts (Shinder et al., 2001), this shows that chaperone proteins help to prevent inclusion formation, possibly by direct interaction with the proteins involved. Data obtained from preliminary experiments, described in the previous chapter, would also support a role for chaperone proteins in inclusion formation. It was shown that endogenous sHSP levels influenced G85R mutant SOD1 inclusion formation.

A model system of G85R mutant SOD1 inclusion formation in HEK293 cells was established, as described in chapter 3. The formation of mutant SOD1 inclusions was followed biochemically. Twenty-four hours after transient transfection of G85R mutant SOD1 into HEK cells and treatment with proteasome inhibitor, cell extracts were prepared. These cell extracts were then separated into soluble and insoluble fractions as described in Materials and Methods. Firstly, the extracts were centrifuged at low speed resulting in a soluble supernatant (SN1) and insoluble pellet (P1). Secondly, a sample of SN1 was centrifuged at high speed resulting in a soluble supernatant (SN2) and

insoluble pellet (P2). P1, resulting from the low speed centrifugation, will contain cytoskeletal components and associated material, as well as nuclear fragments. P2, resulting from the high speed centrifugation, will contain other insoluble material, such as the insoluble mutant SOD1 comprising the inclusions. These four fractions were then analysed by SDS-PAGE and Western blotting using a monoclonal anti-SOD1 antibody. Therefore, the proportion of mutant SOD1 in the insoluble P2 fraction, or the proportion of mutant SOD1 present in inclusions, can be monitored under different conditions.

If wt SOD1 was over-expressed, SOD1 was soluble; SOD1 immunoreactive bands were present in the SN but not P fractions (Figure 4.1A). This is consistent with results from IMF microscopy which showed that over-expression of wt SOD1 and treatment with proteasome inhibitor did not result in inclusion formation (see Figure 3.2) When G85R mutant SOD1 was over-expressed, a proportion of SOD1 was insoluble; SOD1 immunoreactive bands were present in both the SN and P fractions (Figure 4.1B). Again, this is consistent with IMF microscopy, which showed that over-expression of G85R mutant SOD1 and treatment with proteasome inhibitor resulted in mutant SOD1 inclusion formation (Figure 3.2).

In order to study the involvement of sHSPs in inclusion formation, it was decided to investigate the effects of co-expression of sHSPs on the proportion of mutant SOD1 in the insoluble fraction.

Co-expression of SOD1 and αB-crystallin using pBUD

Initially, it was decided to co-express SOD1 and the sHSP, αB-crystallin, using a mammalian expression vector (pBUD) with two multiple cloning sites (MCSs). For these experiments, several pBUD vectors were cloned by insertion of either

wt or G85R mutant SOD1, and wt or R120G αB-crystallin into each of the MCSs. Expression vectors were constructed as described in Materials and Methods. In order to test whether expression of both proteins from these constructs was occurring, they were transiently transfected into HEK293 cells, and treated with the proteasome inhibitor ALLN to induce inclusion formation. However, IMF microscopy studies revealed that SOD1 and αB-crystallin were not being simultaneously expressed within the cell (see Figure 4.2), and hence the vectors were not functioning as expected. In order to overcome this problem and continue with the studies, we decided to achieve co-expression of SOD1 and αB-crystallin by transfection of two separate vectors.

Effects of sHSPs on insoluble G85R mutant SOD1 levels in HEK293 cells

Due to the problems encountered with the pBUD expression system, co-expression of SOD1 and sHSP was carried out using two separate vectors. Cells were transfected, treated and extracts prepared and processed as described above. Over-expression of both αB-crystallin and HSP 27, both sHSPs, resulted in a decrease in the proportion of insoluble G85R mutant SOD1 in these cells. Transfections were carried out in triplicate and representative blots are shown in Figure 4.3 (A, B and C). Quantification of the Western Blots using OptiQuant Imaging software allowed the amount of insoluble SOD1, as a percentage of the total transfected SOD1, to be calculated. For G85R mutant SOD1 alone, 22.4% ± 0.01 of the transfected mutant SOD1 was present in the pellet fractions, i.e. insoluble. Over-expression of αB-crystallin resulted in a decrease in the amount of insoluble mutant SOD1, as evidenced by the absence of SOD1 immunoreactive bands in the pellet fractions. Over-expression of HSP 27 decreased the amount of insoluble mutant

SOD1 to 4.5% ±0.6. To confirm that both vectors were being successfully over-expressed in each case, samples were analysed by SDS-PAGE and Western blotting using either anti αB-crystallin or anti HSP 27 antibodies. The results shown in Figure 4.3 (D and E) show that this is indeed the case. In summary, over-expression of sHSPs decreased the amount of insoluble mutant SOD1 and consequently decreased mutant SOD1 inclusions in this HEK293 cell system.

Mutant sHSPs: are they involved in ALS?

Two recent reports have implicated mutant sHSPs in diseases related to ALS. Mutations in HSP 27 have been linked to CMT disease and distal hereditary motor neuropathy, and neuronal cells transfected with mutated HSP 27 showed a reduced viability when compared to cells expressing wt protein (Evgrafov et al., 2004). Similarly, mutations in HSP 22 have been identified in families with distal hereditary motor neuropathies and cultured cells transfected with mutated HSP 22 formed intracellular inclusions (Irobi et al., 2004). The residues which are mutated in these sHSPs; K141 in HSP 22 and S135 in HSP 27, are conserved residues located in the core α-crystallin domain and hence disrupt protein structure. Is it possible, therefore, that over-expression of mutant sHSPs in our model cell system might have a similar affect and exacerbate the proportion of insoluble mutant SOD1.

Experiments were carried out as described previously, but this time the sHSPs that were co-expressed carried mutations, namely R120G αB-crystallin, S135F and R140G HSP 27. R120G αB-crystallin is the mutation which has been linked to DRM (Perng et al., 1999b) and S135F HSP27 has been linked to CMT disease and distal hereditary motor neuropathy, as described above. Indeed, as shown in Figure 4.4, the presence of these sHSP mutants within the

cell gave rise to increased amounts of insoluble SOD1. Again, using OptiQuant Imaging software, co-expression of R120G αB-crystallin increased the amount of insoluble mutant SOD1 from 22.4% ± 0.01 to 31.8% ± 1.0. In the case of S135F and R140G HSP 27, the amount of insoluble SOD1 was increased from 22.4% ± 0.01 to 30.9% ± 0.4 and 37.3% ± 0.4, respectively.

Thus, sHSPs carrying mutations further exacerbate insoluble mutant SOD1 inclusion formation in this HEK293 cell system. This raises the question as to whether these proteins merely add to the insult on the cell which is already compromised by the presence of mutant SOD1, or whether they are exerting an affect by themselves? To provide insights into this, we co-expressed these mutant sHSPs with wt SOD1. If over-expressed, even in the presence of proteasome inhibitor, wt SOD1 is soluble and no inclusions are formed. Consequently, any affects resulting from the co-expression of mutant sHSPs would be apparent following the preparation and analysis of the soluble and insoluble cell extracts, as described above. Over-expression of R120G αB-crystallin with wt SOD1 increased the amount of insoluble material by 15.3% ± 0.8. In the case of S135F and R140G HSP 27, these values were 15.3% ± 0.5 and 12.2% ± 0.2, respectively. The Western Blots are shown in Figure 4.5. Therefore, these data suggest that mutations in sHSPs result in the formation of inclusions by SOD1, which is soluble under normal conditions. It could be possible, however, that this affect is not specific for SOD1, but is a general affect of the mutant sHSPs. This has not been addressed in this instance, but is an interesting matter for further investigation.

Viability of HEK293 cells in the presence and absence of wt and mutant sHSPs

What affect do these mutant SOD1 inclusions have on the cells in which they are present? Do they, for example, affect cell viability? Durham et al., (1997) and Takeuchi et al., (2002), have demonstrated that mutant SOD1 inclusions do affect cell viability, both in cultured primary MNs and a neuroblastoma cell line. Here, we used a cell viability assay kit (see Materials and Methods) to assay HEK293 cell viability in the presence and absence of mutant SOD1 and mutant SOD1 inclusions. The effects of expression of wt and mutant sHSPs on cell viability were also assessed. The results are shown in Figure 4.6. Over-expression of wt SOD1 and G85R mutant SOD1 had no effect on cell viability. However, mutant SOD1 inclusion formation, induced by over-expression of G85R mutant SOD1 and subsequent proteasome inhibition, reduced cell viability by approximately 50%. This was significantly different from cells treated with proteasome inhibitor only ($p<0.001$). When mutant SOD1 was co-expressed, in the presence of proteasome inhibitor, with αB-crystallin and HSP 27, cell viability was not significantly affected. Similar findings were obtained when mutant sHSPs were co-expressed; cell viability was not significantly affected.

In conclusion, mutant SOD1, in the presence of the proteasome inhibitor ALLN, resulted in a decrease in HEK293 cell viability. From the IMF studies described in chapter 3, over-expression of mutant SOD1 in the presence of ALLN caused inclusion formation, so it can be assumed that mutant SOD1 inclusion formation leads to a decrease in HEK293 cell viability. Co-expression of sHSPs, whether wt or mutant, does not significantly affect cell viability.

Conclusions and discussion

It has been shown that over-expression of G85R mutant SOD1 in HEK293 cells, and subsequent proteasomal inhibition results in the formation of mutant SOD1 inclusions. It has also been shown that this process is affected by sHSPs: αB-crystallin and HSP 27 decrease the amount of insoluble mutant SOD1 and thus act to prevent mutant SOD1 inclusion formation. Mutation of these proteins abolishes these affects and in fact makes the situation worse; their presence coincides with increases in insoluble mutant SOD1 and consequently mutant SOD1 inclusion formation. Results from the cell viability studies show that over-expression of mutant SOD1 and proteasomal inhibition, corresponding to mutant SOD1 inclusion formation, caused a decrease in HEK293 cell viability. Under these conditions, co-expression of wt and mutant sHSPs did not appear to significantly effect viability.

It remains to be determined whether these effects or wt sHSPs will be of benefit in ALS treatment. A report by Kieran et al., (2004), has shown that up-regulation of HSPs, by using a co-inducer of the heat shock response, increases life expectancy in a mouse model of ALS. However, this report did not discuss the mechanisms by which this HSP up-regulation exerts its effects. There is still some controversy as to whether inclusions are formed as a protective mechanism in order to sequester soluble, toxic proteins, or whether it is the inclusions themselves that are toxic, due to sequestration of other cellular proteins or disruption of cellular pathways and responses. To some extent, this appears to be disease dependent. For example, Lewy bodies in Parkinson's disease are thought to have a causative role in the disease, whereas nuclear inclusions in polyglutamine diseases are thought to be protective (reviewed by Tran and Miller, 1999). Although reports by Bruening et al., (1997) and

Takeuchi et al., (2002) suggest that mutant SOD1 inclusion formation causes cell death, a study by Lee et al., (2002) showed that the number of cells with mutant SOD1 inclusions, and the inclusion burden per cell had no significant effect on cell viability and that increased cell viability was not linked to a decrease in inclusions.

Co-expression of wt sHSPs decreases the amount of insoluble mutant SOD1, which in turn, does not significantly affect cell viability. The mutations in αB-crystallin and HSP 27 result in their inability to fold correctly and as a consequence cause them to become more prone to aggregation themselves. This indirectly leads to loss of function (Perng et al., 1999b; Chavez Zobel et al., 2003). Although co-expression of such mis-folded proteins with mutant SOD1 causes further increases in insoluble mutant SOD1, this does not significantly effect cell viability.

Another interesting finding is that, in this model cell system, mutant sHSPs cause a normally soluble protein (wt SOD1) to aggregate. It is not known whether this is specific for SOD1, or whether these mutant sHSPs would have a similar effect on other soluble proteins. Mutations in HSP 22 and 27 have been linked to other neurodegenerative diseases (Irobi et al., 2004 and Evgrafov et al., 2004). Is it possible that sHSPs are also mutated in ALS? The exact mechanisms by which mutant SOD1 exerts its effects in ALS disease pathogenesis remain to be determined. It may be possible that in some cases, mutations which render the protein folding machinery defective, play a role. What about the vast majority of ALS cases that are not linked to mutations in SOD1? Are mutations in chaperone proteins seen here? Presently, all these questions remain unanswered, but studies designed to address them will be important.

Figure 4.1 Mutant, but not wt SOD1, is insoluble

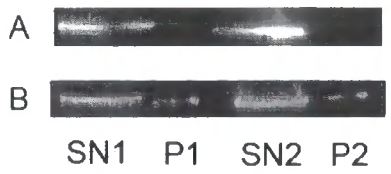

HEK293 cells were transiently transfected with wt or G85R mutant SOD1 and treated with 6.25μgml^{-1} ALLN to induce inclusion formation. Twenty-four hours after transfection, the cells were harvested and cell extracts prepared. These were then subjected to a series of centrifugation steps to obtain soluble and insoluble fractions (see Materials and Methods for details). These fractions were run on 12% (w/v) polyacrylamide gels and analysed for the presence of SOD1 by Western blotting using an anti-SOD1 antibody. (A) Fractions from cells transfected with wt SOD1, (B) Fractions from cells transfected with G85R mutant SOD1. Key: SN1 – supernatant 1; P1 – pellet 1 (both from the low speed centrifugation step); SN2 – supernatant 2; P2 – pellet 2 (both from the high speed centrifugation step). In the case of both wt and mutant fractions, SOD1 is soluble: SOD1 is present in the two supernatant fractions. However, in the case of the mutant fraction, some of the SOD1 is insoluble and consequently detected in the pellet fractions.

Figure 4. 2 Co-expression of G85R mutant SOD1 and αB-crystallin using the pBUD expression vector

To study the effects of sHSPs on mutant SOD1 inclusion formation, we used a mammalian expression vector, pBUD, with two multiple cloning sites, for simultaneous expression of two different proteins. A pBUD vector containing both G85R SOD1 and αB-crystallin was cloned, and transiently transfected into our HEK293 cell system, as described in Materials and Methods. Cells were treated with proteasome inhibitor and processed for IMF microscopy. A-D show cells containing YFP-tagged G85R mutant SOD and E-H show the same cells stained for αB-crystallin. This panel of images shows that some cells express one protein, but not the other (C and G, D and H), thus demonstrating that the pBUD vector was not functioning correctly. In other cases, one cell may show expression of both proteins at comparable levels, whereas another cell shows similar expression of one protein and decreased expression of the other (A and E, B and F). For this reason, subsequent transfections were carried out using two separate vectors.

Figure 4.2

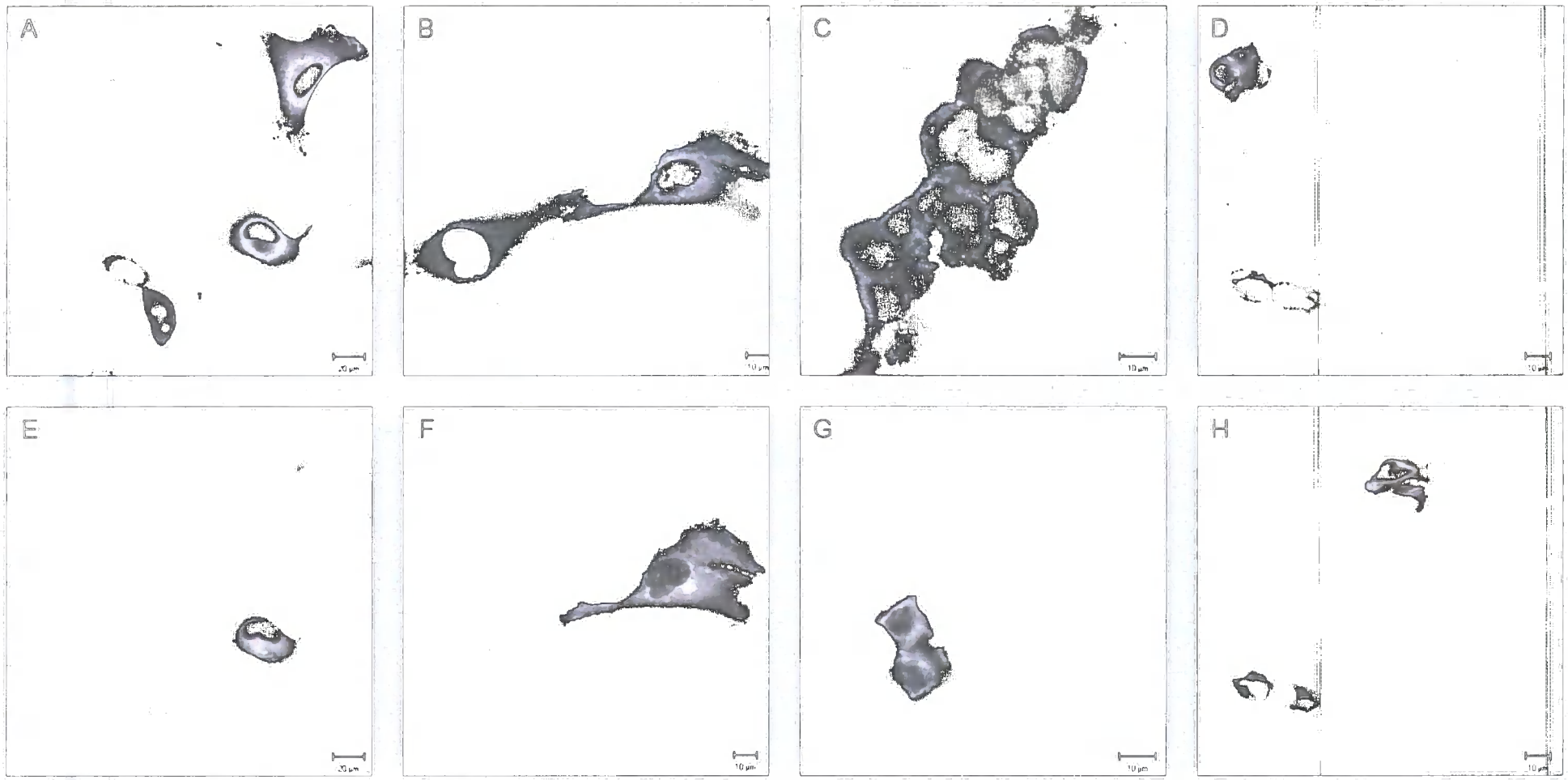

Figure 4.3 sHSPs decrease the amount of insoluble G85R mutant SOD1

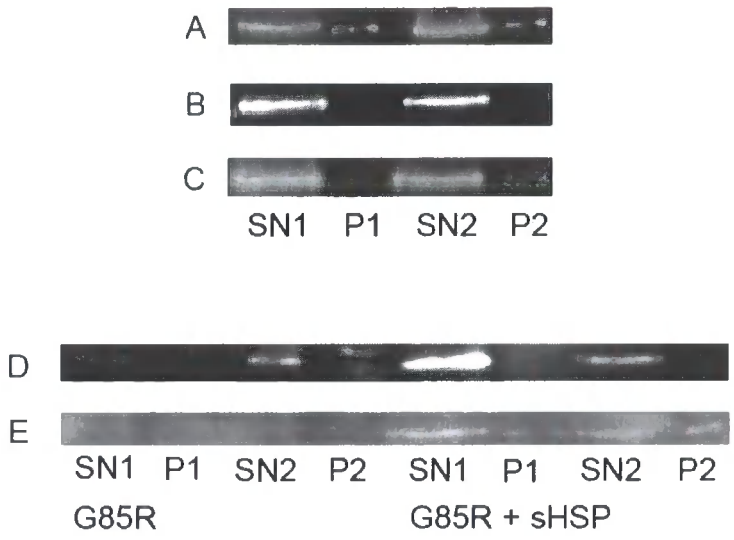

HEK293 cells were transiently transfected with G85R mutant SOD1 together with either αB-crystallin or HSP 27 and soluble and insoluble extracts prepared, as described previously. These fractions were run on 12% (w/v) polyacrylamide gels and analysed for the presence of SOD1 by Western blotting using an anti-SOD1 antibody. The figure shows that co-expression of sHSPs results in a decrease in the amount of insoluble SOD1, as indicated by the decreased intensity of the pellet fractions in the presence of sHSPs. (A) G85R mutant SOD1 only. (B) G85R mutant SOD1 and αB-crystallin. (C) G85R mutant SOD1 and HSP 27. To confirm that both vectors were being successfully over-expressed, these fractions were run on 12% gels and Western blotted using anti αB-crystallin or anti HSP 27 antibodies. (D) shows successful over-expression of αB-crystallin compared to controls and (E) shows successful over-expression of HSP 27 compared to controls. Key: SN1 – supernatant 1; P1 – pellet 1 (both

prepared by the low speed centrifugation step); SN2 – supernatant 2; P2 – pellet 2 (both prepared by the high speed centrifugation step).

Table 4.1
Percentage of mutant SOD1 in pellet fractions

	P1	P2	Total P
A	7.4 ± 0.5	15 ± 0.4	22.4 ± 0.1
B	0	0	0
C	0	4.5 ± 0.6	4.5± 0.6

Table 4.1 shows the amount of mutant SOD1 in each of the pellet fractions, as a percentage of total SOD1, for each cell treatment. (A) G85R mutant SOD1 only. (B) G85R mutant SOD1 and αB-crystallin. (C) G85R mutant SOD1 and HSP 27. P1 – pellet 1, P2 – pellet 2 and total P – total pellet material.

Figure 4.4 Mutant sHSPs further increase the amount of insoluble G85R SOD1

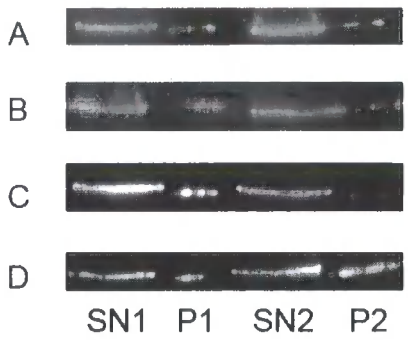

HEK293 cells were transiently transfected with G85R mutant SOD1 together with either R120G mutant αB-crystallin, S135F or R140G mutant HSP 27. Soluble and insoluble extracts were prepared after 24 hr, as described previously. These fractions were run on 12% (w/v) polyacrylamide gels and analysed for the presence of SOD1 by Western blotting using an anti-SOD1 antibody. The figure shows that co-expression of mutant sHSPs further increases the amount of insoluble SOD1, as indicated by the increased intensity of the pellet fractions in the presence of mutant sHSPs. (A) G85R mutant SOD1 only. (B) G85R mutant SOD1 and R120G αB-crystallin. (C) G85R mutant SOD1 and S135F HSP 27. (D) G85R mutant SOD1 and R140G HSP 27. Key: SN1 – supernatant 1; P1 – pellet 1 (both prepared from the low speed centrifugation step); SN2 – supernatant 2; P2 – pellet 2 (both prepared from the high speed centrifugation step).

Table 4.2
Percentage of mutant SOD1 in pellet fractions

	P1	P2	Total P
A	7.4 ± 0.5	15 ± 0.4	22.4 ± 0.05
B	21.8 ± 1.1	10 ± 0.5	31.8 ± 1
C	22.7 ± 0.7	8.1 ± 1.1	30.7 ± 0.4
D	7.9 ± 0.8	29.4 ± 0.4	37.3 ± 0.5

Table 4.2 shows the amount of mutant SOD1 in each of the pellet fractions, as a percentage of total SOD1, for each cell treatment. (A) G85R mutant SOD1 only. (B) G85R mutant SOD1 and R120G αB-crystallin. (C) G85R mutant SOD1 and S135F HSP 27. (D) G85R mutant SOD1 and R140G HSP 27. P1 – pellet 1, P2 – pellet 2 and total P – total pellet material.

Figure 4.5 Mutant sHSPs affect the solubility of wt SOD1

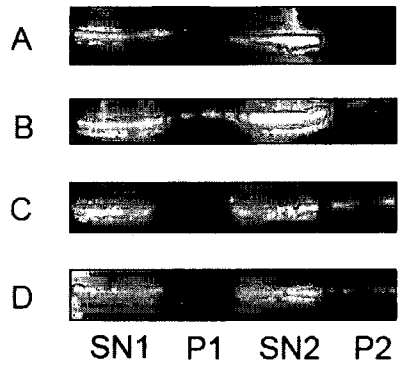

HEK293 cells were transiently transfected with wt SOD1 together with either R120G mutant αB-crystallin, S135F or R140G mutant HSP 27. Soluble and insoluble extracts were prepared after twenty-four hr, as described previously. These fractions were run on 12% (w/v) polyacrylamide gels and analysed for the presence of SOD1 by Western blotting using an anti-SOD1 antibody. The results show that normally, wt SOD1 is soluble. However, the presence of mutant sHSPs affects the solubility of this wt SOD1: in their presence, some of the SOD1 is shifted into the insoluble fraction. (A) wt SOD1 only. (B) wt SOD1 and R120G αB-crystallin. (C) wt SOD1 and S135F HSP 27. (D) wt SOD1 and R140G HSP 27. Key: SN1 – supernatant 1; P1 – pellet 1 (both prepared from the low speed centrifugation step); SN2 – supernatant 2; P2 – pellet 2 (both prepared from the high speed centrifugation step).

Table 4.3
Percentage of mutant SOD1 in pellet fractions

	P1	P2	Total P
A	0	0	0
B	11.9 ± 0.5	3.4 ± 0.4	15.3 ± 0.8
C	0	15.3 ± 0.5	15.3 ± 0.5
D	0	12.2 ± 0.2	12.2 ± 0.2

Table 4.3 shows the amount of mutant SOD1 in each of the pellet fractions, as a percentage of total SOD1, for each cell treatment. (A) wt SOD1 only. (B) wt SOD1 and R120G αB-crystallin. (C) wt SOD1 and S135F HSP 27. (D) wt SOD1 and R140G HSP 27. P1 – pellet 1, P2 – pellet 2 and total P – total pellet material.

Figure 4.6 The effects of sHSPs on the viability of mutant SOD1 inclusion containing HEK293 cells

The figure shows the cell viability of HEK293 cells containing G85R mutant SOD1 inclusions, in the presence and absence of wt and mutant sHSPs. Cells were transiently transfected with the appropriate SOD1 constructs and cell viability assays carried out after twenty-four hours, as described in Materials and Methods. The results shown are the mean values ± SD. Over-expression of wt SOD1 and G85R mutant SOD1 had no effect on cell viability. However, mutant SOD1 inclusion formation, induced by over-expression of G85R mutant SOD1 and subsequent proteasome inhibition, reduced cell viability by approximately 50%. This was significantly different from cells treated with proteasome inhibitor only ($p<0.001$). When mutant SOD1 was co-expressed, in the presence of proteasome inhibitor, with αB-crystallin and HSP 27, cell viability was not significantly affected. Similar findings were obtained when mutant sHSPs were co-expressed; cell viability was not significantly affected.

Figure 4.6

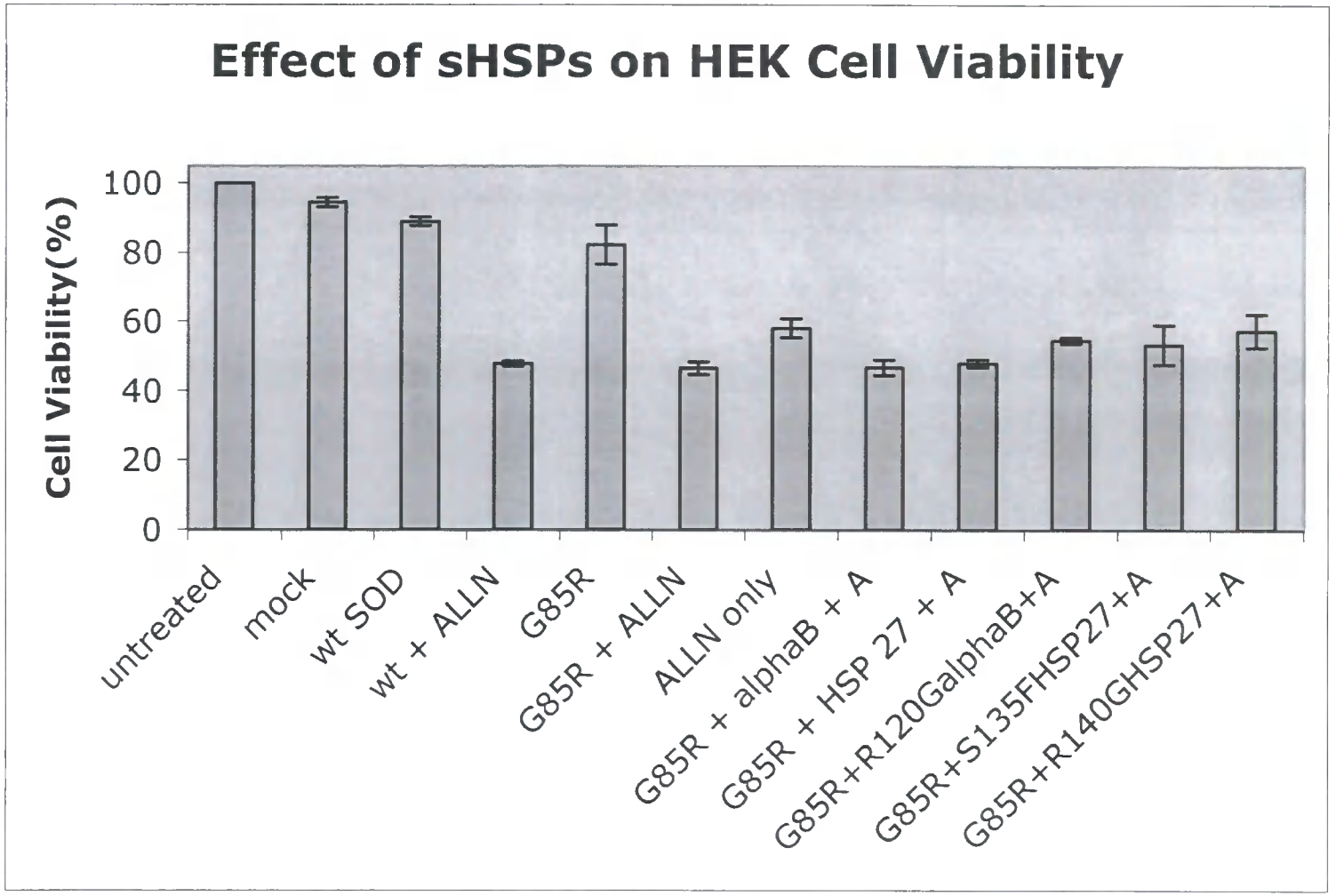
Effect of sHSPs on HEK Cell Viability
Cell Viability(%)
100
80
60
40
20
0
untreated
mock
wt SOD
wt + ALLN
G85R
G85R + ALLN
ALLN only
G85R + alphaB + A
G85R + HSP 27 + A
G85R+R120GalphaB+A
G85R+S135FHSP27+A
G85R+R140GHSP27+A

CHAPTER 5
SOD1 *in vitro* INTERACTIONS STUDIES

The aim of this project is to investigate the role of sHSPs in mutant SOD1 inclusion formation. As well as carrying out these studies in our model cell system, the *in vitro* interactions of SOD1 with sHSPs can also be studied.

Copper and zinc are required for bacterial expression of SOD1

In order to study SOD1 interactions *in vitro*, it was first necessary to produce recombinant SOD1. Wild-type (wt) SOD1 was cloned into the pET23b vector (see Materials and Methods section 2.9). Once this was completed, small scale bacterial inductions were set up to ascertain the best conditions for expression of wt SOD1. BL21(DE3)plysS were transformed with the pET vector and a single colony used to inoculate a starter culture. Then a 50ml culture was grown to the log phase of growth and the bacteria induced with 0.5mM IPTG. Samples were taken before induction and at 1hr intervals for the next 3 hr and samples analysed on 12% (w/v) SDS-PAGE gels with Coomassie Blue staining. The results are shown in Figure 5.1A. Although it is clear from this that there was an increase in the amount of one of the proteins over time, re-running of the gel and Western Blotting, using a monoclonal SOD1 antibody showed that this protein was not SOD1 (Figure 5.1B), as SOD1 was present at similar levels, both before and after induction. This may be due to the codon usage for arginine in the SOD1 construct. BL21(DE3)plysS have preference for specific arginine codons. Rosetta cells, another strain of *E.coli* which can be used for bacterial expression, have different arginine codon preferences and were used to try and overcome this problem. The experiment was repeated using Rosetta

cells, but the results (Figure 5.1C) show that there was no induction of any protein.

SOD1 is a metalloenzyme, which requires both copper and zinc ions as co-factors. Maybe a lack of these metal ions in the growth media was causing this deficiency in bacterial expression. 2μM copper and zinc sulphate were added to the growth media and used to culture BL21(DE3)plysS. The growth of these cells in the presence and absence of copper and zinc sulphate was monitored and no differences were observed. The induction experiments described above were then carried out using BL21(DE3)plysS, grown in the presence of copper and zinc ions. These conditions allowed successful induction of wt SOD1, as shown by SDS-PAGE and Coomassie staining and confirmed by Western Blotting (Figure 5.1D).

Recombinant wt SOD1 was purified as insoluble material from inclusion bodies and also as soluble protein. Insoluble SOD1 was purified from the bacterial pellet as described in Materials and Methods, and eluted on a Fractogel EMD BioSEC 650 column, using a linear gradient of 0-1M NaCl in 6M urea buffer. Eluate fractions were collected and the SOD1 positive fractions determined by SDS-PAGE and Coomassie staining and pooled. The results are shown in Figure 5.2A. For soluble SOD1, the purification was carried out as described in Materials and Methods and eluted on a TMAE sepharose column using a gradient of 0-1M NaCl in a 20mM TrisHCl buffer. Again, eluate fractions were collected and the SOD1 positive fractions determined by SDS-PAGE and Coomassie staining and pooled. The results are shown in figure 5.2B.

Interaction of recombinant SOD1 with αB-crystallin: immunoprecipitation studies

After the successful purification of recombinant wt SOD1 from the bacterial expression system, as both soluble and insoluble protein, *in vitro* experiments were set up to determine whether SOD1 interacts with αB-crystallin. As well as wt SOD1, three different mutants were also used, namely G37R, G85R and G93A. These were kind gifts from Lawrence Hayward (University of Massachusetts). αB-crystallin was kindly provided by Ming Perng (University of Durham). Initially, IP experiments were set up. 10μg each of SOD1 (wt or mutant) and αB-crystallin were incubated at room temperature for 1 hr prior to addition of a monoclonal αB-crystallin antibody for the precipitation step, as described in Materials and Methods. SDS-PAGE on 12% (w/v) gels and Western Blotting, using a polyclonal SOD antibody, were used to analyse the samples. The results are shown in Figure 5.3. Figure 5.3A shows that SOD1, both wt and the two mutants (G85R and G93A), interact with αB-crystallin *in vitro*. Samples from IP using a monoclonal αB-crystallin antibody contain SOD1, as shown by Western Blotting with a polyclonal SOD1 antibody. Figure 5.3B, however, shows results from a control experiment, in which the IP step was omitted. Here, the same results were obtained, indicating that SOD1 interacts with the protein G-coupled beads and thus the interaction seen in Figure 5.3A is not a specific interaction.

Interaction of recombinant SOD1 with αB-crystallin: size exclusion chromatography studies

The results from the IP experiments were inconclusive due to an artificial interaction between SOD1 and the protein G-coupled beads themselves.

Another method of investigating interactions between two proteins is by using SEC. This method is based on the retention time of large and small particles passing through a column. Large particles pass through with a short retention time, whereas smaller ones have a longer retention time, due to adsorption by the column material. If two proteins interact, a shift in particle size occurs, reflected by a shift in retention time. We used this method, as described in Materials and Methods, to see if SOD1 interacts with. αB-crystallin. wt SOD1 and 3 mutant SOD1s were used in these studies. The SEC traces obtained for both wt and mutant SOD1 were the same, whether in the presence or absence of αB-crystallin (Figure5.4). This suggests that neither wt nor mutant SOD1 interacts with αB-crystallin. This was somewhat unexpected, given the results obtained using our model cell system, which showed that sHSPs including αB-crystallin co-localise with mutant SOD1 and have a role in increasing its solubility.

Interaction of recombinant SOD1 with αB-crystallin: Biacore studies

One last method was used to study the possible interaction between SOD1 and αB-crystallin. The Biacore chip system is available in our department. The Biacore system monitors biomolecular interactions on the surface of a sensor chip. One molecule, in this case αB-crystallin, is immobilised on the surface of the chip, whilst the other molecule(s), in this case the wt and mutant SOD1, are injected in a continuous flow over the surface of the chip. Changes in the mass concentration at the surface, which indicate interactions, are then monitored. Using this system, we show that there is no interaction between αB-crystallin and either wt or mutant SOD1. These studies were carried out at several

different temperatures, including the physiological temperature of 37°C. These data are consistent with those obtained using SEC.

Conclusions

We have used two independent methods to study the possible interaction of both wt and mutant SOD1 with αB-crystallin, and both have shown that both wt and mutant SOD1 do not interact with αB-crystallin *in vitro,* even at 37°C. This is somewhat unexpected, given the results obtained using our model cell system, which show that sHSPs including αB-crystallin co-localise with mutant SOD1 and have a role in increasing its solubility. It is possible that the interaction occurring *in situ* in the HEK293 cell system is not a direct interaction, but one involving other proteins. This may explain why no interaction was observed between SOD1 and αB-crystallin *in vitro.* This is unlikely, however, as a report by Shinder et al., (2001), showed co-immunoprecipitation of mutant SOD1 with HSP 70, 40 and αB-crystallin. It is possible that the two methods used here were not best suited to these types of studies and that other methods of studying *in vitro* interactions may have yielded different results. Also, the SOD1 used in these *in vitro* studies was in a soluble form, and it would also be of interest to investigate possible interactions between aggregated insoluble SOD1 and αB-crystallin. Unfortunately this was not possible in the time available.

Figures 5.1A and B Bacterial induction of SOD1 in BL21(DE3)plysS

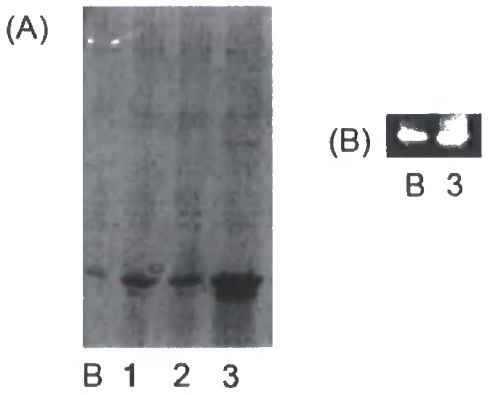

BL21(DE3)plysS were transformed with a pET23 vector containing a wt SOD1 construct. A single colony was used to inoculate a starter culture and this used to inoculate a 50ml culture. At the log phase of growth, the bacteria were induced with 0.5mM IPTG. Samples were taken before induction and at 1hr intervals over the next 3 hr, before analysis on 12% SDS-PAGE gels with Coomassie staining. The gel in (A) shows induction of a protein of approximately 20kDa, a similar size to SOD1 (17kDa). When two samples were re-run and Western blotted (before and 3 hr after induction), however, the amounts of SOD1 in each were shown to be similar (B), indicating that the induced protein was not actually SOD1.

Key: B – before induction, 1 – 1hr after induction, 2 – 2hr after induction and 3 – 3hr after induction.

Figure 5.1C Bacterial induction of SOD1 in Rosetta cells

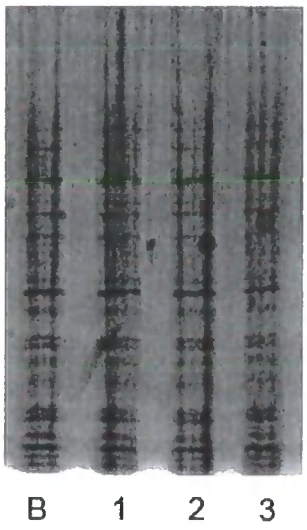

A bacterial induction was set up using Rosetta cells. These cells were transformed with a wt SOD1 containing pET vector. A single colony was used to inoculate a starter culture and this used to inoculate a 50ml culture. At the log phase of growth, the bacteria were induced with 0.5mM IPTG. Samples were taken before induction and then after induction at 1hr intervals for 3 hr. These samples were analysed by 12% SDS-PAGE and Coomassie staining, as shown. This figure shows that no protein induction occurred under these conditions.

Key: B – before induction, 1 – 1hr after induction, 2 – 2hr after induction and 3 – 3hr after induction.

Figures 5.1D and E Bacterial induction of SOD1 in the presence of copper and zinc

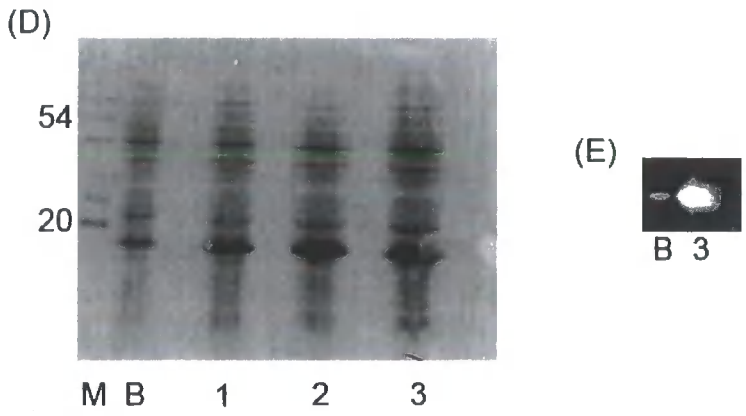

A bacterial induction was set up, using BL21(DE3)plysS grown in media containing 2μM copper and zinc sulphate. These cells were transformed with a wt SOD1 containing pET vector. A single colony was used to inoculate a starter culture and this used to inoculate a 50ml culture. At the log phase of growth, the bacteria were induced with 0.5mM IPTG. Samples were taken before induction and then after induction at 1hr intervals for 3 hr. These samples were analysed by 12% SDS-PAGE and Coomassie staining. As shown in (D), the amount of a protein, approximately 17kDa, increases over time after induction. Two samples were re-run (before and 3 hr after induction), and Western blotting using an anti-SOD1 antibody confirmed that this protein was indeed SOD1 (E).

Key: B – before induction, 1 – 1hr after induction, 2 – 2hr after induction and 3 – 3hr after induction. M – molecular weight in kD.

Figure 5.2A Purification of insoluble SOD1

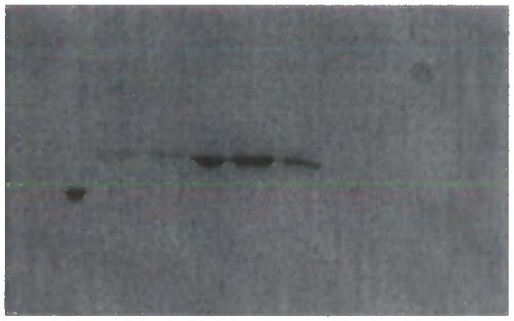

The fractions eluted from the TMAE column, used to purify insoluble SOD1 from inclusion bodies, were analysed by SDS-PAGE on 15% gels and visualised by Coomassie staining. As shown here, some of the fractions were SOD1 positive, and these were pooled for use in subsequent *in vitro* studies. M – bovine SOD marker, 15.6kDa.

Figure 5.2B Purification of soluble SOD1

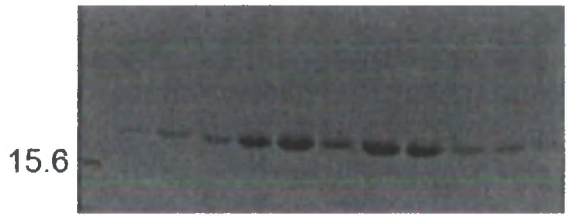

The fractions eluted from the TMAE column, used to purify soluble SOD1 from the bacterial expression system, were analysed by SDS-PAGE on 15% gels, with Coomassie staining. As shown here, some of the fractions were SOD1 positive, and these were pooled and for use in subsequent *in vitro* studies. M – bovine SOD1 marker, 15.6kDa.

Figure 5.3 Immunoprecipitation results

(A)

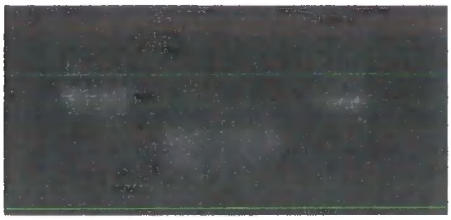

G93A G85R wt

(B)

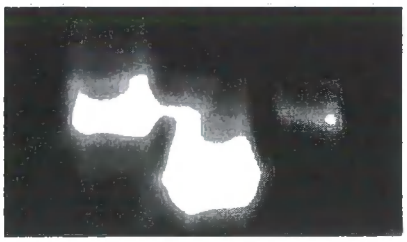

G93A G85R wt

This figure shows results from IP experiments. The IP was carried out as described in Materials and Methods section 2.12. Samples were analysed by SDS-PAGE and Western Blotting, using a polyclonal SOD1 antibody. (A) shows that wt, G85R and G93A mutant SOD1 all interact with αB-crystallin, as in each case SOD1 is present in the immunoprecipitated material. (B), however, shows the results of the control experiment, in which the IP step was omitted. SOD1, both wt and mutant, is still present, indicating that SOD1 interacts non-specifically with the protein G-coupled beads.

Figure 5.4A Size exclusion chromatography traces

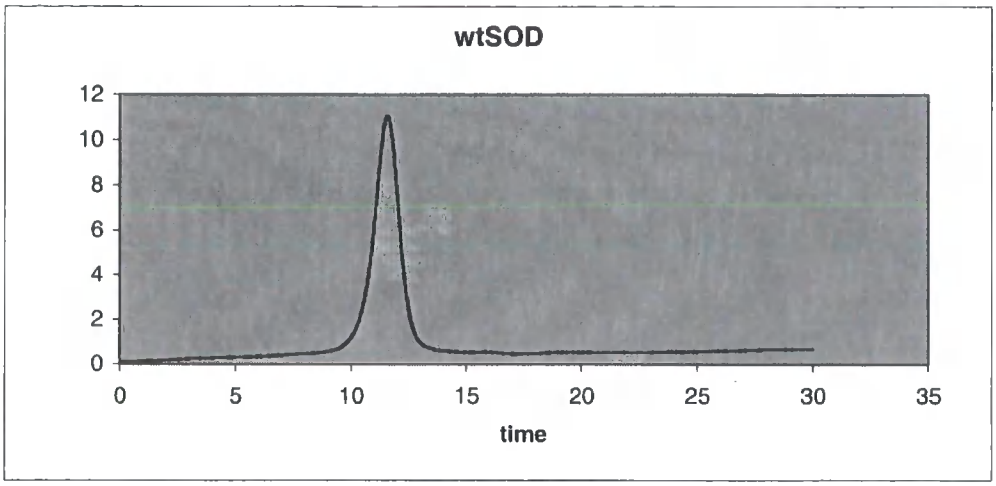

Figure 5.4B

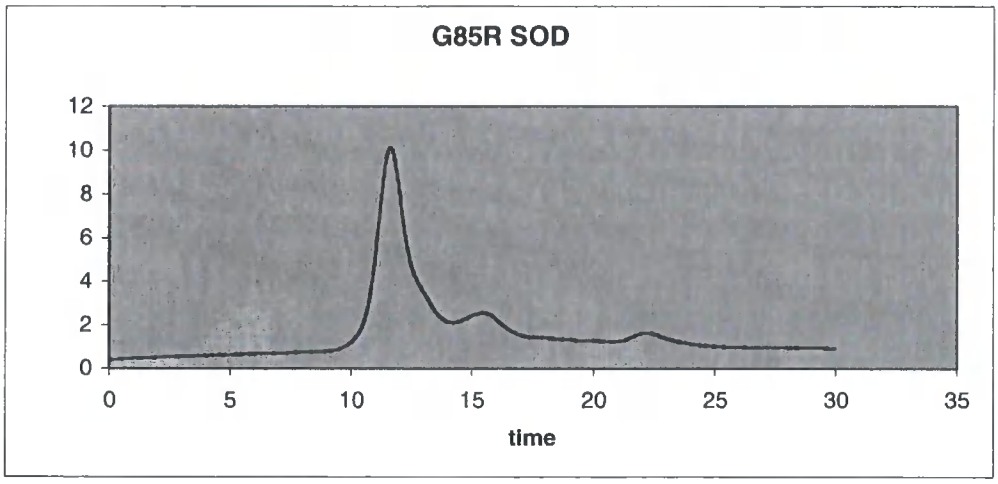

Figure 5.4C

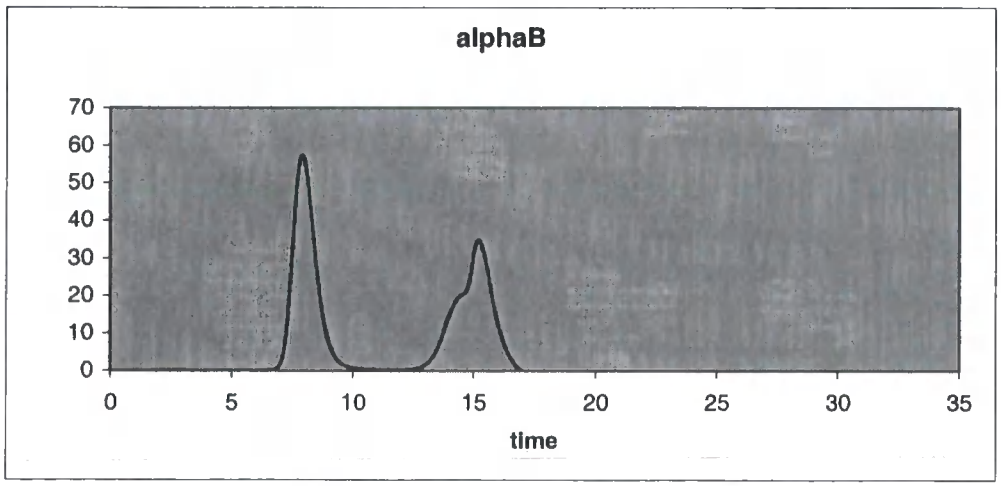

Figure 5.4D

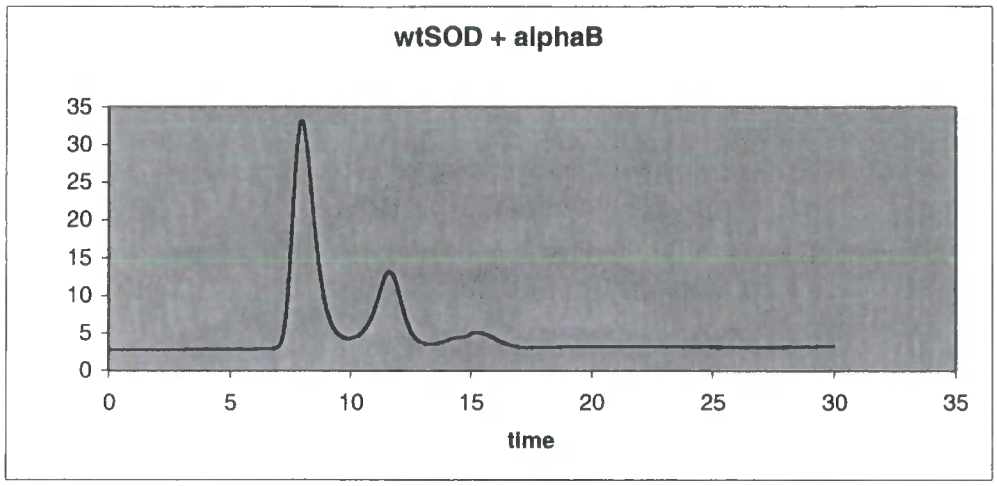

Figure 5.4E

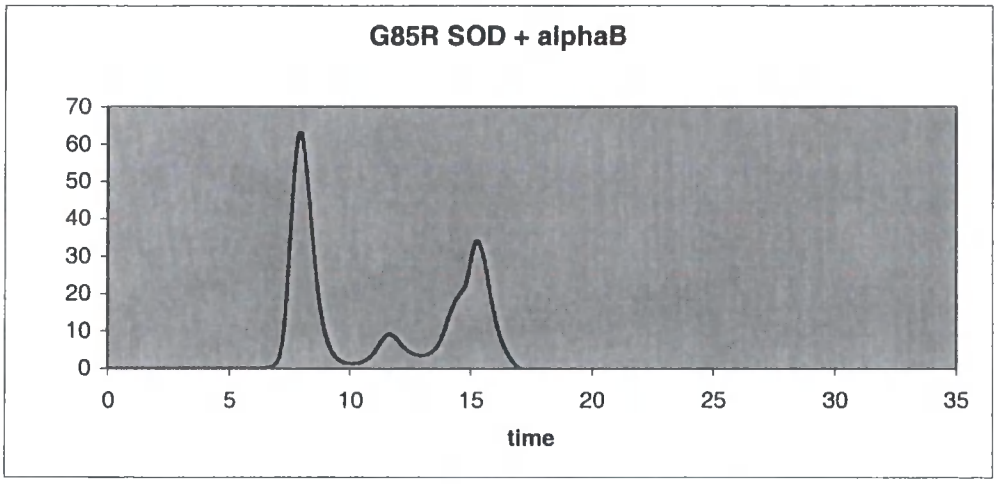

Figure 5.4A shows the SEC trace obtained for wt SOD1. The retention time of wt SOD1 is approximately 11min. This is the same as for G85R mutant SOD1 (figure 5.4B) and the other mutants. The small peak at 15min for the G85R mutant SOD1 trace is a component of the buffer. Figure 5.4C shows the trace obtained for αB-crystallin. The peak at 8min is the αB-crystallin and the later peak at 15min is unexpected, likely due to contamination. When SOD1, whether wt or mutant, is mixed with αB-crystallin, no interaction occurs. Figure 5.4D shows an αB-crystallin peak with an unchanged retention time of 8min and the wt SOD1 peak also has an unchanged retention time of 11min. Figure 5.4E

shows an αB-crystallin peak with an unchanged retention time of 8min and the G85R mutant SOD1 peak also has an unchanged retention time of 11min. If these proteins were interacting, a change in size would occur, resulting in a shift in retention time.

NB – the traces for the other two mutants, G37R and G93A, are not shown here, but in each case are the same as for G85R mutant SOD1.

CHAPTER 6
PARALLEL STUDIES IN NEURONAL CELLS

The results presented here have shown that sHSPs influence mutant SOD1 inclusion formation in a HEK293 cell model system. Although mutant SOD1 inclusions are observed in MNs and astrocytes of G85R mutant SOD1 transgenic mice (Bruijn et al., 1998) and in spinal cord samples from FALS patients (Shibta et al., 1996), it is MNs that undergo selective degeneration during disease progression. A neuronal cell model system would, therefore, be more appropriate to study sHSP involvement in mutant SOD1 linked-FALS. Thus, parallel studies were carried out in a murine neuroblastoma cell line: Neuro 2a (N2a) cells. Mutant SOD1 inclusion formation was induced in these cells and the insoluble SOD1 analysed biochemically. The data obtained was then compared to that obtained using the HEK293 cell system, and possible insights into the selective vulnerability of MNs determined.

Initially, N2a cells were transiently transfected with either YFP-tagged wt or G85R mutant SOD1 and processed for subsequent IMF microscopy, as described in Materials and Methods. Figure 6.1 shows a representative confocal image of N2a cells transfected with YFP-tagged G85R mutant SOD1. Propidium iodide was used to stain the nuclei. The image shows that over-expression of G85R mutant SOD1 alone did not result in mutant SOD1 inclusion formation. This result was the same as that obtained for HEK293 cells. Figure 6.1 also shows that the transfection rate was low. In HEK293 cells, mutant SOD1 inclusion formation was induced by the addition of the proteasome inhibitor ALLN to cells over-expressing mutant SOD1. Accordingly, ALLN was also used to try and induce mutant SOD1 inclusion formation in N2a cells. A range of different ALLN concentrations was used, including the same concentration

(6.25μgml^{-1}) as that used to induce inclusion formation in HEK293 cells. However, at a concentration of 3μgml^{-1}, the N2a cells appeared to be more susceptible to the joint stresses of mutant SOD1 over-expression and proteasome inhibition, as they washed off the slides during processing. However, as shown in Figure 6.2, this concentration of ALLN was sufficient to induce inclusion formation in N2a cells over-expressing YFP-tagged G85R mutant SOD1.

To study the effects of sHSPs on insoluble mutant SOD1, YFP-tagged G85R mutant SOD1 was over-expressed and inclusion formation induced with ALLN, as described above. Twenty-four hrs after transfection, cell extracts were prepared and processed into soluble and insoluble fractions, as described in Material and Methods. However, biochemical analysis could not be carried out as the level of transfected SOD1 in these cell extracts was too low and could not be detected by Western blotting. As shown by the cell images in Figures 6.1 and 6.2 this was most likely due to the low transfection rate in this cell line.

An alternative method for determining the effects of sHSPs on mutant SOD1 inclusion formation in N2a cells is IMF microscopy. Although the transfection rate was low, it has been shown, none the less, that mutant SOD1 inclusion formation can be induced. Cells can then be scored for presence, or absence of inclusions under different experimental conditions. N2a cells were seeded onto chamber slides and transiently transfected with YFP-tagged G85R mutant SOD1 using GeneJuice, as described in Materials and Methods. Inclusion formation induced by the addition of 3μgml^{-1} ALLN 6hrs after transfection. Twenty-four hr after transfection, the cells were processed for subsequent IMF microscopy, as described in Materials and Methods. It was planned that cells could then be scored for the presence or absence of mutant

SOD1 inclusions. Unfortunately, these experiments were difficult to carry out. A large proportion of the cells were either rounded up, or detatched from the surface of the slide, which lead to ambiguity in the assigning of inclusions to cells. Also, as mentioned previously, a proportion of the cells washed off the slide surface during processing for IMF microscopy. This detachment could possibly bias the results obtained through such analysis, as it would be logical to suppose that those cells containing higher levels of transfected SOD1 are the most susceptible to do this. However, one observation made during this microscopic analysis was that the appearance of the SOD1 inclusions appeared to be different in the presence of sHSPs. The montage in Figure 6.3 shows examples of the different phenotypes of mutant SOD1 inclusions in N2a cells in the presence and absence of both αB-crystallin and HSP 27. In the absence of sHSPs, the inclusions are dense, tight structures, whereas in the presence of the sHSPs, they appear to be much more diffuse. Results published in a report by Takeuchi et al., (2002) support this observation. They showed that the over-expression of HSPs 70 and 40 in N2a cells changed the appearance of mutant SOD1 inclusions such that they became diffuse throughout the cytoplasm. These results would support our findings in the HEK293 cell system. Here, it was shown by biochemical analysis, that over-expression of wt sHSPs decreased the proportion of mutant insoluble SOD1. If there were less mutant insoluble SOD1 present within a cell, then it might be expected that the inclusion phenotype would become more diffuse.

The results from these N2a cell studies suggest that sHSPs decrease the amount of insoluble mutant SOD1. This supports our previous findings from the HEK293 cell model. The low transfection rates ruled out any biochemical analysis of insoluble mutant SOD1 within the cell but it has been shown that

over-expression of sHSPs changes the phenotype of mutant SOD1 inclusions, causing them to appear more diffusely distributed throughout the cytoplasm, as opposed to over-expression of mutant SOD1 alone, where inclusions appear as intense green structures.

If extra time had been available, it would have been of interest to use alternative neuronal cell lines or primary neuronal cultures in order to study the role of sHSPs in mutant SOD1 inclusion formation. The N2a cells, due to their low transfection rate and susceptibility to washing off the slides during IMF microscopy processing, were not a good model system. The N2a cells were transfected using GeneJuice, as described in Materials and Methods. One way to overcome this low transfection rate would be to use a viral transfection system, but it is possible that other neuronal cells would be easier to transfect. The ability to carry out biochemical analyses in neuronal cells would allow a direct comparison with the results obtained from the HEK293 cell system. At present, the results presented in this chapter support those from the HEK293 cell system, but more extensive studies on the role of sHSPs in mutant SOD1 inclusion formation in neuronal cells is required before any meaningful conclusions can be reached.

Figure 6.1 Over-expression of YFP-tagged G85R SOD1 in N2a cells

The figure shows two representative confocal images of N2a cells transfected with YFP-tagged G85R mutant SOD1. N2a cells were seeded onto chamber slides and transiently transfected with this mutant SOD1 construct. Twenty-four hrs following transfection, the cells were fixed and stained with propidium iodide (red), to visualise the nuclei. YFP-tagged SOD1 is green.

Figure 6.1

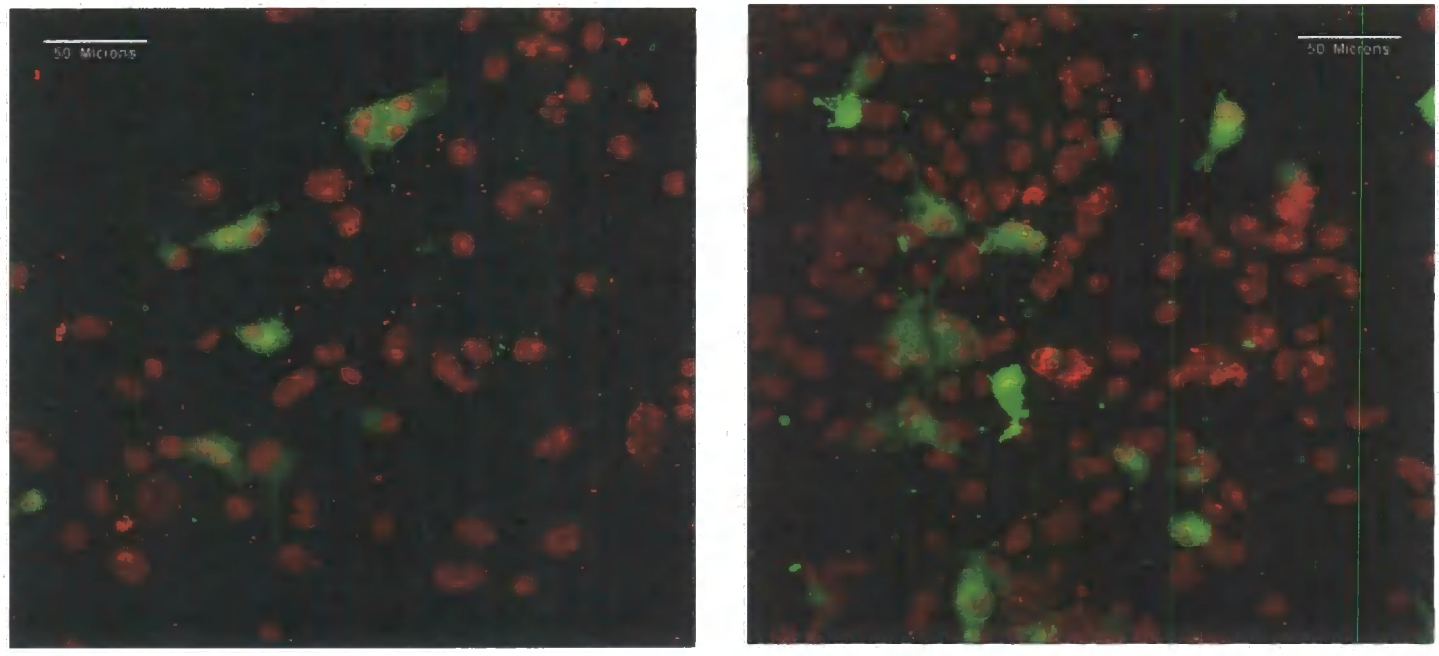

Figure 6.2 Proteasomal inhibiton induces inclusions in N2a cells over-expressing YFP-tagged G85R mutant SOD1

The proteasome inhibitor ALLN was used to induce inclusion formation in N2a cells over-expressing YFP-tagged G85R mutant SOD1. Cells were seeded onto chamber slides and transiently transfected with this mutant SOD1. Six hr after transfection, cells were treated with $3\mu gml^{-1}$ ALLN. After a further 18 hr in culture, the cells were fixed and stained with propidium iodide (red) to visualise the nuclei. YFP-tagged SOD1 is green.

Figure 6.2

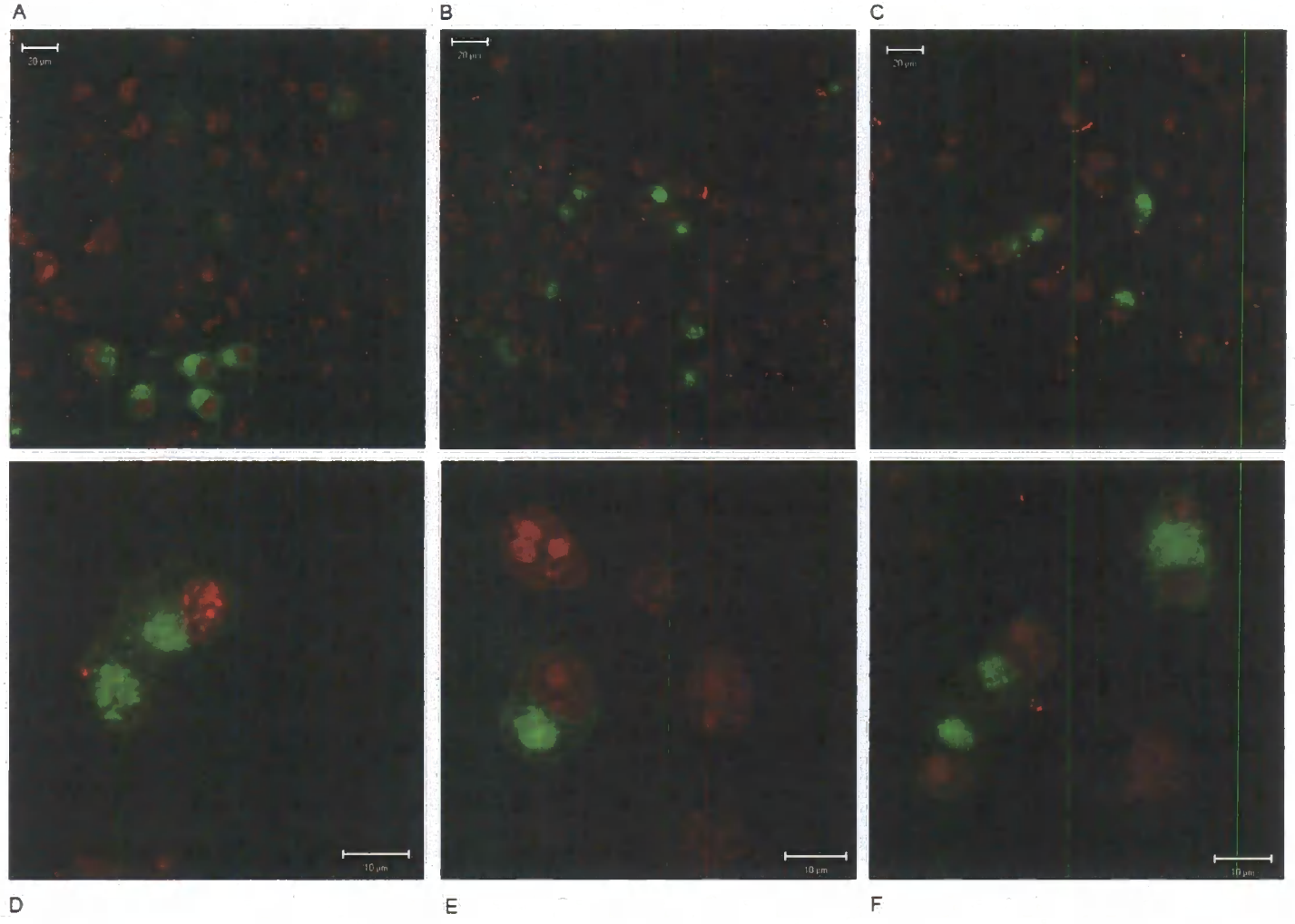

Figure 6.3 Over-expression of sHSPs changes the appearance of mutant SOD1 inclusions in N2a cells

The figure shows that when mutant SOD1 and sHSPs are co-expressed in N2a cells, the appearance of the inclusions changes. (A) Shows that over-expression of mutant SOD1 resultsin dense inclusions, whereas in (B-C) and (D-E), co-expression of αB-crystallin or HSP 27, respectively, changes the appearance of the inclusions to a diffuse pattern distributed throughout the cytoplasm. N2a cells were seeded onto chamber slides, transiently transfected with YFP-tagged G85R mutant SOD1, and either αB-crystallin of HSP 27. After 6 hr the cells were treated with $3\mu gml^{-1}$ ALLN to induce mutant SOD1 inclusion formation. After a further 18 hr in culture, the cells were fixed and stained, using the appropriate sHSP antibody. SOD1 is green and in each case sHSP is stained red.

Figure 6.3

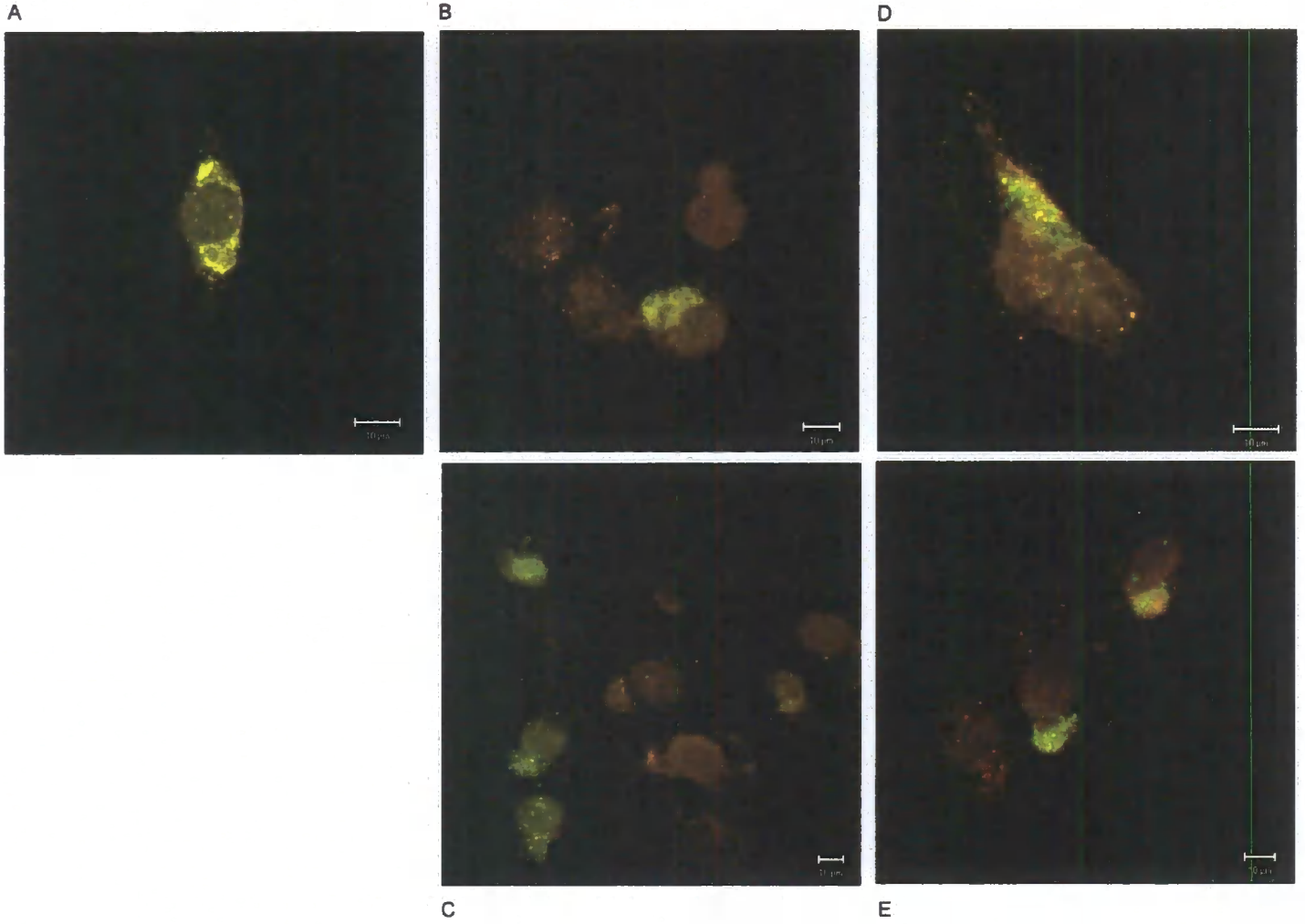

CHAPTER 7
DISCUSSION

ALS is a debilitating neurodegenerative disease, the most common adult onset motor neurone disease. The motor neurone diseases are a group of disorders affecting MNs. The primary pathogenic processes underlying ALS are currently unknown, but it is probable that multiple factors contribute to the disease mechanism. A number of major hypotheses have been postulated to explain disease progression, including cytoskeletal abnormalities (Xu et al., 1993, Cote et al., 1993), excitotoxicty (Rothstein et al., 1992, Shaw et al., 1994) and protein aggregation (Deng et al., 1993, Shibata et al., 1996, Durham et al., 1997). A number of these contributing factors have been discussed in the introduction. The work presented in this study has concentrated on the role of protein aggregation in ALS.

Protein aggregates or inclusions are a common feature of many neurodegenerative diseases, including Parkinson's, polyglutamine diseases such as Huntington's, SBMA and ALS. The process of aggregate or inclusion formation has been characterised (Johnston et al., 1998). They proposed that inclusion formation is a general cellular response to the accumulation of un-degraded or aggregated protein, which occurs when the capacity of the proteasomal degradation machinery, (the UPS), is saturated. They also proposed that once formed, these inclusions are delivered, by retrograde transport on MTs, to an Ub containing structure at the MTOC. Here, they are ensheathed in IF protein and the resultant aggregates are called aggresomes. Whether protein inclusions are toxic, or whether they act as a 'sink', protecting the cell against toxic soluble intermediates, is an area of controversy in this field. To some extent, it appears to be disease specific (reviewed by Tran and

Miller, 1999). Lewy bodies in Parkinson's Disease (intracytoplasmic inclusions with a dense eosinophilic core and pale surrounding halo) are thought to have a causative role in the disease, whereas nuclear inclusions observed in Huntington's Disease are thought to have a protective role (Arrasate et al., 2004).

In ALS, inclusions are thought to contribute to neurodegeneration. Twenty percent of FALS cases are linked to mutations in SOD1. These mutations may cause SOD1 to mis-fold and thus render it more prone to aggregation, resulting in the formation of toxic inclusions. Mutations in SOD1 occur throughout all five exons, suggestive of altered protein conformation; X-ray crystallography has shown that conformation of the active site is indeed altered in mutant SOD (Deng et al., 1993). Durham et al., (1997), have shown that over-expression of mutant, (but not wt), SOD1 in primary neuronal cell cultures leads to inclusion formation and cell death, and SOD1-positive inclusions are frequently found in ALS patient spinal cord samples and mouse models of ALS (Shibata et al., 1996, Bruijn et al., 1998, respectively).

Chaperone proteins, present in all cells and organelles, function to support the correct folding of proteins. Therefore, chaperones may be a key factor in the ability of cells to protect themselves against the aggregation of mutant SOD1. Chaperone proteins have been shown to be up-regulated in cells and tissues containing mutant, but not wt, SOD1 (Bruening et al., 1999). However, this up-regulation, was not observed in the spinal cord of mutant SOD1 transgenic mice, leading Brueining et al., (1999), to propose that mutant, mis-folded SOD1 present within a cell may divert the chaperone proteins towards trying to re-fold it and thus away from the re-folding of other proteins. This process may have detrimental affects on the cell, leading to aggregation of

other proteins, thereby rendering the cell more susceptible to other environmental and physiological stresses and ultimately leading to dysfunction and death. Most cells are able to up-regulate chaperones but it is possible that MNs are deficient in their ability to do this. A report by Batulan et al., (2003), investigated the heat shock response in MNs and showed that these cells have a high threshold for this response, due to lack of activation of HSF 1. In stressed cells, containing insufficient levels of HSPs, HSF1 trimerises and binds HSEs. Multiple phosphorylation then causes conformational changes, finally resulting in the recruitment of transcription machinery and transcription of heat shock protein genes (Morimoto and Santoro, 1998). The deficiency of MNs in their ability to initiate the heat shock response may render them selectively vulnerable in ALS. Bruening et al., (1999) tested this hypothesis by co-injecting HSP 70 and mutant SOD1 into cultured primary MNs. This led to a decrease in the number of cells containing mutant SOD1 inclusions and prolonged cell survival.

Mutant SOD1 from NIH3T3 cell extracts and G93A mutant SOD1 transgenic mice spinal cord extract is detergent insoluble, and chaperone proteins, namely HSPs 70, 40 and αB-crystallin, co-immunoprecipitate with mutant SOD1 from NIH3T3 cells (Shinder et al., 2001). Studies using the Neuro 2a cell line have shown that mutant, but not wt, SOD1 induces inclusion formation, fewer neurites and cell death (Takeuchi et al., 2002). Over-expression of HSPs 70 and 40 suppresses this aggregation of mutant SOD1, promotes neurite outgrowth and suppresses cell death in these Neuro 2a cells (Takeuchi et al., 2002). Thus far, these studies, demonstrating the beneficial role of HSPs in mutant SOD1 inclusion formation have been carried out in cell models *in vitro*. A more recent report, however, showed that up-regulation of

HSPs in a mouse model of ALS increased the life expectancy of these animals (Kieran et al., 2004). This up-regulation of HSPs was induced by the administration of the drug arimoclomol to G93A mutant SOD1 transgenic mice, and led to improved muscle function and increased MN survival, resulting in a 22% increase in lifespan. Arimoclomol is a hydroxylamine derivative which acts as a co-inducer of HSP expression by prolonging activation of HSF1 (Hargitai et al., 2003). Kieran et al., (2004), showed that in the G93A mutant SOD1 transgenic mice, arimoclomol acts, through HSF1, to up-regulate HSP 90 and 70. HSP 27 was not up-regulated in response to arimoclomol, but the up-regulation of other sHSPs, such as αB-crystallin, was not studied. The mechanism by which this up-regulation of HSPs leads to an increase in life expectancy in these mice was not addressed in this study. Thus it is not known whether HSP 90 and 70 are capable of ameliorating the effects of mutant SOD1 inclusions in this *in vivo* system. In light of the presence of mutant SOD1 inclusions in animal models (Bruijn et al., 1998) and patients (Shibata et al., 1996), and evidence that HSPs decrease mutant SOD1 inclusion formation in cell systems (Buening et al., 1999, Takeuchi et al., 2002), it is likely that this is indeed the case, although it is possible that they are exerting their effects in other ways. However a recent report has demonstrated that increasing HSP 70 in mutant SOD1 transgenic mice gave no protection against disease pathogenesis (Liu et al., 2005).

This protective role of HSPs extends to other neurodegenerative diseases. Using *Drosophila melanogaster* as a model of polyglutamine disease, Warrick et al., (1999), showed that the directed expression of HSP 70 suppressed polyglutamine mediated neurodegeneration. Over-expression of HSPs 70 and 40 reduced aggregate formation and suppressed apoptosis in a

neuronal cell model of SBMA (Kobayashi et al., 2000). SCA1 is another example of a polyglutamine disease. High levels of HSP 70 in SCA1 transgenic mice were shown to suppress neuropathology and improve motor function (Cummings et al., 2001).

From the data reviewed above, it can be concluded that chaperone proteins play an important role in protein aggregation during the process of neurodegeneration. Furthermore, mutations in HSPs have recently been linked to neurodegenerative diseases (Irobi et al., 2004 and Evgrafov et al., 2004), further supporting this role. The work presented in this study has focussed on investigating the role of sHSPs in the process of mutant SOD1 inclusion formation.

In order to study this, it was first necessary to establish a model system in which these investigations could be carried out. HEK293 cells displayed good transfection rates and it was possible to induce mutant SOD1 inclusion in these cells, as shown by IMF microscopy (see chapter 3, mutant SOD1 inclusion formation in culture cells). Over-expression of wt YFP-tagged SOD1 in HEK293 cells did not lead to inclusion formation, either in the presence or absence of proteasome inhibitor. Over-expression of YFP-tagged mutant SOD1s in HEK293 cells lead to inclusion formation in the presence, but not the absence, of proteasome inhibitor. This over-expression of mutant SOD1 in HEK293 cells and subsequent treatment with the proteasome inhibitor ALLN provides a model cell system of mutant SOD1 inclusion formation which could be used for further studies. Over-expression of YFP-tagged mutant SOD1 was also carried out using other cell lines available in the laboratory, (namely mH36, MCF7 and U373), and during these studies it was noticed that endogenous levels of sHSPs affected mutant SOD1 inclusion levels. MCF7 and U373 cells, which

have higher levels of αB-crystallin and HSP 27, have lower numbers of inclusions compared to mH36 and HEK293 cells, which have lower levels of these proteins. These findings support previous reports, which showed that experimentally increasing the level of chaperone proteins resulted in a decrease in the number of mutant SOD1 inclusions (Brueining et al., 1999, Takeuchi et al., 2002). Bruening et al., (1999) demonstrated that increasing HSP 70 levels decreased mutant SOD1 inclusions and prolonged survival in cultured primary MNS, and Takeuchi et al., (2002), reported similar findings following the over-expression of HSP 70 and 40 in Neuro 2a cells.

Having established this model cell system of mutant SOD1 inclusion formation, cell staining and IMF microscopy were carried out and used to show that chaperone proteins and components of the UPS co-localised to these inclusions. This result was in fact expected; Shinder et al., (2001), showed, using IP studies, that mutant SOD1 interacts with αB-crystallin, HSP 40 and 70 in NIH 3T3 cells, and Bruijn et al., (1998), showed in FALS patients and mouse models of the disease, that mutant SOD1 inclusions contain ubiquitin. Dorfin (an E3 ligase) expression has also been shown to be elevated in the spinal cord of ALS patients (Ishigaki et al., 2002) and is present in inclusions in both FALS and SALS (Niwa et al., 2002). Over-expression of dorfin has been shown to prevent cell death induced by mutant protein, presumably by promoting its degradation via the UPS (Niwa et al., 2002).

Ubiquitin containing inclusions have frequently been observed in many neurodegenerative diseases. The UPS constitutes the protein degradation machinery of the cell and is responsible for the removal of mis-folded proteins tagged with Ub. The presence of Ub containing inclusions within a cell is probably related to a deficiency in the UPS and, consequently its inability to

remove mis-folded proteins. Protein aggregates can inhibit the UPS (Bence et al., 2001), but this creates a positive feedback loop, as protein aggregates are also the products of UPS inhibition. Is it possible, therefore, that this feedback mechanism may have a role in the loss of neuronal function which characterises the progression of many of these neurodegenerative diseases? At present, this remains unanswered. Urushitani et al., (2002), have shown that the presence of mutant mis-folded SOD1 reduces the catalytic activity of the UPS in a neuroblastoma cell line. Furthermore, this is not due to incorporation of proteasome components into inclusions, as occurs in some other neurodegenerative diseases (Cummings et al., 1998). Urushitani et al., (2002), also proposed a model of disease pathogenesis in ALS: mutant, mis-folded and polyubiquitinated SOD1 overloads the UPS, leading to its further accumulation. Such accumulation will have an affect on the normal functioning of SOD1 i.e. it will cause impairment of the defence mechanisms that protect against stress. As a consequence of this, the increased stress may cause further mis-folding of proteins, including mutant SOD1, thereby exacerbating the substrate overload on the UPS even further. All this results in a self-perpetuating cycle occurring within the cell.

It is of interest that in both cell types used in this study, over-expression of mutant SOD1 alone was not sufficient to induce inclusion formation. In both HEK293 and N2a cells (used in later experiments), the addition of proteasome inhibitor was also required in order to induce inclusion formation. This suggests that the cells may be subject to multiple stresses before mutant SOD1 inclusion formation can occur. Is there a similar occurrence in ALS patients? If so this could go some way to explain the selective degeneration of MNs during disease progression. SOD1 is ubiquitously expressed throughout the nervous system,

and indeed the body, and the question as to why MNs are selectively vulnerable is central to the understanding of ALS disease pathogenesis. If mutant SOD1 alone is insufficient to form inclusions, and a combination of other stresses is also required, it could be the case that MNs, compared to other cell types, are more susceptible to these other stresses, e.g. physiological or oxidative stress. Evidence to support this includes the demonstration that MNs have a high threshold for the activation of the heat shock response, due to lack of activation of HSF1 (Batulan et al., 2003). Also, due to their role in relaying electrical impulses and effecting muscle movement, MNs are continually subjected to the physiological stress of a high excitatory input.

In other neurodegenerative diseases, mutant protein has been shown to affect transcription, which in turn may contribute to neurodegeneration. Huntingtin is the protein which causes Huntington's disease when its polyglutamine tract is extended above thirty-seven polyglutamie residues. Truncated N-terminal mutant Huntingtin represses transcription, whereas wt huntingtin does not (Kegel et al., 2002). In Alzheimer's disease, a phosphorylated, C-terminal fragment of APP, the precursor of plaque forming amyloid protein, is present in the nucleus and localises to the splicing factor compartment (Muresan and Muresan, 2004). This indicates that APP may have a role in pre-mRNA splicing and/or transcription in this disease. We investigated the possibility as to whether mutant SOD1 could contribute to ALS disease progression in a similar way by affecting transcription. Speckles, or interchromatin granules, are distinct nuclear structures involved in the processing and transcription of RNA (Wei et al., 1999). They can be detected using antibodies to components of the spliceosome, either snRNP components e.g. Sm and UIA, or non-snRNP components e.g. SC35 and TMG (Antoniou et

al., 1993). By looking at the pattern of speckles obtained with such antibodies, insights into the transcriptional activity of the cell can be gleaned. Using such antibodies, we showed that mutant SOD1 did not affect transcription in our HEK293 system of mutant SOD1 inclusion formation, as no difference in speckle pattern was observed in cells expressing wt or mutant SOD1 (Figure 3.6). This suggests that alterations in transcription by mutant SOD1 do not have a role in the disease pathogenesis of ALS.

Biochemical analysis of cell extracts from HEK293 cells containing mutant SOD1 inclusions showed that 22.4% of the mutant SOD1 was insoluble. Over-expression of αB-crystallin and HSP 27 under these conditions decreased the proportion of insoluble SOD1 from 22.4% to 0% for αB-crystallin and 4.4% for HSP 27 (see chapter 4, effects of sHSPs on insoluble G85R SOD1 levels in HEK293 cells). Although the question as to whether inclusions are either directly toxic, or act as a protective sink mechanism remains controversial; these data support the findings of an earlier report (Kieran et al., 2004), which showed that a co-inducer of HSPs improved disease pathogenesis in mutant SOD1 mice. When mutant forms of these sHSPs were over-expressed under these conditions, the proportion of insoluble mutant SOD1 was further increased, to 31.8% for R120G αB-crystallin and 30.9% and 37.3% for S135F and R140G HSP 27, respectively (see chapter 4, mutant sHSPs: are they involved in ALS?). These mutations result in the proteins being unable to fold correctly and thus indirectly lead to their dysfunction (Bova et al., 1999, Perng et al., 1999b, Chavez Zobel et al., 2003). Bruening et al., (1999), showed that over-expression of HSP 70 prevented mutant SOD1 inclusion formation and subsequent cell death in cultured primary MNs. Furthermore, Takeuchi et al., (2002), showed that over-expression of HSP 40 and 70 in N2a cells which

contained mutant SOD1 inclusions, suppressed the aggregation of mutant SOD1, promoted neurite outgrowth and prolonged cell survival. All these data, together with that presented by Kieran et al., (2004), would support a protective role for HSPs. Similar findings have been reported in other neurodegenerative diseases. Over-expression of HSP 70 has been shown to suppress polyglutamine mediated neurodegeneration, (Warrick et al., 1999), neuropathology in SCA1 mice (Cummings et al., 2001) and decreased inclusion formation and suppressed apoptosis in a cell model of SBMA (Kobayashi et al., 2002). However, this assumes that inclusions are toxic. As previously mentioned, there are still contradicting views as to whether inclusions are toxic, or whether they act as a 'sink' for toxic soluble proteins. This subject has been reviewed by Tran and Miller (1999). Reports by Bruening et al., (1999) and Takeuchi et al., (2002), showed that mutant SOD1 inclusion formation results in cell death. In this study cell viability assays were carried out on HEK293 cells containing mutant SOD1 inclusions in the presence and absence of wt and mutant sHSPs. Although over-expression of mutant SOD1 alone did not result in any adverse effects, the addition of proteasome inhibitor, to induce inclusion formation, resulted in a significant increase in cell death. This suggests that additional stresses are detrimental to cells which already express mutant SOD1. As MNs are already compromised in their stress response (Batulan et al., 2003), it is easy to see how expression of mutant SOD1 in these cells could lead to cell dysfunction and death. Under these conditions over-expression of either wt or mutant sHSPs, did not significantly affect cell viability, despite their effects on the proportions of insoluble mutant SOD1. As with all the other experiments presented here, these viability studies were carried out twenty-four hr following transfection. It might be the case that after prolonged exposure to

the inclusions, additional effects would have become apparent. Although these data show that αB-crystallin and HSP 27 both interact with mutant SOD1 *in vivo*, and in doing so alter the proportions of insoluble material, this interaction may not be a direct one. The interaction of both wt and mutant SOD1 with αB-crystallin was studied *in vitro*. Although three different methods were used, namely IP, SEC and Biacore, none of these demonstrated an interaction between the two proteins (see chapter 5). This is somewhat unexpected: (a) due to our *in vivo* results described above, and (b) due to the results from Shinder et al., (2001), where it was demonstrated that HSP 70, 40 and αB-crystallin co-immunoprecipitated with mutant SOD1 from NIH-3T3 cells. From our results alone, it would be easy to argue that the mutant SOD-sHSP interaction is not a direct one, but one which involves other proteins *in vivo* which are not present in the *in vitro* assays. However, the data presented by Shinder et al., (2001), does not support this. Maybe our three chosen methods are not best suited to the studies carried out. They were selected due to departmental availability, but it is possible that there are other methods which would have been better suited, for example Far Western Blotting or yeast two-hybrid analysis. Unfortunately, for the IP experiments, the protein-G coupled beads themselves interacted with the SOD1. If this problem had been overcome, maybe a true interaction could have been demonstrated. It is also possible that aggregated SOD1 interacts with αB-crystallin; soluble SOD1 was utilised in the experiments described here.

When wt SOD1 was over-expressed in the HEK293 cell system, even in the presence of proteasome inhibitor, it remained soluble, as shown by IMF microscopy and biochemical analysis. However, when mutant αB-crystallin and mutant HSP 27 were over-expressed together with wt SOD1, followed by

treatment with proteasome inhibitor, some of the normally soluble SOD1 was shifted into the insoluble fraction. Mutations in sHSPs have recently been linked to neurodegenerative diseases. Mutations in HSP 27 have been linked to CMT disease and distal hereditary motor neuropathy (Evgrafov et al., 2004) and mutations in HSP 22 have been identified in families with distal hereditary motor neuropathies (Irobi et al., 2004). Is it possible that sHSPs are also mutated in ALS and contribute to protein aggregation? What about the vast majority of ALS cases that are not linked to mutations in SOD1? Are mutations in chaperone proteins seen here? Mutations in sHSPs result in their being unable to fold correctly, consequently rendering them prone to aggregation and affecting their activity (Bova et al., 1999, Perng et al., 1999b, Chavez Zobel et al., 2003). If, through some as yet unidentified interaction, they are able to sequester proteins, which are normally soluble, into inclusions, as has been observed in these studies for mutant SOD1, this may have deleterious effects on the cells, thus making them more susceptible to other stresses. SOD1 is involved in protecting cells from oxidative stress, so decreasing the amount of available SOD1 would lead to an increase in superoxide radicals which could damage cellular macromolecules. Again, these findings could hint at the selective vulnerability of MNs in ALS, as MNs are subject to a high excitatory input compared to other cell types. Thus, MNs may be particularly sensitive to increased levels of oxidative stress.

The results obtained from the HEK293 cell system showed that over-expression of sHSPs decreased the proportion of insoluble mutant SOD1. Do sHSPs have similar effects in N2a cells? Compared to the HEK293 cell model, a neuronal cell line could provide a model system better suited to studying ALS. It was shown that over-expression of YFP-tagged G85R mutant SOD1 and

subsequent treatment with proteasome inhibitor induced SOD1 inclusions in N2a cells. However, as the transfection rate was low in this cell line it was not possible to quantify the proportion of insoluble mutant SOD1, as was the case in the HEK293 cell system. Over-expression of sHSPs affected the physical appearance of the mutant SOD1 inclusions. Instead of dense inclusions observed when mutant SOD1 alone is expressed, the presence of αB-crystallin and HSP 27 resulted in the inclusions being more diffuse in phenotype. Similar findings have been reported by Takeuchi et al., (2002). They showed that over-expression of HSPs 70 and 40 in Neuro 2a cells resulted in a change in the appearance of inclusions to a more diffuse pattern throughout the cytoplasm. The results from the HEK293 cell system support these findings for a role of sHSPs in mutant SOD1 inclusion formation. To obtain more definite conclusions about this possible role, it would be of use to study the effects of sHSPs on mutant SOD1 inclusion formation in another neuronal cell line which would be easier to transfect and better suited to IMF microscopy studies.

It has been shown here that over-expression of sHSPs in a model cell system of mutant SOD1 inclusion formation decreases the proportion of insoluble mutant SOD1 (see chapter 4) It is likely that decreasing the insolubility of mutant SOD1, as determined biochemically, coincides with a decrease in mutant SOD1 inclusions, although we have not been able to demonstrate this directly, due to treated HEK293 cells becoming detached from the slides during processing for IMF microscopy. This supports numerous other reports (Bruening et al., 1999, Warrick et al., 1999, Kieran et al., 2004), which show that up-regulation of HSPs are beneficial both in cell and animal models for a range of neurodegenerative diseases. But how exactly is this up-regulation of HSPs beneficial? They decrease the amount of insoluble mutant SOD1 and the

numbers of mutant SOD1 inclusions, but how is this achieved? This has not been addressed here. Studies in NIH3T3 cells (Shinder et al., 2001) showed that mutant SOD1 co-immunoprecipitates with HSP 70, 40 and αB-crystallin, suggesting that HSPs interact directly with the mutant SOD1. Results from our *in vitro* studies however, do not support these findings (discussed previously). Another question is whether HSPs and sHSPs act co-operatively in their roles to decrease mutant SOD1. Most of the studies to date which have implicated a role for chaperone proteins in mutant SOD1 inclusion formation in ALS (Bruening et al., 1999, Takeuchi et al., 2002, Kieran et al., 2004), have shown that it is an increase in HSPs which decrease mutant SOD1 inclusions. The results presented here show a similar role for sHSPs. Does raising the capacity of one component of a cells chaperone machinery lead to increases in levels of others? All HSPs are up-regulated in response to stress (Morimoto et al., 1997), but whether over-expression of one HSP in cell and animal systems leads to increases in others has not been directly addressed. A report by Lee et al., (1997), proposed that energy-independent sHSPs trap non-native proteins during stress conditions, thus protecting them from aggregation. Under permissive conditions, energy-dependent chaperones can then complete the refolding of this reservoir of folding-competent protein. Thus, sHSPs prevent rapid protein aggregation by initiation of binding events while other chaperones primarily refold non-native protein. This suggests that both sHSPs and HSPs would be required to decrease mutant SOD1 inclusions within cells, so maybe HSPs do act co-operatively and that an increase in one chaperone component leads to increases in other chaperone components.

Whether these effects of HSPs will be of any therapeutic benefit remains to be determined. However, it must be remembered that the over-expression of

mutant SOD1 in these animals is much greater than is seen in ALS patients. Although such animals provide a good model for ALS and allow important insights into disease mechanisms, this must be taken into account when considering these systems.

It has also been shown that over-expression of mutant, inactive sHSPs results in an increase in the insolubility of normally soluble proteins. Two recent reports have linked mutations in sHSPs to related neurodegenerative diseases (Irobi et al., 2004, Evgrafov et al., 2004). It is possible that such mutations may contribute to disease pathogenesis in the majority of those ALS cases not linked to mutant SOD1. This is potentially an interesting area of new research, which warrants further investigation.

The results presented here are based around mutant SOD1, which can mis-fold and form inclusions. Ten percent of ALS cases are inherited (FALS cases), and of these, only 20% are linked to mutant SOD1. What is happening in the 90% of non-inherited ALS cases? Can the findings presented here help us to understand the pathogenesis of these sporadic cases? It is possible, of course, that SOD1 is mutated in some of these non-inherited cases, but there are other factors which have been shown to contribute to ALS disease pathogenesis. The accumulation and abnormal assembly of NFs are a hallmark of ALS (Carpenter, 1968), and mutations in NFs have been shown to result in degeneration of MNs (Xu et al., 1993, Cote et al., 1993). Excitotoxicity has been shown to contribute to ALS and increased glutamate in cerebrospinal fluid from ALS patients has been reported (Rothstein et al., 1990, Rothstein et al., 1991, Shaw et al., 1995). Loss of the astroglial glutamate transported EAAT2 has been shown to be responsible for abnormal glutamate transport (Rothstein et al., 1995). Other factors implicated in this disease include mitochondrial defects

such as vacuolation, which can be detected early in disease progression (Kong and Xu, 1998), activation of apoptosis (Martin 1999, Pedersen et al., 2000) and reduced VEGF expression (Lambrechts et al., 2003).

Can the results obtained here help us to understand these mechanisms and how they lead to MN degeneration? Our experiments were designed to address aggregation of mutant SOD1 and the results show that increased levels of sHSPs decrease the insolubility of mutant SOD1. These other contributing factors in ALS described above are not known to involve protein aggregation, so whether increased levels of sHSPs will be beneficial in these cases is not clear. One role of HSPs is in stabilising the cytoskeleton (Perng et al., 1999a), so their up-regulation may be beneficial in the case of NF disruption, but this is unlikely as currently there are no reports demonstrating that they are themselves involved in this disruption. Other reported roles of sHSPs include inhibition of apoptosis (Bruey et al., 2000, Kamradt et al., 2001, Mehlen et al., 1996). As activation of apoptosis has been reported in ALS patients (Martin 1999, Pedersen et al., 2000) and may contribute to disease pathogenesis, it is therefore possible that in these cases, the up-regulation of sHSPs can confer some protection against apoptosis and its possible contribution to disease progression. In the case of glutamate-mediated excitotoxicity, there is a link between FALS and SALS. Howland et al., (2002), have reported that decreased levels of EAAT2 are observed in a rat model of ALS and Trotti et al., (1999), showed that mutant, but not wt, SOD1 inactivates EAAT2. If mutant SOD1 mediates this inactivation through inclusion related mechanisms, up-regulation of sHSPs may help to prevent this inactivation of EAAT2.

A recent report by Clement et al., (2003), suggested that mutant SOD1 mediated toxicity is non-cell autonomous. Using chimeric mice, they

demonstrated that mutant SOD1, acting within non-neuronal cells, is required in order to cause damage to MNs, and that non-neuronal cells, which do not express mutant SOD1, improve survival of mutant SOD1 expressing MNs. The mechanisms by which normally functioning non-neuronal cells could prevent degeneration in neighbouring MNs is presently unknown. The results presented by Clement et al., (2003), support a body of evidence, discussed previously, which suggests that up-regulation of chaperone proteins helps to reduce mutant SOD1 inclusion formation and improve survival in various cell models and in G93A mutant SOD1 transgenic mice. There is speculation that MNs may be deficient in their ability to up-regulate chaperone proteins (Batulan et al., 2003), and that this may be key to their selective dysfunction and degeneration in ALS. However, the fact that mutant SOD1 inclusions in MNs alone *per se* do not cause dysfunction and death (Clement et al., 2003), suggests that the heat shock response in MNs is not a problem. Maybe the other non-neuronal cells which contribute to MN dysfunction and death have deficiencies in their heat shock response and expression and accumulation of mutant SOD1 within these cells leads to detrimental effects on surrounding cells including MNs.

The surrounding non-neuronal cells support MNs; for example, astrocytes provide MNs with nutrients and neurotrophic factors, as well as scavenging neurotransmitters, such as glutamate (Oppenheim et al., 1988, Lin et al., 1993). It is possible that the presence of mutant SOD1 inclusions within these non-neuronal cells affects their ability to carry out these support functions efficiently. It is not known exactly how inclusions exert their affects, but hypotheses include co-aggregation with other proteins, resulting in the cells being depleted of essential components, burdening of the UPS, disruption of axonal transport and induction of apoptosis. Such events in these cells may

impair their ability to efficiently support the surrounding MNs, leading to their degeneration and death. As we have demonstrated here, increasing HSP protein levels decreases the amount of insoluble mutant SOD1. How is this relevant in relation to the results presented by Clement et al., (2003)? Findings similar to ours have been reported in a mouse model of ALS (Kieran et al., 2004). Increasing HSP levels in G93A mutant SOD1 transgenic mice leads to increased MN survival and prolongs life expectancy in these animals (Kieran et al., 2004). Maybe the HSPs decrease mutant SOD1 inclusions present within non-neuronal cells, allowing them to function more efficiently in their role of providing MNs with nutrients and growth factors, thus improving MN survival and prolonging life expectancy. Clearance of mutant SOD1 from surrounding non-neuronal cells may improve their functioning and consequently their ability to support MNs, thereby helping to prevent their degeneration and death.

In conclusion, the results of this study show that increases in sHSPs can help prevent mutant SOD1 inclusion formation in a model cell system. This supports other evidence for beneficial roles of chaperones in mutant SOD1 inclusion formation in cell and animal models of ALS. How this relates to the vast majority of non-SOD1 linked ALS cases is not clear. If these cases involve protein aggregation, then increases in sHSPs are likely to be beneficial, as they are not specific for mutant SOD1. Also, it has been shown that mutant sHSPs cause increased insolubility of mutant SOD1. Mutations in sHSPs in related neurodegenerative diseases were reported last year (Irobi et al., 2004, Evgrafov et al., 2004). It is possible that mutant sHSPs contribute to ALS in the non-SOD1 linked cases, by increasing the insolubility of proteins which, under normal cellular conditions are soluble. ALS is a disease in which multiple factors and pathways have been shown to contribute to disease pathogenesis.

Increasing levels of chaperones proteins may be of therapeutic benefit in cases that involve protein aggregation and inclusion formation but a lot more research is needed to better understand the mechanisms which underlie the degeneration of MNs in ALS, such that therapeutic strategies can be designed to treat and prevent this debilitating disease.

REFERENCES

Ackerley, S., A.J. Grierson, S. Banner, M.S. Perkinton, J. Brownlees, H.L. Byers, M. Ward, P. Thornhill, K. Hussain, J.S. Waby, B.H. Anderton, J.D. Cooper, C. Dingwall, P.N. Leigh, C.E. Shaw, and C.C. Miller. 2004. p38alpha stress-activated protein kinase phosphorylates neurofilaments and is associated with neurofilament pathology in amyotrophic lateral sclerosis. *Mol Cell Neurosci.* 26:354-64.

Al-Chalabi, A., P.M. Andersen, P. Nilsson, B. Chioza, J.L. Andersson, C. Russ, C.E. Shaw, J.F. Powell, and P.N. Leigh. 1999. Deletions of the heavy neurofilament subunit tail in amyotrophic lateral sclerosis. *Hum Mol Genet.* 8:157-64.

Al-Chalabi, A., M.D. Scheffler, B.N. Smith, M.J. Parton, M.E. Cudkowicz, P.M. Andersen, D.L. Hayden, V.K. Hansen, M.R. Turner, C.E. Shaw, P.N. Leigh, and R.H. Brown, Jr. 2003. Ciliary neurotrophic factor genotype does not influence clinical phenotype in amyotrophic lateral sclerosis. *Ann Neurol.* 54:130-4.

Alexianu, M.E., B.K. Ho, A.H. Mohamed, V. La Bella, R.G. Smith, and S.H. Appel. 1994. The role of calcium-binding proteins in selective motoneuron vulnerability in amyotrophic lateral sclerosis. *Ann Neurol.* 36:846-58.

Alexianu, M.E., M. Kozovska, and S.H. Appel. 2001. Immune reactivity in a mouse model of familial ALS correlates with disease progression. *Neurology.* 57:1282-9.

Almer, G., C. Guegan, P. Teismann, A. Naini, G. Rosoklija, A.P. Hays, C. Chen, and S. Przedborski. 2001. Increased expression of the pro-inflammatory enzyme cyclooxygenase-2 in amyotrophic lateral sclerosis. *Ann Neurol.* 49:176-85.

Almer, G., P. Teismann, Z. Stevic, J. Halaschek-Wiener, L. Deecke, V. Kostic, and S. Przedborski. 2002. Increased levels of the pro-inflammatory prostaglandin PGE2 in CSF from ALS patients. *Neurology.* 58:1277-9.

Anand, P., A. Parrett, J. Martin, S. Zeman, P. Foley, M. Swash, P.N. Leigh, J.M. Cedarbaum, R.M. Lindsay, R.E. Williams-Chestnut, and et al. 1995. Regional changes of ciliary neurotrophic factor and nerve growth factor levels in post mortem spinal cord and cerebral cortex from patients with motor disease. *Nat Med.* 1:168-72.

Anderson, P.M. 2001. Genetics of sporadic ALS. *ALS and other Motor Neurone Disorders.* 2:(Suppl 1), S37-41.

Anderson, P.M., K.B. Sims, W.W. Xin, R. Kiely, G. O'Neill, J. Ravits, E. Pioro, Y. Harati, R.D. Brower, J.S.Levine, H.U. Heinicke, W. Seltzer, M. Boss, and R.H. Brown, Jr. 2003. *ALS and other Motor Neurone Disorders.* 4:62-73.

Andreassen, O.A., R.J. Ferrante, P. Klivenyi, A.M. Klein, L.A. Shinobu, C.J. Epstein, and M.F. Beal. 2000. Partial deficiency of manganese superoxide dismutase exacerbates a transgenic mouse model of amyotrophic lateral sclerosis. *Ann Neurol.* 47:447-55.

Antoniou, M., M. Carmo-Fonseca, J. Ferreira, and A.I. Lamond. 1993. Nuclear organization of splicing snRNPs during differentiation of murine erythroleukemia cells in vitro. *J Cell Biol.* 123:1055-68.

Aoki, M., C.L. Lin, J.D. Rothstein, B.A. Geller, B.A. Hosler, T.L. Munsat, H.R. Horvitz, and R.H. Brown, Jr. 1998. Mutations in the glutamate transporter EAAT2 gene do not cause abnormal EAAT2 transcripts in amyotrophic lateral sclerosis. *Ann Neurol.* 43:645-53.

Arrasate, M., S. Mitra, E.S. Schweitzer, M.R. Segal, and S. Finkbeiner. 2004. Inclusion body formation reduces levels of mutant huntingtin and the risk of neuronal death. *Nature.* 431:805-10.

Arrigo, A.P., J.P Suhan, and W.J. Welch. 1988. Dynamic changes in the structure and intracellular locale of mammalian low-molecular weight heat shock proteins. *Mol Cell Biol.* 12:5059-71.

Azzouz, M., G.S. Ralph, E. Storkebaum, L.E. Walmsley, K.A. Mitrophanous, S.M. Kingsman, P. Carmeliet, and N.D. Mazarakis. 2004. VEGF delivery with retrogradely transported lentivector prolongs survival in a mouse ALS model. *Nature.* 429:413-7.

Batulan, Z., G.A. Shinder, S. Minotti, B.P. He, M.M. Doroudchi, J. Nalbantoglu, M.J. Strong, and H.D. Durham. 2003. High threshold for induction of the stress response in motor neurons is associated with failure to activate HSF1. *J Neurosci.* 23:5789-98.

Beal, M.F., R.J. Ferrante, S.E. Brown, R.T. Matthews, N.W. Kowall, and R.H. Brown, Jr. 1997.Increased 3-nitrotyrosine in both sporadic and familial amyotrophic lateral sclerosis. *Ann Neurol.* 42:646- 54.

Beaulieu, J.M., M.D. Nguyen, and J.P. Julien. 1999. Late onset of motor neurons in mice overexpressing wild-type peripherin. *J Cell Biol.* 147:531-44.

Beckman, J.S., M. Carson, C.D. Smith, and W.H. Koppenol. 1993. ALS, SOD and peroxynitrite. *Nature.* 364:584.

Bence, N.F., R.M. Sampat, and R.R. Kopito. 2001. Impairment of the ubiquitin-proteasome system by protein aggregation. *Science.* 292:1552-5.

Bogdanov, M.B., L.E. Ramos, Z. Xu, and M.F. Beal. 1998. Elevated "hydroxyl radical" generation in vivo in an animal model of amyotrophic lateral sclerosis. *J Neurochem.* 71:1321-4.

Borchelt, D.R., M.K. Lee, H.S. Slunt, M. Guarnieri, Z-S. Xu, P.C. Wong, R.H. Brown, Jr., D.L. Price, S.S. Sisodia, and D.W. Cleveland. 1994.

Superoxide dismutase 1 with mutations linked to familial amyotrophic lateral sclerosis possesses significant activity. *Proc Natl Acad Sci U S A.* 91:8292-96.

Borthwick, G.M., M.A. Johnson, P.G. Ince, P.J. Shaw, and D.M. Turnbull. 1999. Mitochondrial enzyme activity in amyotrophic lateral sclerosis: implications for the role of mitochondria in neuronal cell death. *Ann Neurol.* 46:787-90.

Bova, M.P., O. Yaron, Q. Huang, L. Ding, D.A. Haley, P.L. Stewart, and J. Horwitz. 1999. Mutation R120G in alphaB-crystallin, which is linked to a desmin-related myopathy, results in an irregular structure and defective chaperone-like function. *Proc Natl Acad Sci U S A.* 96:6137-42.

Bowling, A.C., E.E. Barkowski, D. McKenna-Yasek, P. Sapp, H.R. Horvitz, M.F. Beal, and R.H. Brown, Jr. 1995. Superoxide dismutase concentration and activity in familial amyotrophic lateral sclerosis. *J Neurochem.* 64:2366-9.

Brownlees, J., S. Ackerley, A.J. Grierson, N.J. Jacobsen, K. Shea, B.H. Anderton, P.N. Leigh, C.E. Shaw, and C.C. Miller. 2002. Charcot-Marie-Tooth disease neurofilament mutations disrupt neurofilament assembly and axonal transport. *Hum Mol Genet.* 11:2837-44.

Bruening, W., J. Roy, B. Giasson, D.A. Figlewicz, W.E. Mushynski, and H.D. Durham. 1999. Up-regulation of protein chaperones preserves viability of cells expressing toxic Cu/Zn-superoxide dismutase mutants associated with amyotrophic lateral sclerosis. *J Neurochem.* 72:693-9.

Bruey, J.M., C. Ducasse, P. Bonniaud, L. Ravagnan, S.A. Susin, C. Diaz-Latoud, S. Gurbuxani, A.P. Arrigo, G. Kroemer, E. Solary, and C. Garrido. 2000. Hsp27 negatively regulates cell death by interacting with cytochrome c. *Nat Cell Biol.* 2:645-52.

Bruijn, L.I., M.F. Beal, M.W. Becher, J.B. Schulz, P.C. Wong, D.L. Price, and D.W. Cleveland. 1997a. Elevated free nitrotyrosine levels, but not protein-bound nitrotyrosine or hydroxyl radicals, throughout amyotrophic lateral sclerosis (ALS)-like disease implicate tyrosine nitration as an aberrant in vivo property of one familial ALS-linked superoxide dismutase 1 mutant. *Proc Natl Acad Sci U S A.* 94:7606-11.

Bruijn, L.I., M.W. Becher, M.K. Lee, K.L. Anderson, N.A. Jenkins, N.G. Copeland, S.S. Sisodia, J.D. Rothstein, D.R. Borchelt, D.L. Price, and D.W. Cleveland. 1997b. ALS-linked SOD1 mutant G85R mediates damage to astrocytes and promotes rapidly progressive disease with SOD1-containing inclusions. *Neuron.* 18:327-38.

Bruijn, L.I., M.K. Houseweart, S. Kato, K.L. Anderson, S.D. Anderson, E. Ohama, A.G. Reaume, R.W. Scott, and D.W. Cleveland. 1998. Aggregation and motor neuron toxicity of an ALS-linked SOD1 mutant independent from wild-type SOD1. *Science.* 281:1851-4.

Buchner, J. 1996. Supervising the fold: functional principles of molecular chaperones. *Faseb J.* 10:10-9.

Carpenter, S. 1968. Proximal axonal enlargement in motor neuron disease. *Neurology.* 18:841-51.

Carroll, M.C., J.B. Girouard, J.L. Ulloa, J.R. Subramaniam, P.C. Wong, J.S. Valentine and V.C. Culotta. 2004. Mechanisms for activating Cu- and Zn-containing superoxide dimutase in the absence of the CCS Cu chaperone. *Proc Natl Acad Sci U S A.* 101:5964-69.

Chavez Zobel, A.T., A. Loranger, N. Marceau, J.R. Theriault, H. Lambert, and J. Landry. 2003. Distinct chaperone mechanisms can delay the formation of aggresomes by the myopathy-causing R120G alphaB-crystallin mutant. *Hum Mol Genet.* 12:1609-20.

Ciechanover, A., and P. Brundin. 2003. The ubiquitin proteasome system in neurodegenerative diseases: sometimes the chicken, sometimes the egg. *Neuron.* 40:427-46.

Clark, J.I., and P.J. Muchowski. 2000. Small heat-shock proteins and their potential role in human disease. *Curr Opin Struct Biol.* 10:52-9.

Clement, A.M., M.D. Nguyen, E.A. Roberts, M.L. Garcia, S. Boillee, M. Rule, A.P. McMahon, W. Doucette, D. Siwek, R.J. Ferrante, R.H. Brown, Jr., J.P. Julien, L.S. Goldstein, and D.W. Cleveland. 2003. Wild-type nonneuronal cells extend survival of SOD1 mutant motor neurons in ALS mice. *Science.* 302:113-7.

Corbo, M., and A.P. Hays. 1992. Peripherin and neurofilament protein coexist in spinal spheroids of motor neuron disease. *J Neuropathol Exp Neurol.* 51:531-7.

Corson, L.B., J.J. Strain, V.C. Culotta, and D.W. Cleveland. 1998. Chaperone-facilitated copper binding is a property common to several classes of familial amyotrophic lateral sclerosis-linked supeoxide dismutase mutants. *Proc Natl Acad Sci U S A.* 95:6361-6.

Cote, F., J.F. Collard, and J.P. Julien. 1993. Progressive neuronopathy in transgenic mice expressing the human neurofilament heavy gene: a mouse model of amyotrophic lateral sclerosis. *Cell.* 73:35-46.

Couillard-Despres, S., Q. Zhu, P.C. Wong, D.L. Price, D.W. Cleveland, and J.P. Julien. 1998. Protective effect of neurofilament heavy gene overexpression in motor neuron disease induced by mutant superoxide dismutase. *Proc Natl Acad Sci U S A.* 95:9626-30.

Crow, J.P., J.B. Sampson, Y. Zhuang, J.A. Thompson, and J.S. Beckman. 1997. Decreased zinc affinity of amyotrophic lateral sclerosis mutants leads to enhanced catalysis of tyrosine nitration by peroxynitrite. *J Neurochem.* 69:1936-44.

Culotta, V.C., L.W.J. Klomp, J. Strain, R.L.B. Casareno, B. Krems, and J.D. Gitlin. 1997. The copper chaperone for superoxide dismutase. *J Biol Chem.* 272;23469-72.

Cummings, C.J., M.A. Mancini, B. Antalffy, D.B. DeFranco, H.T. Orr, and H.Y. Zoghbi. 1998. Chaperone suppression of aggregation and altered subcellular proteasome localization imply protein misfolding in SCA1. *Nat Genet.* 19:148-54.

Cummings, C.J., Y. Sun, P. Opal, B. Antalffy, R. Mestril, H.T. Orr, W.H. Dillmann, and H.Y. Zoghbi. 2001. Over-expression of inducible HSP70 chaperone suppresses neuropathology and improves motor function in SCA1 mice. *Hum Mol Genet.* 10:1511-8.

De Jong, W.W., J.A.M. Leunissen, P.J.M. Leenen, A. Zweeres, and M. Versteeg. 1998. Dogfish α-crystallin sequences. *J Biol Chem.* 263:5141-49.

De Jonghe, P., I. Mersivanova, E. Nelis, J. Del Favero, J.J. Martin, C. Van Broeckhoven, O. Evgrafov, and V. Timmerman. 2001. Further evidence that neurofilament light chain gene mutations can cause Charcot-Marie-Tooth disease type 2E. *Ann Neurol.* 49:245-9.

Deng, H.X., A. Hentati, J.A. Tainer, Z. Iqbal, A. Cayabyab, W.Y. Hung, E.D. Getzoff, P. Hu, B. Herzfeldt, R.P. Roos, and et al. 1993. Amyotrophic lateral sclerosis and structural defects in Cu,Zn superoxide dismutase. *Science.* 261:1047-51.

Dubois-Dauphin, M., H. Frankowski, Y. Tsujimoto, J. Huarte, and J-C. Martinou. 1994. Proc Natl Acad Sci U S A. 91:2459-

Durham, H.D., J. Roy, L. Dong, and D.A. Figlewicz. 1997. Aggregation of mutant Cu/Zn superoxide dismutase proteins in a culture model of ALS. *J Neuropathol Exp Neurol.* 56:523-30.

Elliott, J.L. 2001. Cytokine upregulation in a murine model of familial amyotrophic lateral sclerosis. *Brain Res Mol Brain Res.* 95:172-8.

Estevez, A.G., J.P. Crow, J.B. Sampson, C. Reiter, Y. Zhuang, G.J. Richardson, M.M. Tarpey, L. Barbeito, and J.S. Beckman. 1999. Induction of nitric oxide-dependent apoptosis in motor neurons by zinc-deficient superoxide dismutase. *Science.* 286:2498-500.

Evgrafov, O.V., I. Mersiyanova, J. Irobi, L. Van Den Bosch, I. Dierick, C.L. Leung, O. Schagina, N. Verpoorten, K. Van Impe, V. Fedotov, E. Dadali, M. Auer-Grumbach, C. Windpassinger, K. Wagner, Z. Mitrovic, D. Hilton-Jones, K. Talbot, J.J. Martin, N. Vasserman, S. Tverskaya, A. Polyakov, R.K. Liem, J. Gettemans, W. Robberecht, P. De Jonghe, and V. Timmerman. 2004. Mutant small heat-shock protein 27 causes axonal Charcot-Marie-Tooth disease and distal hereditary motor neuropathy. *Nat Genet.* 36:602-6.

Facchinetti, F., M. Sasaki, F.B. Cutting, P. Zhai, J.E. Macdonald, D. Reif, M.F. Beal, P.L. Huang, T.M. Dawson, M.E. Gurney, and V.L. Dawson. 1999. Lack of involvement of neuronal nitric oxide synthase in the pathogenisis of a transgenic mouse model of familial amyotrophic lateral sclerosis. *Neuroscience.* 90:1483-92.

Ferrante, R.J., S.E. Browne, L.A. Shinobu, A.C. Bowling, M.J. Baik, U. MacGarvey, N.W. Kowall, R.H. Brown, Jr., and M.F. Beal. 1997. Evidence of increased oxidative damage in both sporadic and familial amyotrophic lateral sclerosis. *J Neurochem.* 69:2064-74.

Fridovich, I. 1986. Superoxide dismutases. *Adv Enzymol Relat Areas Mol Biol.* 58:61-97.

Friedlander, R.M., R.H. Brown, V. Gagliardini, J. Wang, and J. Yuan. 1997. Inhibition of ICE slows ALS in mice. *Nature.* 388:31.

Gaudette, M., M. Hirano, and T. Siddique. 2000. Current status of SOD1 mutations in familial amyotrophic lateral sclerosis. *ALS and other Motor Neurone Disorders.* 1:83-9.

Giess, R., B. Holtmann, M. Braga, T. Grimm, B. Muller-Myhsok, K.V. Toyka, and M. Sendtner. 2002. Early onset of severe familial amyotrophic lateral sclerosis with a SOD-1 mutation: potential impact of CNTF as a candidate modifier gene. *Am J Hum Genet.* 70:1277-86.

Gonatas, N.K., A. Stieber, Z. Mourelatos, Y. Chen, J.O. Gonatas, S.H. Appel, A.P. Hays, W.F. Hickey, and J.J. Hauw. 1992. Fragmentation of the Golgi apparatus of motor neurons in amyotrophic lateral sclerosis. *Am J Pathol.* 140:731-7.

Gong, Y.H., A.S. Parsadanian, A. Andreeva, W.D. Snider, and J.L. Elliott. 2000. Restricted expression of G86R Cu/Zn superoxide dismutase in astrocytes results in astrocytosis but not cause motorneurondegeneration. *J Neurosci.* 20;660-5.

Guegan, C., M. Vila, G. Rosoklija, A.P. Hays, and S. Przedborski. 2001. Recruitment of the mitochondrial-dependent apoptotic pathway in amyotrophic lateral sclerosis. *J Neurosci.* 21:6569-76.

Gurney, M.E.. H. Pu, A.Y. Chiu, M.C Dal Canto, C.Y. Polchow, D.D. Alexander, J. Caliendo, A. Hentati, Y.W. Kwon, H-X. Deng, W. Chen, P. Zhai, R.L. Sufit and T. Siddique. 1994. Motor neurone degeneration in mice that express a human Cu, Zn superoxide dismutase mutation. *Science.* 264:1772-5.

Hadano, S., Y. Yanagisawa, J. Skaug, K. Fichter, J. Nasir, D. Martindale, B.F. Koop, S.W. Scherer, D.W. Nicholson, G.A. Rouleau, J. Ikeda, and M.R. Hayden. 2001. Cloning and characterization of three novel genes, ALS2CR1, ALS2CR2, and ALS2CR3, in the juvenile amyotrophic lateral

sclerosis (ALS2) critical region at chromosome 2q33-q34: candidate genes for ALS2. *Genomics.* 71:200-13.

Hafezparast, M., R. Klocke, C. Ruhrberg, A. Marquardt, A. Ahmad-Annuar, S. Bowen, G. Lalli, A.S. Witherden, H. Hummerich, S. Nicholson, P.J. Morgan, R. Oozageer, J.V. Priestley, S. Averill, V.R. King, S. Ball, J. Peters, T. Toda, A. Yamamoto, Y. Hiraoka, M. Augustin, D. Korthaus, S. Wattler, P. Wabnitz, C. Dickneite, S. Lampel, F. Boehme, G. Peraus, A. Popp, M. Rudelius, J. Schlegel, H. Fuchs, M. Hrabe de Angelis, G. Schiavo, D.T. Shima, A.P. Russ, G. Stumm, J.E. Martin, and E.M. Fisher. 2003. Mutations in dynein link motor neuron degeneration to defects in retrograde transport. *Science.* 300:808-12.

Hargitai, J., H. Lewis, I. Boros, T. Racz, A. Fiser, I. Kurucz, I. Benjamin, L. Vigh, Z. Penzes, P. Csermely, and D.S. Latchman. 2003. Bimoclomol, a heat shock protein co-inducer, acts by the prolonged activation of heat shock factor-1. *Biochem Biophys Res Commun.* 307:689-95.

Hartl, F.U., and M. Hayer-Hartl. 2002. Molecular chaperones in the cytosol: from nascent chain to folded protein. *Science.* 295:1852-8.

Hentati, A., K. Bejaoui, M.A. Pericak-Vance, F. Hentati, M.C. Speer, W.Y. Hung, D.A. Figlewicz, J. Haines, J. Rimmler, C. Ben Hamida, and et al. 1994. Linkage of recessive familial amyotrophic lateral sclerosis to chromosome 2q33-q35. *Nat Genet.* 7:425-8.

Higgins, C.M., C. Jung, H. Ding, and Z. Xu. 2002. Mutant Cu, Zn superoxide dismutase that causes motoneuron degeneration is present in mitochondria in the CNS. *J Neurosci.* 22:RC215.

Hopwood, D., S. Moitra, B. Vojtesek, J.A. Johnston, J.F. Dillon, and T.R. Hupp. 1997. Biochemical analysis of the stress protein response in human oesophageal epithelial. *Gut.* 41:156-63.

Howland, D.S., J. Liu, Y. She, B. Goad, N.J. Maragakis, B. Kim, J. Erickson, J. Kulik, L. DeVito, G. Psaltis, L.J. DeGennaro, D.W. Cleveland, and J.D. Rothstein. 2002. Focal loss of the glutamate transporter EAAT2 in a transgenic rat model of SOD1 mutant-mediated amyotrophic lateral sclerosis (ALS). *Proc Natl Acad Sci U S A.* 99:1604-9.

Ince, P., N. Stout, P. Shaw, J. Slade, W. Hunziker, C.W. Heizmann, and K.G. Baimbridge. 1993. Parvalbumin and calbindin D-28k in the human motor system and in motor neuron disease. *Neuropathol Appl Neurobiol.* 19:291-9.

Irobi, J., K. Van Impe, P. Seeman, A. Jordanova, I. Dierick, N. Verpoorten, A. Michalik, E. De Vriendt, A. Jacobs, V. Van Gerwen, K. Vennekens, R. Mazanec, I. Tournev, D. Hilton-Jones, K. Talbot, I. Kremensky, L. Van Den Bosch, W. Robberecht, J. Van Vandekerckhove, C. Broeckhoven, J. Gettemans, P. De Jonghe, and V. Timmerman. 2004. Hot-spot residue in small heat-shock protein 22 causes distal motor neuropathy. *Nat Genet.* 36:597-601.

Ishigaki, S., J. Niwa, Y. Ando, T. Yoshihara, K. Sawada, M. Doyu, M. Yamamoto, K. Kato, Y. Yotsumoto, and G. Sobue. 2002. Differentially expressed genes in sporadic amyotrophic lateral sclerosis spinal cords--screening by molecular indexing and subsequent cDNA microarray analysis. *FEBS Lett.* 531:354-8.

Jaarsma, D., F. Rognoni, W. van Duijn, H.W. Verspaget, E.D. Haasdijk, and J.C. Holstege. 2001. CuZn superoxide dismutase (SOD1) accumulates in vacuolated mitochondria in transgenic mice expressing amyotrophic lateral sclerosis-linked SOD1 mutations. *Acta Neuropathol (Berl).* 102:293-305.

Jakob, U., M. Gaestel, K. Engel, and J. Buchner. 1993. Small heat shock proteins are molecular chaperones. *J Biol Chem.* 268:1517-20.

Johnston, J.A., M.J. Dalton, M.E. Gurney, and R.R. Kopito. 2000. Formation of high molecular weight complexes of mutant Cu, Zn-superoxide dismutase in a mouse model for familial amyotrophic lateral sclerosis. *Proc Natl Acad Sci U S A.* 97:12571-6.

Johnston, J.A., C.L. Ward, and R.R. Kopito. 1998. Aggresomes: a cellular response to misfolded proteins. *J Cell Biol.* 143:1883-98.

Jolly, C., L. Konecny, D.L. Grady, Y.A. Kutskova, J.J. Cotto, R.I. Morimoto, and C. Vourc'h. 2002. *In vivo* binding of active heat shock transcription factor 1 to human chromosome 9 heterochromatin during stress. *J Cell Biol.* 156:775-81.

Jung, C., J.T. Yabe, and T.B. Shea. 2000. C-terminal phosphorylation of the high molecular weight neurofilament subunit correlates with decreased neurofilament axonal transport velocity. *Brain Res.* 856:12-9.

Kaal, E.C., A.S. Vlug, M.W. Versleijen, M. Kuilman, E.A. Joosten, and P.R. Bar. 2000. Chronic mitochondrial inhibition induces selective motoneuron death in vitro: a new model for amyotrophic lateral sclerosis. *J Neurochem.* 74:1158-65.

Kamradt, M.C., F. Chen, and V.L. Cryns. 2001. The small heat shock protein alpha B-crystallin negatively regulates cytochrome c- and caspase-8-dependent activation of caspase-3 by inhibiting its autoproteolytic maturation. *J Biol Chem.* 276:16059-63.

Kaspar, B.K., J. Llado, N. Sherkat, J.D. Rothstein, and F.H. Gage. 2003. Retrograde viral delivery of IGF-1 prolongs survival in a mouse ALS model. *Science.* 301:839-42.

Kawamata, T., H. Akiyama, T. Yamada, and P.L. McGeer. 1992. Immunologic reactions in amyotrophic lateral sclerosis brain and spinal cord tissue. *Am J Pathol.* 140:691-707.

Kegel, K.B., A.R. Meloni, Y. Yi, Y.J. Kim, E. Doyle, B.G. Cuiffo, E. Sapp, Y. Wang, Z.H. Qin, J.D. Chen, J.R. Nevins, N. Aronin, and M. DiFiglia. 2002. Huntingtin is present in the nucleus, interacts with the transcriptional corepressor C-terminal binding protein, and represses transcription. *J Biol Chem.* 277:7466-76.

Kieran, D., B. Kalmar, J.R. Dick, J. Riddoch-Contreras, G. Burnstock, and L. Greensmith. 2004. Treatment with arimoclomol, a coinducer of heat shock proteins, delays disease progression in ALS mice. *Nat Med.* 10:402-5.

King, R.J.B., J.R. Finley, A.I. Coffer, R.R. Millis, and R.D. Rubens. 1987. Characterisation and biological relevance of a 29-kDa, oestrogen receptor-related protein. *J Steroid Biochem.* 27: 471-75.

Klivenyi, P., R.J. Ferrante, R.T. Matthews, M.B. Bogdanov, A.M. Klein, O.A. Andreassen, G. Mueller, M. Wermer, R. Kaddurah-Daouk, and M.F. Beal. 1999. Neuroprotective effects of creatine in a transgenic animal model of amyotrophic lateral sclerosis. *Nat Med.* 5:347-50.

Kobayashi, Y., A. Kume, M. Li, M. Doyu, M. Hata, K. Ohtsuka, and G. Sobue. 2000. Chaperones Hsp70 and Hsp40 suppress aggregate formation and apoptosis in cultured neuronal cells expressing truncated androgen receptor protein with expanded polyglutamine tract. *J Biol Chem.* 275:8772-8.

Kong, J., and Z. Xu. 1998. Massive mitochondrial degeneration in motor neurons triggers the onset of amyotrophic lateral sclerosis in mice expressing a mutant SOD1. *J Neurosci.* 18:3241-50.

Kong, J., and Z. Xu. 2000. Overexpression of neurofilament subunit NF-L and NF-H extends survival of a mouse model for amyotrophic lateral sclerosis. *Neurosci Lett.* 281:72-4.

Kostic, V., V. Jackson-Lewis, F. de Bilbao, M. Dubois-Dauphin, and S. Przedborski. 1997. Bcl-2: prolonging life in a transgenic mouse model of familial amyotrophic lateral sclerosis. *Science.* 277:559-62.

Kriz, J., M.D. Nguyen, and J.P. Julien. 2002. Minocycline slows disease progression in a mouse model of amyotrophic lateral sclerosis. *Neurobiol Dis.* 10:268-78.

Kunst, C.B., L. Messer, J. Gordon, J. Haines, and D. Patterson. 2000. Genetic mapping of a mouse modifier gene that can prevent ALS onset. *Genomics.* 70:181-9.

Laemmli, U.K. 1970. Cleavage of structural proteins during the assembly of the head of bacteriophage T4. *Nature.* 227:680-5.

Lambrechts, D., E. Storkebaum, M. Morimoto, J. Del-Favero, F. Desmet, S.L. Marklund, S. Wyns, V. Thijs, J. Andersson, I. van Marion, A. Al-Chalabi, S. Bornes, R. Musson, V. Hansen, L. Beckman, R. Adolfsson, H.S. Pall,

H. Prats, S. Vermeire, P. Rutgeerts, S. Katayama, T. Awata, N. Leigh, L. Lang-Lazdunski, M. Dewerchin, C. Shaw, L. Moons, R. Vlietinck, K.E. Morrison, W. Robberecht, C. Van Broeckhoven, D. Collen, P.M. Andersen, and P. Carmeliet. 2003. VEGF is a modifier of amyotrophic lateral sclerosis in mice and humans and protects motoneurons against ischemic death. *Nat Genet.* 34:383-94.

LaMonte, B.H., K.E. Wallace, B.A. Holloway, S.S. Shelly, J. Ascano, M. Tokito, T. Van Winkle, D.S. Howland, and E.L. Holzbaur. 2002. Disruption of dynein/dynactin inhibits axonal transport in motor neurons causing late-onset progressive degeneration. *Neuron.* 34:715-27.

Lariviere, R.C., J.M. Beaulieu, M.D. Nguyen, and J.P. Julien. 2003. Peripherin is not a contributing factor to motor neuron disease in a mouse model of amyotrophic lateral sclerosis caused by mutant superoxide dismutase. *Neurobiol Dis.* 13:158-66.

Lee, G.J., A.M. Roseman, H.R. Saibil, and E. Vierling. 1997. A small heat shock protein stably binds heat-denatured model substrates and can maintain a substrate in a folding-competent state. *Embo J.* 16:659-71.

Lee, J.P., C. Gerin, V.P. Bindokas, R. Miller, G. Ghadge, and R.P. Roos. 2002. No correlation between aggregates of Cu/Zn superoxide dismutase and cell death in familial amyotrophic lateral sclerosis. *J Neurochem.* 82:1229-38.

Leigh, P.N., H. Whitwell, O. Garofalo, J. Buller, M. Swash, J.E. Martin, J-M. Gallo, R.O. Weller, and B.H. Anderton. 1991. Ubiqutin-immunoreactive intraneuronal inclusions in amyotrophic lateral sclerosis. *Brain.* 114:775-88.

Levine, J.B., J. Kong, M. Nadler, and Z. Xu. 1999. Astrocytes interact intimately with degenerating motor neurons in mouse amyotrophic lateral sclerosis (ALS). *Glia.* 28:215-24.

Li, M., V.O. Ona, C. Guegan, M. Chen, V. Jackson-Lewis, L.J. Andrews, A.J. Olszewski, P.E. Stieg, J.P. Lee, S. Przedborski, and R.M. Friedlander. 2000. Functional role of caspase-1 and caspase-3 in an ALS transgenic mouse model. *Science.* 288:335-9.

Lin, C.L., L.A. Bristol, L. Jin, M. Dykes-Hoberg, T. Crawford, L. Clawson, and J.D. Rothstein. 1998. Aberrant RNA processing in a neurodegenerative disease: the cause for absent EAAT2, a glutamate transporter, in amyotrophic lateral sclerosis. *Neuron.* 20:589-602.

Lin, L.F., D.H. Doherty, J.D. Lile, S. Bektesh, and F. Collins. 1993. GDNF: a glial cell line-derived neurotrophic factor for midbrain dopaminergic neurons. *Science.* 260:1130-2.

Lino, M.M., C. Schneider, and P. Caroni. 2002. Accumulation of SOD1 mutants in postnatal motorneurons does not cause motorneuron pathology or motorneuron disease. *J Neurosci.* 22:4825-32.

Lyons, T.J., H. Liu, J.J. Goto, A. Nersissian, J.A. Roe, J.A. Graden, C. Cafe, L.M. Ellerby, D.E. Bredesen, E.B. Gralla, and J.S. Valentine. 1996. Mutations in copper-zinc superoxide dismutase that cause amyotrophic lateral sclerosis alter the zinc binding site and the redox behavior of the protein. *Proc Natl Acad Sci U S A.* 93:12240-4.

Martin, L.J. 1999. Neuronal death in amyotrophic lateral sclerosis is apoptosis: possible contribution of a programmed cell death mechanism. *J Neuropathol Exp Neurol.* 58:459-71.

Masu, Y., E. Wolf, B. Holtmann, M. Sendtner, G. Brem, and H. Thoenen. 1993. Disruption of the CNTF gene results in motor neuron degeneration. *Nature.* 365:27-32.

Mehlen, P., K. Schulze-Osthoff, and A.P. Arrigo. 1996. Small stress proteins as novel regulators of apoptosis. Heat shock protein 27 blocks Fas/APO-1- and staurosporine-induced cell death. *J Biol Chem.* 271:16510-4.

Mersiyanova, I.V., A.V. Perepelov, A.V. Polyakov, V.F. Sitnikov, E.L. Dadali, R.B. Oparin, A.N. Petrin, and O.V. Evgrafov. 2000. A new variant of Charcot-Marie-Tooth disease type 2 is probably the result of a mutation in the neurofilament-light gene. *Am J Hum Genet.* 67:37-46.

Meyer, T., A. Fromm, C. Munch, B. Schwalenstocker, A.E. Fray, P.G. Ince, S. Stamm, G. Gron, A.C. Ludolph, and P.J. Shaw. 1999. The RNA of the glutamate transporter EAAT2 is variably spliced in amyotrophic lateral sclerosis and normal individuals. *J Neurol Sci.* 170:45-50.

Migheli, A., C. Atzori, R. Piva, M. Tortarolo, M. Girelli, D. Schiffer, and C. Bendotti. 1999. Lack of apoptosis in mice with ALS. *Nat Med.* 5:966-7.

Morimoto, R.I. 1998. Regulation of the heat shock transcriptional response: cross talk between a family of heat shock factors, molecular chaperones, and negative regulators. *Genes Dev.* 12:3788-96.

Morimoto, R.I., and M.G. Santoro. 1998. Stress-inducible responses and heat shock proteins: new pharmacologic targets for cytoprotection. *Nat Biotechnol.* 16:833-8.

Morimoto, R.I., M.P. Kline, D.N. Bimston, J.J. Cotto. 1997. The heat-shock response: regulation and function of heat-shock proteins and molecular chaperones. *Essays Biochem.* 32:17-29.

Muresan, Z., and V. Muresan. 2004. A phosphorylated, carboxy-terminal fragment of beta-amyloid precursor protein localizes to the splicing factor compartment. *Hum Mol Genet.* 13:475-88.

Nguyen, M.D., R.C. Lariviere, and J.P. Julien. 2001. Deregulation of Cdk5 in a mouse model of ALS: toxicity alleviated by perikaryal neurofilament inclusions. *Neuron.* 30:135-47.

Niwa, J., S. Ishigaki, M. Doyu, T. Suzuki, K. Tanaka, and G. Sobue. 2001. A novel centrosomal ring-finger protein, dorfin, mediates ubiquitin ligase activity. *Biochem Biophys Res Commun.* 281:706-13.

Niwa, J., S. Ishigaki, N. Hishikawa, M. Yamamoto, M. Doyu, S. Murata, K. Tanaka, N. Taniguchi, and G. Sobue. 2002. Dorfin ubiquitylates mutant SOD1 and prevents mutant SOD1-mediated neurotoxicity. *J Biol Chem.* 277:36793-8.

Olsen, M.K., S.L. Roberds, B.R. Ellerbrock, T.J. Fleck, D.K. McKinley, and M.E. Gurney. 2001. Disease mechanisms revealed by transcription profiling in SOD1-G93A transgenic mouse spinal cord. *Ann Neurol.* 50:730-40.

Oosthuyse, B., L. Moons, E. Storkebaum, H. Beck, D. Nuyens, K. Brusselmans, J. Van Dorpe, P. Hellings, M. Gorselink, S. Heymans, G. Theilmeier, M. Dewerchin, V. Laudenbach, P. Vermylen, H. Raat, T. Acker, V. Vleminckx, L. Van Den Bosch, N. Cashman, H. Fujisawa, M.R. Drost, R. Sciot, F. Bruyninckx, D.J. Hicklin, C. Ince, P. Gressens, F. Lupu, K.H. Plate, W. Robberecht, J.M. Herbert, D. Collen, and P. Carmeliet. 2001. Deletion of the hypoxia-response element in the vascular endothelial growth factor promoter causes motor neuron degeneration. *Nat Genet.* 28:131-8.

Oppenheim, R.W., L.J. Haverkamp, D. Prevette, J.L. McManaman, and S.H. Appel. 1998. Reduction of naturally motoneuron death in vivo by a target-derived neurotrophic factor. *Science.* 240: 919-20.

Otomo, A., S. Hadano, T. Okada, H. Mizumura, R. Kunita, H. Nishijima, J. Showguchi-Miyata, Y. Yanagisawa, E. Kohiki, E. Suga, M. Yasuda, H. Osuga, T. Nishimoto, S. Narumiya, and J.E. Ikeda. 2003. ALS2, a novel guanine nucleotide exchange factor for the small GTPase Rab5, is implicated in endosomal dynamics. *Hum Mol Genet.* 12:1671-87.

Pasinelli, P., D.R. Borchelt, M.K. Houseweart, D.W. Cleveland, and R.H. Brown, Jr. 1998. Caspase-1 is activated in neural cells and tissue with amyotrophic lateral sclerosis-associated mutations in copper-zinc superoxide dismutase. *Proc Natl Acad Sci U S A.* 95:15763-8.

Pedersen, W.A., H. Luo, I. Kruman, E. Kasarskis, and M.P. Mattson. 2000. The prostate apoptosis response-4 protein participates in motor neuron degeneration in amyotrophic lateral sclerosis. *Faseb J.* 14:913-24.

Perng, M.D., L. Cairns, I.P. van den, A. Prescott, A.M. Hutcheson, and R.A. Quinlan. 1999a. Intermediate filament interactions can be altered by HSP27 and alphaB-crystallin. *J Cell Sci.* 112 (Pt 13):2099-112.

Perng, M.D., P.J. Muchowski, I.P. van Den, G.J. Wu, A.M. Hutcheson, J.I. Clark, and R.A. Quinlan. 1999b. The cardiomyopathy and lens cataract mutation in alphaB-crystallin alters its protein structure, chaperone activity, and interaction with intermediate filaments in vitro. *J Biol Chem.* 274:33235-43.

Pompl, P.N., L. Ho, M. Bianchi, T. McManus, W. Qin, and G.M. Pasinetti. 2003. A therapeutic role for cyclooxygenase-2 inhibitors in a transgenic mouse model of amyotrophic lateral sclerosis. *Faseb J.* 17:725-7.

Puls, I., C. Jonnakuty, B.H. LaMonte, E.L. Holzbaur, M. Tokito, E. Mann, M.K. Floeter, K. Bidus, D. Drayna, S.J. Oh, R.H. Brown, Jr., C.L. Ludlow, and K.H. Fischbeck. 2003. Mutant dynactin in motor neuron disease. *Nat Genet.* 33:455-6.

Reaume, A.G., J.L. Elliott, E.K. Hoffman, N.W. Kowall, R.J. Ferrante, D.F. Siwek, H.M. Wilcox, D.G. Flood, M.F. Beal, R.H. Brown, Jr., R.W. Scott, and W.D. Snider. 1996. Motor neurons in Cu/Zn superoxide dismutase-deficient mice develop normally but exhibit enhanced cell death after axonal injury. *Nat Genet.* 13:43-7.

Ripps, M.E., G.W. Huntley, P.R. Hof, J.H. Morrison, and J.W. Gordon. 1995. Transgenic mice expressing an altered murine superoxide dismutase gene provide an animal model of amyotropic lateral sclerosis. *Proc Natl Acad Sci U S A.* 92:689-93.

Robertson, J., J.M. Beaulieu, M.M. Doroudchi, H.D. Durham, J.P. Julien, and W.E. Mushynski. 2001. Apoptotic death of neurons exhibiting peripherin aggregates is mediated by the proinflammatory cytokine tumor necrosis factor-alpha. *J Cell Biol.* 155:217-26.

Robertson, J., M.M. Doroudchi, M.D. Nguyen, H.D. Durham, M.J. Strong, G. Shaw, J.P. Julien, and W.E. Mushynski. 2003. A neurotoxic peripherin splice variant in a mouse model of ALS. *J Cell Biol.* 160:939-49.

Rordorf, G., W.J. Koroshetz, and J.V. Bonventre. 1991. Heat shock protects cultured neurons from glutamate toxicity. *Neuron.* 7:1043-51.

Rosen, D.R. 1993. Mutations in Cu/Zn superoxide dismutase gene are associated with familial amyotrophic lateral sclerosis. *Nature.* 364:362.

Rothstein, J.D., M. Dykes-Hoberg, C.A. Pardo, L.A. Bristol, L. Jin, R.W. Kuncl, Y. Kanai, M.A. Hediger, Y. Wang, J.P. Schielke, and D.F. Welty. 1996. Knockout of glutamate transporters reveals a major role for astroglial transport in excitotoxicity and clearance of glutamate. *Neuron.* 16:675-86.

Rothstein, J.D., R. Kuncl, V. Chaudhry, L. Clawson, D.R. Cornblath, J.T. Coyle, and D.B. Drachman. 1991. Excitatory amino acids in amyotrophic lateral sclerosis: an update. *Ann Neurol.* 30:224-5.

Rothstein, J.D., L.J. Martin, and R.W. Kuncl. 1992. Decreased glutamate transport by the brain and spinal cord in amyotrophic lateral sclerosis. *N Engl J Med.* 326:1464-8.

Rothstein, J.D., G. Tsai, R.W. Kuncl, L. Clawson, D.R. Cornblath, D.B. Drachman, A. Pestronk, B.L. Stauch, and J.T. Coyle. 1990. Abnormal

excitatory amino acid metabolism in amyotrophic lateral sclerosis. *Ann Neurol.* 28:18-25.

Rothstein, J.D., M. Van Kammen, A.I. Levey, L.J. Martin, and R.W. Kuncl. 1995. Selective loss of glial glutamate transporter GLT-1 in amyotrophic lateral sclerosis. *Ann Neurol.* 38:73-84.

Sawada, K., K. Agata, A. Yoshiki, and G. Eguchi. 1993. A set of anti-crystallin monoclonal antibodies for detecting lens specificities: beta-crystallin as a specific marker for detecting lentoidogenesis in cultures of chicken lens epithelial cells. *Jpn J Ophthalmol.* 37:355-68.

Schultz, A., .1999. Interindividual heterogeneity in the hypoxic regualtion of VEGF: significance for the development of the coronary artery collateral circulation. *Circulation.* 100:547-552.

Shaw, P.J., R.M. Chinnery, and P.G. Ince. 1994. (^{3}H)D-Aspartate binding sites in the normal spinal cord and changes in motor neuron disease: a quantitative autoradiographic study. *Brain Res.* 655:195-201.

Shaw, P.J., V. Forrest, P.G. Ince, J.P. Richardson, and H.J. Wastell. 1995. CSF and plasma amino acid levels in motor neuron disease: elevation of CSF glutamate in a subset of patients. *Neurodegeneration.* 4:209-16.

Shibata, N., A. Hirano, M. Kobayashi, T. Siddique, H.X. Deng, W.Y. Hung, T. Kato, and K. Asayama. 1996. Intense superoxide dismutase-1 immunoreactivity in intracytoplasmic hyaline inclusions of familial amyotrophic lateral sclerosis with posterior column involvement. *J Neuropathol Exp Neurol.* 55:481-90.

Shinder, G.A., M. Lacourse, S. Minotti, and H.D. Durham. 2001. Mutant Cu/Zn-superoxide dismutase proteins have altered solubility and interact with heat shock/stress proteins in models of amyotrophic lateral sclerosis. *J Biol Chem.* 276:12791-96.

Sobue, G., Y. Hashizume, T. Yasuda, E. Mukai, T. Kumagai, T. Mitsuma, and J.Q. Trojanowski. 1990. Phosphorylated high molecular weight neurofilament protein in lower motor neurons in amyotrophic lateral sclerosis and other neurodegenerative diseases involving ventral horn cells. *Acta Neuropathol (Berl).* 79:402-8.

Spencer, P.S., G.E. Kisby, S.M. Ross, D.N. Roy, J. Hugon, A.C. Ludolph, and P.B. Nunn. 1993. Guam ALS-PDC: possible causes. *Science.* 262:825-6.

Strong, M.J., M.M. Sopper, J.P. Crow, and J.S. Beckman. 1998. Nitration of the low molecular weight neurofilament is equivalent in sporadic amyotrophic lateral sclerosis and control cervical spinal cord. *Biochem Biophys Res Com.* 248:157-64.

Subramaniam, J.R., W.E. Lyons, J. Liu, T.B. Bartnikas, J. Rothstein, D.L. Price, D.W. Cleveland, and P.C. Wong. 2002. Mutant SOD1 causes motor

neuron disease independent of copper chaperone-mediated copper loading. *Nature Neurosci.* 5:301-7.

Takahashi, R., H. Yokoji, H. Misawa, M. Hayashi, J. Hu, and T. Deguchi. 1994. A null mutation in the human CNTF gene is not causally related to neurological diseases. *Nat Genet.* 7:79-84.

Takeuchi, H., Y. Kobayashi, T. Yoshihara, J. Niwa, M. Doyu, K. Ohtsuka, and G. Sobue. 2002. Hsp70 and Hsp40 improve neurite outgrowth and suppress intracytoplasmic aggregate formation in cultured neuronal cells expressing mutant SOD1. *Brain Res.* 949:11-22.

Tortarolo, M., P. Veglianese, N. Calvaresi, A. Botturi, C. Rossi, A. Giorgini, A. Migheli, and C. Bendotti. 2003. Persistent activation of p38 mitogen-activated protein kinase in a mouse model of familial amyotrophic lateral sclerosis correlates with disease progression. *Mol Cell Neurosci.* 23:180-92.

Tran, P.B., and R.J. Miller. 1999. Aggregates in neurodegenerative disease: crowds and power? *Trends Neurosci.* 22:194-7.

Trotti, D., A. Rolfs, N.C. Danbolt, R.H. Brown, Jr., and M.A. Hediger. 1999. SOD1 mutants linked to amyotrophic lateral sclerosis selectively inactivate a glial glutamate transporter. *Nat Neurosci.* 2:848.

Trotti, D., M. Aoki, P. Pasinelli, U.V. Berger, N.C. Danbolt, R.H. Brown, Jr., and M.A. Hediger. 2001. Amyotrophic lateral sclerosis-linked glutamate transporter mutant has impaired glutamate clearance capacity. *J Biol Chem.* 276:576-82.

Troy, C.M., N.A. Muma, L.A. Green, D.L. Price, and M.L. Shelanski. 1990. Regulation of peripherin and neurofilament expression in regenerating rat motor neurons. *Brain Res.* 529:232-8.

Uney, J.B., J.N. Kew, K. Staley, P. Tyers, and M.V. Sofroniew. 1993. Transfection-mediated expression of human Hsp70i protects rat dorsal root ganglian neurones and glia from severe heat stress. *FEBS Lett.* 334:313-6.

Urushitani, M., J. Kurisu, K. Tsukita, and R. Takahashi. 2002. Proteasomal inhibition by misfolded mutant superoxide dismutase 1 induces selective motor neuron death in familial amyotrophic lateral sclerosis. *J Neurochem.* 83:1030-42.

Vigh, L., P.N. Literati, I. Horvath, Z. Torok, G. Balogh, A. Glatz, E. Kovacs, I. Boros, P. Ferdinandy, B. Farkas, L. Jaszlits, A. Jednakovits, L. Koranyi, and B. Maresca. 1997. Bimoclomol: a nontoxic, hydroxylamine derivative with stress protein-inducing activity and cytoprotective effects. *Nat Med.* 3:1150-4.

Vukosavic, S., L. Stefanis, V. Jackson-Lewis, C. Guegan, N. Romero, C. Chen, M. Dubois-Dauphin, and S. Przedborski. 2000. Delaying caspase

activation by Bcl-2: A clue to disease retardation in a transgenic mouse model of amyotrophic lateral sclerosis. *J Neurosci.* 20:9119-25.

Wang, J., G. Xu, V. Gonzales, M. Coonfield, D. Fromholt, N.G. Copeland, N.A. Jenkins and D.R. Borchelt. 2002. Fibrillar inclusions and motor neurone degeneration in transgenic mice expressing superoxide dismutase 1 with a disrupted copper-binding site. *Neurobiol Dis.* 10:128-38.

Warrick, J.M., H.Y. Chan, G.L. Gray-Board, Y. Chai, H.L. Paulson, and N.M. Bonini. 1999. Suppression of polyglutamine-mediated neurodegeneration in Drosophila by the molecular chaperone HSP70. *Nat Genet.* 23:425-8.

Wei, X., S. Somanathan, J. Samarabandu, and R. Berezney. 1999. Three-dimensional visualization of transcription sites and their association with splicing factor-rich nuclear speckles. *J Cell Biol.* 146:543-58.

Wiedau-Pazos, M., J.J. Goto, S. Rabizadeh, E.B. Gralia, J.A. Roe, M.K. Lee, J.S. Valentine, and D.E. Bredesen. 1996. Altered reactivity of superoxide dismutase in familial amyotrophic lateral sclerosis. *Science.* 271:515-8.

Williamson, T.L., L.I. Bruijn, Q. Zhu, K.L. Anderson, S.D. Anderson, J.P. Julien, and D.W. Cleveland. 1998. Absence of neurofilaments reduces the selective vulnerability of motor neurons and slows disease caused by a familial amyotrophic lateral sclerosis-linked superoxide dismutase 1 mutant. *Proc Natl Acad Sci U S A.* 95:9631-6.

Williamson, T.L., and D.W. Cleveland. 1999. Slowing of axonal transport is a very early event in the toxicity of ALS-linked SOD1 mutants to motor neurons. *Nat Neurosci.* 2:50-6.

Wong, P.C., C.A. Pardo, D.R. Borchelt, M.K. Lee, N.G. Copeland, N.A. Jenkins, S.S. Sisodia, D.W. Cleveland, and D.L. Price. 1995. An adverse property of a familial ALS-linked SOD1 mutation causes motor neuron disease characterized by vacuolar degeneration of mitochondria. *Neuron.* 14:1105-16.

Xu, Z., L.C. Cork, J.W. Griffin, and D.W. Cleveland. 1993. Increased expression of neurofilament subunit NF-L produces alterations that resemble the pathology of human motor neurone disease. *Cell.* 73:23-33.

Yamanaka, K., C. Vande Velde, E. Eymard-Pierre, E. Bertini, O. Boespflug-Tanguy, and D.W. Cleveland. 2003. Unstable mutants in the peripheral endosomal membrane component ALS2 cause early-onset motor neuron disease. *Proc Natl Acad Sci U S A.* 100:16041-6.

Yang, Y., A. Hentati, H.X. Deng, O. Dabbagh, T. Sasaki, M. Hirano, W.Y. Hung, K. Ouahchi, J. Yan, A.C. Azim, N. Cole, G. Gascon, A. Yagmour, M. Ben-Hamida, M. Pericak-Vance, F. Hentati, and T. Siddique. 2001. The gene encoding alsin, a protein with three guanine-nucleotide exchange factor domains, is mutated in a form of recessive amyotrophic lateral sclerosis. *Nat Genet.* 29:160-5.

Yasojima, K., W.W. Tourtellotte, E.G. McGeer, and P.L. McGeer. 2001. Marked increase in cyclooxygenase-2 in ALS spinal cord: implications for therapy. *Neurology.* 57:952-6.

Yenari, M.A., S.L. Fink, G.H. Sun, L.K. Chang, M.K. Patel, D.M. Kunis, D. Onley, D.Y. Ho, R.M. Sapolsky and G.K. Steinberg. 1998. Gene therapy with HSP72 is neuroprotective in rat models of stroke and epilepsy. *Ann Neurol.* 44:581-3.

Zhang, B., P. Tu, F. Abtahian, J.Q. Trojanowski and V.M.-Y. Lee. 1997. Neurofilaments and orthograde transport are reduced in ventral root axons of transgenic mice that express human SOD1 with a G93A mutation. *J Cell Biol.* 139:1307-15.

Zhu, S., I.G. Stavrovskaya, M. Drozda, B.Y. Kim, V. Ona, M. Li, S. Sarang, A.S. Liu, D.M. Hartley, C. Wu du, S. Gullans, R.J. Ferrante, S. Przedborski, B.S. Kristal, and R.M. Friedlander. 2002. Minocycline inhibits cytochrome c release and delays progression of amyotrophic lateral sclerosis in mice. *Nature.* 417:74-8.